Processes and controls of meander development in the Allier, France

a case study on meander change in the period 1960 – 2003

final version

Supervisors: Dr. H. Middelkoop
Dr. J.H. van den Berg

November, 2005

Maarten Bakker
9907610

Universiteit Utrecht

Department Physical Geography
Faculty of Geosciences

Contents

Preface

This report was written as part of Master's research in Physical Geography at Utrecht University. It contains the results and conclusions from graduate fieldwork done along the Allier river in the summer of 2003.

I would like to thank everyone that was involved in the fieldwork. Supervisors Dr. H. Middelkoop and Dr. J.H. van den Berg for their guidance and constructive discussions. Fieldwork partners Sander van Rooy and Eisse Wijma for the good cooperation in the field and behind the computer, but also for the good times we had. The staff of the Moscow State University, TU Delft and Seva, Maxim, Misha, Emilie and Mathys for their help in the field.

Summary

Morphological development was researched along five meanders in the Allier river, France. This includes large scale development of meander form and direction and guiding factors and processes. On a smaller scale channel processes that form morphology, including bars and (secondary) channels.

Five meanders in the Allier river, France, demonstrated various types of development in time and space; lateral, downstream, rotational, compound bends and cutoffs. Bend radii decreased with lateral meander development, that occurred where bends were long enough to develop helicoidal flow (adjustment length) and where pointbar vegetation forced flow outwards. Downstream meander propagation and increasing bend radius occurred along resistant banks and recent cutoffs, that directed flow in downstream direction. The development of rotational and compound bends result from lateral (in the first case) and downstream (second case) erosion where flow meanders within bends.

Meander migration increased with discharge. Lateral erosion and sedimentation are (significantly) related to discharges above 550 m^3/s, that accounted for 20-30 % of their variation. Downstream sedimentation showed the strongest relationship with average discharge, accounting for 10-15 % of variation. Helicoidal flow was fully developed halfway most bends, causing lateral development, while lower discharges "meandered" within a bend causing bend expansion near the downstream end (and upstream for compound bends). A curve that related bend radius to erosion amounts, accounted for about 40 % of variation, while no correlation was found with sedimentation. Relative Bend radius (greater than 2.5) was related to maximum lateral and downstream sedimentation amounts (together with erosion). The steepest and clearest trend was found with erosion. Bend radius and discharge provided conditions that controlled potential erosion and sedimentation, while local factors (vegetation, bank resistance, upstream meander development etc.) limited actual amounts.

Average pointbar slopes near the apex increased from 0.025 to 0.035 with decreasing bend radius (till 2.5) and strengthening helicoidal flow. Sedimentation intensity, visible through the presence and amount of scroll bars, was greatest where slopes deviated most from the steeper equilibrium slope. When the bank became steeper, opposite of a resistant bank, scroll bars were stopped in their development and erosion could temporarily take place. Scroll bars are distinguishable through swales, that develop best in large bends, where there was more space than along the sharp inner bends. Pointbar morphology and scroll bar development were often influenced by the crossing of flow (riffles). Erosive channels often crossed long, narrow pointbars to a swale located on the inside of the pointbar, increasing the local waterlevel gradient. Riffles developed along long complex pointbars with average discharges, but were remoulded to scroll bars by high discharges. At the upstream end of a pointbar, riffles or riffle sections migrated downstream forming the newest phase of scroll bar development.

The potential of meanders in the Allier to cause erosion and sedimentation is largely determined by bend radius and discharge. Actual meander development, form and direction, is related to the local factors vegetation, bend length, bank resistance and upstream meander development.

1. Introduction

1.1 Research background

For many centuries the Dutch have been in conflict with flooding rivers for the control of land. This struggle continues because rivers and the adjoining land provide man with various resources. The land offers fertile grounds, building materials (gravel, sand and clay) and can be used for urban development with access to the river. Rivers supply fresh (cooling) water, a transport route, possibilities for recreation and more. Future usage of river space and resources combined with a changing climate and river behaviour, will lead to the persistence or growth of the conflict between man and river.

To enable the usage of rivers and adjacent land, large rivers such as the Rhine and Meuse have been straightened and narrowly enclosed by dikes. This was done primarily to protect the surrounding land from floods and allow the rivers to be navigated by large ships. Floods and high waters in the 1990's, however, called for more space for rivers to drain high discharges. Apart from increasing discharge capacity, larger floodplains can also accommodate more natural development and promote recreation and tourism. Instead of the strict protection of isolated patches of 'nature', river processes are allowed to develop nature on a larger scale (van Looy, 2003). Rivers can connect areas of natural development and act as corridor for species between such areas (Wolfert, 2002). This new approach in river management facilitates more, larger scale and sustainable natural development.

The implementation of more natural development in river management will have its effect on the whole river system. The system is expected to become more dynamic (natural), making it harder for man to control or steer development. Channel and floodplain morphology, including vegetation distribution, will change in space and time through local erosion and sedimentation. The changing river morphology is the concrete result of acting river processes while also guiding these processes. The morphology also forms the basis on which man interacts with rivers, determining where, how and under what circumstances human activities take place along the rivers. Examples include where navigation routes for ships lie, how high discharges are drained and where recreation conditions are most suitable. A shift towards more natural development and with it changes in river morphology and morphodynamics can lead to conflicts in the interaction between man and river. More space for high discharges and natural development comes at the cost of urban or agricultural land. Increased amounts of vegetation, however, can also cause an increase in flow resistance and the risk of floods, while channel sedimentation and the development of secondary channels can impede shipping. With close interaction between man and nature, it is necessary to understand natural river processes and their relation to river morphology. Research in river morphodynamics allows man to optimally cooperate with nature and benefit from it, while keeping it intact.

'Natural' rivers, that resemble the Dutch rivers (similar discharge, sediment size, gradient etc.), were chosen to study river behaviour. Rijkswaterstaat uses the Lower Volga in Russia, between Volgograd and the Caspian sea, and the upstream part of the Allier (figure 2.1), a tributary of the Loire in southern central France, as 'natural' analogues for the Dutch Rhine and Border Meuse (Lambeek and Klaassen, 1994). Insight in river processes and morphological development from these 'natural' analogues, can be used in future management of the Rhine, Border Meuse and other rivers.

Research in the Volga is concentrated on large scale morphology and vegetation dynamics related to regulated discharges. Since 1999 Utrecht University and the Moscow State

University have been involved in the research, done for Dutch governmental organisations such as the RIZA and NWO. The Allier is a smaller scale, more dynamic river. The research in the Allier finds its roots in the flooding of the Meuse in the Netherlands, notably the ones in 1993 and 1995 (Lambeek and Klaassen, 1994). Research in the Allier is concentrated on the development of the natural structure of river bed and floodplain (Helmer et al., 1991). Research in the Allier is done by: Utrecht University, TU Delft and the Radboud University Nijmegen.

In 1995 students of Utrecht University made a general overview of river characteristics and parameters of the Allier. Between 1996 and 1998 research continued, concentrating on the river bed, including sediment characteristics and morphology such as barchans and pavements. In the period 1998-1999 the focus of the research shifted towards flow patterns and discharge characteristics, while the TU Delft modelled meander development and flow patterns. The latest research phase is concentrated on the vegetational and morphological development of floodplains in the meandering part of the river. The history of research in Allier is summarised on the internet by Wilbers (see references).

1.2 Research objectives

The main question of research in the Allier is how natural riverbeds and floodplains develop in a small-scale dynamic river. The goals of this specific research were the following: *To determine how meander development is influenced by discharge, bend radius and form, bank resistance and pointbar vegetation. To understand the morphology of bars and their development in space and time.*

Research was done in the Allier to meet the abovementioned goals. These goals are worked out and further specified in the following sub-questions:

1. How are erosion and sedimentation, in lateral and downstream direction, related to discharge; average, maximum or number of days with discharge greater than 550 m^3/s?
2. How are erosion and sedimentation, in lateral and downstream direction, related to bend radius?
3. How do meander form and migration direction develop; downstream, lateral, compound bends, cutoffs? What (combination of) factors cause these types of development; resistant banks, pointbar vegetation, bend form and length?
4. How is lateral sedimentation related to erosion on the opposite bank? Do equilibrium conditions prevail along the pointbar slope or is there a lag in sedimentation?
5. What factors influence the presence and dimensions of scroll bars; bend radius, pointbar slope, flow obstacles? How do scroll bars develop and what is the role of lateral sedimentation, riffle development and their interaction?

To understand the morphological behaviour of a “natural” river, five bends near Moulins were examined (chapters 6 – 10). Changes in meander shape, morphological features (bars and channels) and vegetation in the period ± 1960 – 1992 were described using aerial photographs (sections 6.1, 7.1, 8.1 etc). In later years additional photographs, accurate plan form and elevation measurements and field observations allowed the analyses of morphological development in space and time (sections 6.2, 7.2, 8.2 etc). Quantitative results and a general outline of meander development was given in sections 6.3, 7.3, 8.3 etc. The findings of the individual bends were combined, compared and developed in chapters 11 – 15. Here the conditions and processes that controlled morphological development were discussed. The bases of chapters 11 – 15 were formed by sub-questions 1-5 (mentioned above). A

statistical approach to meander development was given in chapters 11 and 12, analysing the influence of discharge and bend radius. Large scale meander development was analysed in chapter 13 from a qualitative perspective. The relation between lateral sedimentation and erosion was discussed in chapter 14. Small scale morphology and sedimentation (/erosion) processes were analyzed to comprehend the development of scroll bars in chapter 15.

2. Description of research area

2.1 The Allier river

The Allier is a gravel bed river in south-central France (figure 2.1) with a catchment area of about 14000 km^2 (Bouchardy, 1991). It originates in the Cévennes, the southeastern part of the Massif Central, and flows northwards ending in the Loire River near the city of Nevers. The river follows a route of approximately 410 km from the foot of the Moure de la Gardille (1500 m) to Bec-d'Allier at 186 m (Bouchardy, 1991).

From the Massif Central the river flows through the Limange graben (geologically faulted depression), where it formed a series of terraces during the Pleistocene (Wilbers, 1997). The river now lies embedded in its own alluvial deposits, occasionally encountering older geologic formations near the valley edge. In the basin of Paris the Allier confluences with the Loire.

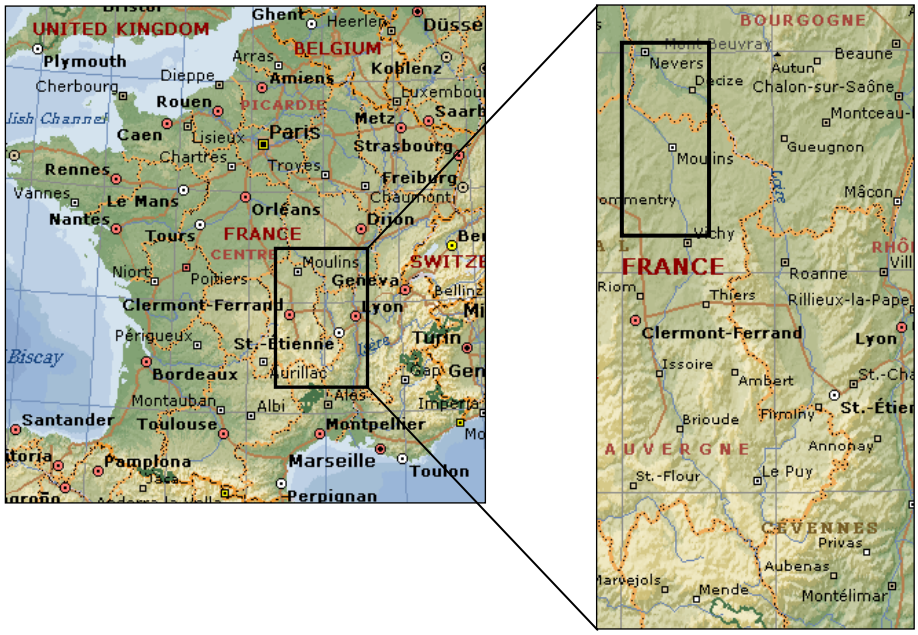

Figure 2.1: The location of the Allier river in France.(Expedia Maps) In the insert the Allier is the river west of the Loire along the places Brioude, Issoire, Vichy and Moulins. The box in the insert shows the location of the map in figure 2.4 that shows the different research areas.

The Allier is fed mostly by rain that falls in the Massif Central. The average discharge in the period 1968 – 2000 near Moulins was 132 m^3/s. Discharges vary considerably, ranging from a maximum of 1422 m^3/s to minima slightly less than 20 m^3/s (figure 2.2). The high discharges occur mainly in the winter and spring. Over the last 50 years the Allier showed a decreasing trend in (maximum and average) discharge amounts (de Kramer, 1998).

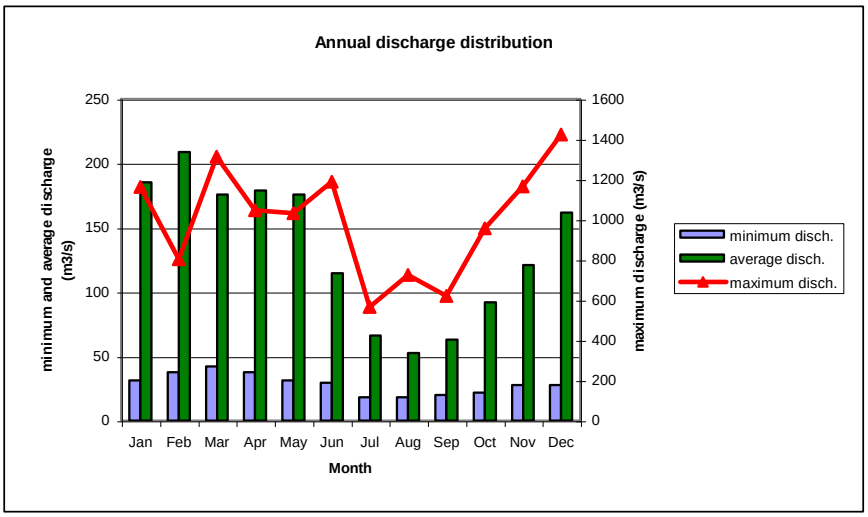

Figure 2.2: Allier at Moulins, monthly discharge distribution between 1968 and 2000 (data from Direction Departemental de l'equipement).

2.2 Study area near Moulins

This research was mainly concentrated on the meandering part of the Allier, upstream (south) of Moulins (figure 2.3). Downstream from Moulins a braiding pattern dominates (Wilbers, 1997). The meandering part of the river has a channel, about 90 meters wide, and a floodplain that ranges from a few hundred meters to a kilometer in width.

Sediment along the channel has a bimodal composition ranging from (coarse) sand to gravel/pebbles (figure 2.3) with a d90 (90 % by weight is finer) of approximately 2 cm. The river gradient is approximately $6*10^{-4}$ while the valley slopes down at about $5*10^{-4}$.

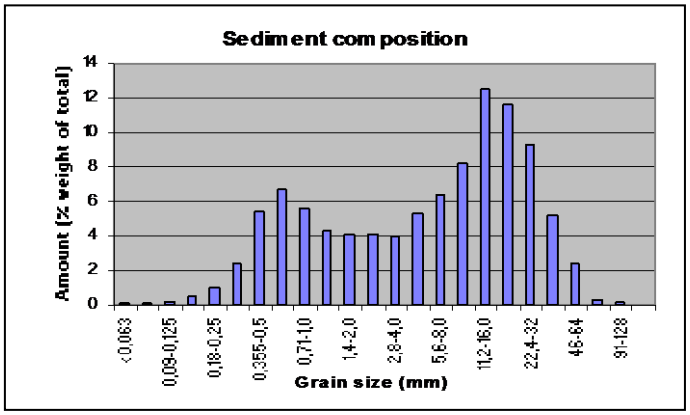

Figure 2.3: Sediment grain size composition from a number of river bends between Moulins and Varennes (Wilbers, 1997).

Vegetation on pointbars of the Allier is characterised by poplars in the form of bushes and trees. Grasses and other vegetation types develop mainly alongside and behind poplar strokes that provide protection against strong flow. The succession of vegetation, ranging from pioneer species to softwood forests, have been described by Van den Berg and Balyuk (2004).

2.3 Study sites (meanders)

Research was carried out at five meander bends: St. Loup, Châtel de Neuvre, Chemilly, Château de Lis, and Beauregard. The location and an aerial photograph of each of the bends is shown in figure 2.4. The bends will be presented in this report starting upstream (in the north) at St. Loup, moving downstream to Beauregard.

The meander St. Loup lies just upstream from the confluence of the Sioule with the Allier. It lies about two kilometers WSW of the town it is named after, 24 kilometers south of Moulins. At the downstream end of the bend a railroad bridge crosses the river. Revetments on both banks protect the bridge, limiting the river in its movement. Nearly the complete pointbar is vegetated with strokes of trees and pioneer vegetation.

The following bend in downstream direction is Châtel de Neuvre. The bend is named after the town that lies a kilometer Southwest of it. Châtel de Neuvre lies about 17 kilometers south of Moulins. The river is free in its movement. The only protected bank lies on the outside of the bend upstream from “Châtel de Neuvre”, near the local camping. Across the pointbar lies a stroke of trees that separates an unvegetated area along the river from an area with predominantly grasses on the inside.

The meander designated as “Chemilly” lies a kilometer to the NE of the town Chemilly and about eight kilometers south from Moulins. Floodplain edges pose limitations to meandering, especially on the western side where the river cuts deeply into a Pleistocene terrace. At the upstream end of the eastern bank revetments also hamper meander movement. The pointbar has a concentration of trees at its center, surrounded by pioneer vegetation.

The meander “Château de Lis” is separated from “Chemilly” by one bend in downstream direction. The bend is named after the castle on the west bank that lies about seven kilometers south of Moulins. The river has a lot of space to meander shown by meander expansion and cut-offs that occurred several times in the last 50 years. Only the western bank, near the castle, is protected. The pointbar is only partially covered with low vegetation including pioneer vegetation, grass and sporadically shrubs.

The Beauregard meander lies downstream (north) of Moulins, in a slightly braiding stretch of river. It lies about 26 km northwest of Moulins. The bend is named after the castle that lies on the slope of a hill on the bank opposite of the point bar. Since 1993 it is hampered in its movement on the south western bank, because of naturally resistant bedrock that crops out at the valley edge. Vegetation on the pointbar is dominated by trees.

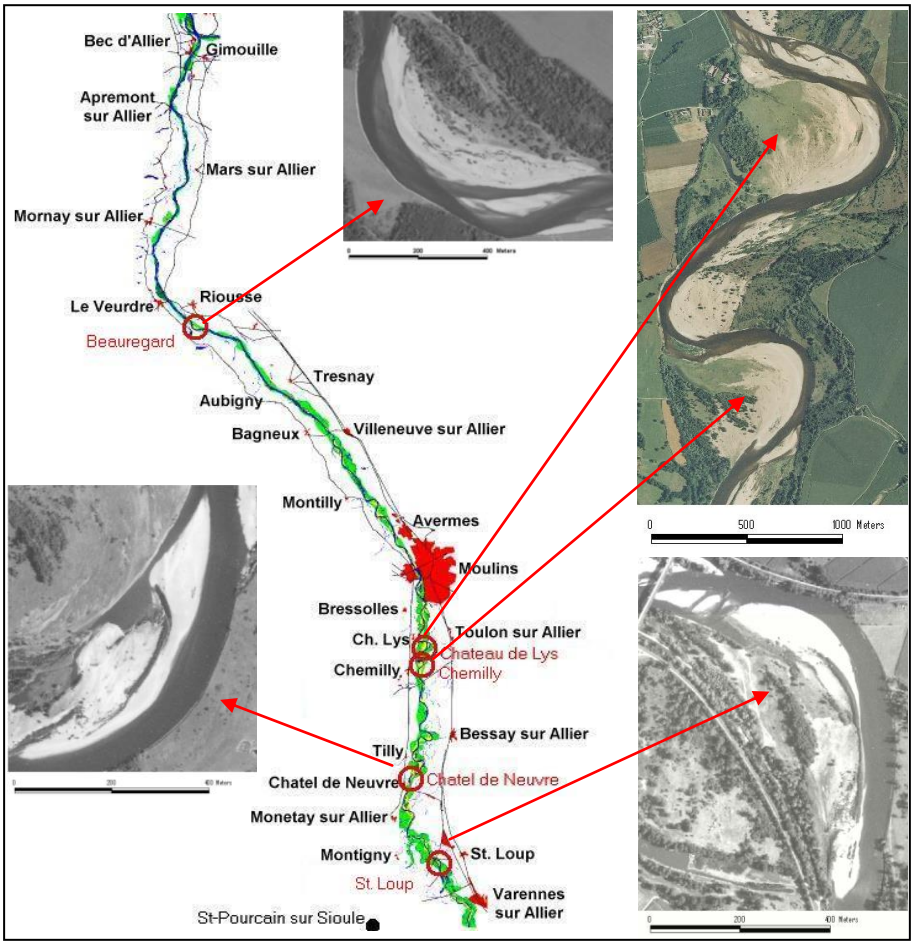

Figure 2.4: The locations of the research meanders, marked in red, along the Allier with aerial photographs from 2000, adapted from Wilbers (website).

3. Meander flow and morphological development

3.1 Secondary flow in meanders

Secondary flow, perpendicular to the primary downstream flow (figure 3.1), can develop as a result of changes in flow direction (bends) or local cross sectional irregularities (Prandtl, 1952). In a meander bend secondary circulation is caused by an imbalance along the flow-depth between curvature-induced centrifugal force (outwards) and a pressure gradient (inwards) associated with transverse sloping water surface (figure 3.1, cell 1). At the water surface, flow velocity is large, resulting in a large centrifugal force and outward motion. Along the channel bed flow velocities are low and the dominant hydrostatic force causes inward motion. The combined primary and secondary flow lead to helicoidal motion in meander bends.

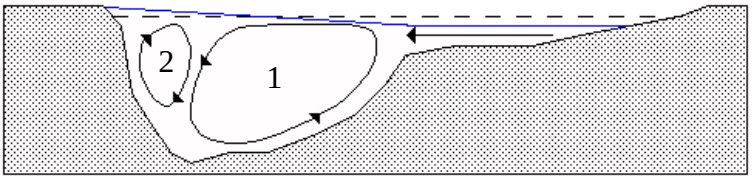

Figure 3.1: Secondary flow in a meander cross section, adapted from Roy Richardson, 1997.

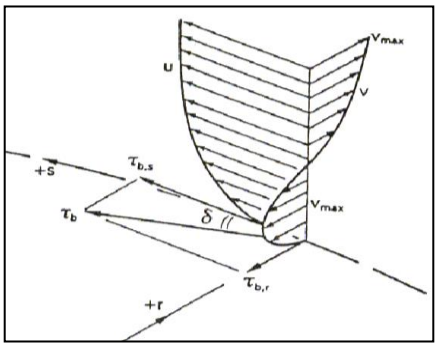

Figure 3.2: Helicoidal flow in two dimensions (van Rijn, 1990).

The lateral component of flow is expressed in equation 1 (Rozovski, 1960) and increases with decreasing bend radius.

$$\tan\delta = a\frac{h}{r} \qquad [1]$$

δ = deviation bend tangent (figure 3.2), a = constant $\approx$ 11, h = flow depth, r = bend radius.

Lokal bank irregularities and varying bank resistance can also cause secondary circulation, including outer bank cells (figure 3.1, cell 2). Additional circulation cells can also be a relict from an upstream bend that gradually get replaced by a cell from the present bend (Toebes and Sooky, 1967; Thorne and Hey, 1979). Along the upstream part of a shallow inner bend, flow experiences high bed resistance causing a decrease in the transverse waterlevel gradient (figure 3.1) and outerward movement of water (Thorne and Rais, 1983).

3.2 Meander development

3.2.1 Progressive meander development

The form of a meander is in constant change, caused by erosion and sedimentation. Conversely, meander form also influences the location and amount of erosion, and implicitly sedimentation, that occurs (section 3.3.3). This interaction leads to a few characteristic types of meander development, shown in figure 3.3.

The development and form of a meander are related to its maturity (Hickin, 1974) or

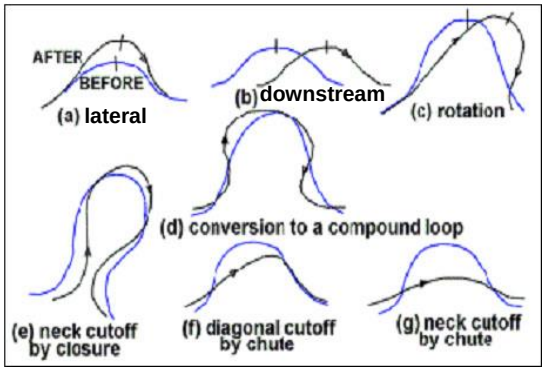

Figure 3.3: Modes of meander development Brice and Blodgett (1978).

proximity to equilibrium conditions (Friedkin, 1945). Lateral development (figure 3.3 a) is characteristic for meanders with a low amplitude, in their early stages of development. Approaching equilibrium conditions meanders with a larger amplitude will predominantly migrate downstream (b), changing little in form. Meandering behaviour is often assumed as a stable equilibrium state, but meanders also show gradual evolution and increased form complexity (Hooke, 2004). This leads to the development of complex meanders c,d and possible bend cutoffs e,f,g that will be discussed in sections 3.2.2 and 3.2.3.

Meander development is affected by the alignment of the flow that enters it from upstream bends (Lagasse et al., 1995). The direction of incoming flow determines where and at what angle flow encounters a bank (or other morphological entity) and therefore also where and with what intensity erosion can take place. The spatial distribution of bank resistance also guides flow and meander development. Resistance can be caused by bedrock, sub soil and vegetation, but in the Allier manmade bank revetments are most prominent. The revetments confine rivers laterally, forcing meander development in downstream direction (Lagasse et al., 1995).

3.2.2 Compound bend formation

Compound bends are characterized by two sections of strong curvature, where outer bank erosion takes place, separated by a section that shows little to no curvature or even curvature reversal, shown in figure 3.3(d). An additional pool-riffle sequence is present in such a bend (Lancaster and Bras, 2002). Compound bends develop through the coalescence of following bends with different migration velocity's (Brice, 1974), or the development of a sufficiently large bend into two or more (sub)bends (Hooke and Harvey, 1983; Lancaster and Bras, 2002). The breaking up of long bends is assigned to secondary flow (Hooke and Harvey, 1983) and/or the unsustainability of sediment transport (Thompson, 1986). Sun et al. (1996) and Lancaster and Bras (2002) developed models showing the importance of bank heterogeneity and the interaction between flow and bank.

3.2.3 Meander cutoff

Meander cutoffs can be considered as an integral part of meander evolution (Hooke, 2004). In the final stages of progressive meander development a meander can reach a critical state of equilibrium that leads to a cutoff (Bak et al., 1987; Stolum 1996). Cutoffs are also assigned to external triggering influences (Hooke, 2004), such as a high discharges or (artificial) upstream cutoffs. Bank stability plays an important role in determining cutoff type (Lagasse et al., 1995). Neck cutoffs (figure 3.3 e) need sufficiently stable banks to develop an elongated loop before closure, while chute cutoffs (f,g) occur along unstable banks. Wolfert (2002) found that meanders that encounter a resistant bank will often continue downstream, tighten and a neck-cutoff will occur upstream (figure 3.4).

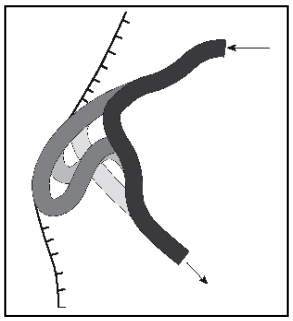

Figure 3.4. Bend cutoff along resistant bank (darker courses are older) (Wolfert, 2002).

The cut-off of a meander has profound influences on up- and downstream meanders. A cutoff leads to an increase in stream gradient and scour that propagates upstream from the cutoff. Increased erosion will lead to increased sedimentation downstream from the cutoff, where the gradient decreases (Lagasse et al., 1995). Cutoffs are often found in clusters (Hooke, 2004). A meander that is cut-off can impose conditions on (downstream) meanders that lead to their cutoff. A group of meanders in a critical state of equilibrium can be cut-off (Bak et al., 1987; Stolum, 1996), not necessarily progressing downstream as found by Hooke (2004).

3.3 Erosion and sedimentation

3.3.1 Beginning of motion

The movement of sediment is dependent on flow velocity and sediment characteristics. At a certain threshold, flow velocity along the bedding is strong enough to cause the movement of sediment grains. This threshold is determined by grain form, density and above all its size. Sediment motion can be determined with the Shields parameter (θ; equation 2) and curve (figure 3.5).

$$\theta = \frac{Ri}{(s-1)d} \qquad [2]$$

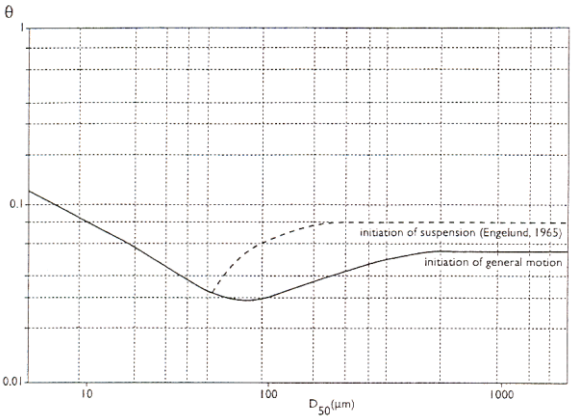

Figure 3.5: Shields curve, θ is the mobility (Shields) parameter.

R = hydraulic radius ≈ h, waterdepth for wide rivers (van Rijn, 1990); i = water surface slope ($6*10^{-4}$); s = density ratio between sediment and water (2.65); d = grain diameter.

Flow velocity (u) can be measured or determined theoretically / empirically using river parameters as shown in equation 3:

$$u = C\sqrt{hi}\ ,\ C = 18\log\left(\frac{12R}{ks}\right) \qquad [3]$$

C = Chezy coefficient, R ≈ h, waterdepth; i = water surface slope ($6*10^{-4}$); ks = d90 (0.02 m) for flat gravel bed.

The discharge at which sediment transport commences in the Allier was calculated using equations 2 and 3. As representative sediment size the Allier channel modus was used, d = 0.014 m (figure 2.3), was used. Although sediment from the outer bank (that gets laterally eroded) is on average smaller, it is more cohesive. Using Shield's curve (figure 3.5) and equation (2) the waterdepth (h) at which transport is initiated was calculated. Using equation 3 flow velocity was calculated from which a discharge of 460 m^3/s was determined (multiplied by waterdepth (h) and flow width (b)). This is an indication with what discharge sediment transport along the outer bank initiates.

On a larger scale, channel migration rates are controlled by stream power, discharge (3.3.2) and channel gradient, and channel morphology, bend radius (3.3.3) and channel dimensions. These factors represent flow velocity and its distribution throughout a channel. Factors that resist erosion (3.3.4), apart from sediment characteristics, include bank height, cohesiveness, vegetation and sediment transport.

3.3.2 Discharge

The capacity of discharge to erode and transport sediment is dependent on local flow velocities, flow configuration (secondary flow, including divergence and convergence) and its distribution in time (occurrence frequency). Increasing discharges are accompanied by increasing flow velocities (above the threshold of movement), channel area (sediment source) and sediment transport amounts. At a certain discharge height, however, flow starts to follow a straighter path across the river bed and diverges across the floodplain, impeding helicoidal flow and sediment transport capacity. The maximum amount of sediment transport occurs at dominant discharge, which is approximated by bankfull discharge (Richards, 1982). The frequency distribution of discharges determines what amounts of sediment discharges actually

transport. Low discharges have a low erosive capacity but occur relatively often, while high discharges might have a high capacity but occur infrequently.

Amounts of transport are dependent not only on flow velocity but also on the mechanism of sediment transport; bed (Allier), saltating or suspensive load. Relating flow velocities to amounts of eroded sediment gives variable results among authors. Erosion, that occurs at flow velocities above the threshold of motion, is proportional to flow velocity taken to powers ranging from 1 to 5 (e.g Ikeda et al., 1981; Engelund and Hansen, 1967). Meyer-Peter & Muller (1948) developed a dimensionless transport parameter (ϕ) for large amounts of gravel transport, using a fixed threshold for motion ($\theta = 0.047$):

$$\phi = 8\left(\theta C^{1.5} - 0.047\right)^{1.5}, \qquad C = \text{Chezy coeff (eq. 3)}\ \ \theta = \text{Shields par. (eq. 2).} \qquad [4]$$

3.3.3 Bend radius

A meander bend can be portrayed as a circle. The radius of the circle is considered to be a measure for the curvature of the bend. The ratio between bend radius and mean channel width is known as the relative meander radius and allows the comparison of bends from different rivers or river sections.

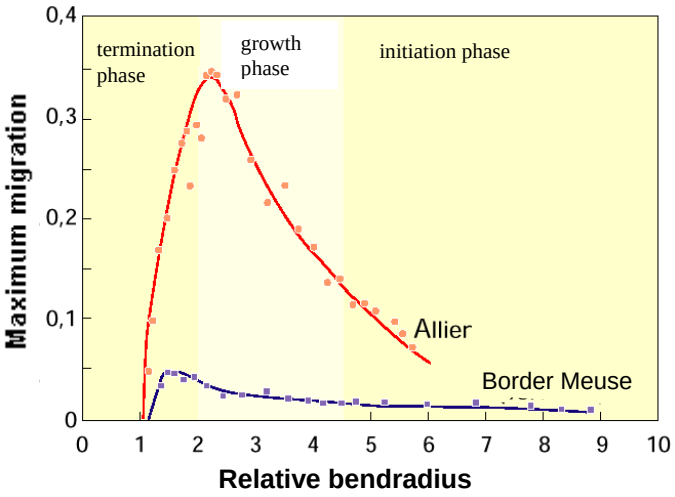

Figure 3.6: Meander migration as a function of relative bend radius. Migration is in meters per year / bed width (adapted from de Kramer et al, 2000).

Hickin (1977) described standard meander bend development as the progressive sharpening of a bend through local erosion at the outer bank (figure 3.6). Initially, the bend radius decreases slowly and there is little channel migration. Strengthening helicoidal flow causes the rate of lateral migration and bend sharpening to increase. A bend reaches maximum erosive capacity near a (relative) radius between 2.5 and 3 (figure 3.6). In sharper bends the erosive capacity decreases due to the development of turbulence and a shift of maximum shear stress towards the inner bank, causing erosion at the pointbar instead of in the outer bend (Nanson and Hickin, 1983). This development sequence assumes that the location of maximum erosion remains fairly stationary along the bend. In practice however, this location usually shifts as result of changes in the form of the upstream bend, a change in bank resistance, variation in discharge etc. A shift in the location where maximum erosion takes place can cause an increase in bend radius (Hickin, 1974).

Apart from influencing the amount of erosion in a bend, meander curvature also influences where erosion takes place. Maximum erosion along the outer bank occurs at the end or just past the section of maximum curvature (figure 3.7). Flow here is concentrated in the outer bend and helicoidal flow is strong. In the outerbend the waterlevel super-elevation is maximum due to helicoidal flow. This leads to a relative low waterlevel gradient upstream of the apex and a relatively high gradient downstream, where the strongest erosion takes place (NEDECO, 1959). Near the innerbend the opposite is true; waterlevels are low, causing a low downstream gradient and sedimentation to occur.

3.3.4 Resistance to flow

Apart from individual sediment grains other forms of resistance to flow are found along the channel bed and banks. Trees, rocks and cohesive lumps of earth, that influence flow and local bend migration, are usually found along the outer margin of the channel, where they have been dislodged from the bank by erosion. The width-depth ration of a channel is often used as a measure of bank resistance (Wolfert, 2002; Schumm, 1968), where relatively deep channels have banks that are difficult to erode. The bank height determines the amount of sediment that has to be removed for a channel to migrate.

Debris in a channel can cause sedimentation, through flow blockage and energy dissipation, and scour, through flow deflection (Wallerstein and Thorne, 2004). Upstream of large woody debris, helicoidal flow can be strengthened due to the inward redirection of flow (that makes a sharper turn), while downstream from the debris helicoidal flow diminishes (Daniels and Rhoads, 2003). Thompson et al. (1999) found that obstacles, in pools, cause a narrower flow cross section and increased water surface gradients causing high flow velocities and erosion.

3.4 Flow – morphology equilibrium

3.4.1 Upstream influences on meander development; adaptation length

A change in stream power or resistance to flow between bends can cause a change in transport capacity and therefore lead to erosion or sedimentation. The sediment balance of a bend is therefore dependent on characteristics of the bend, the river upstream, and the amount of incoming sediment.

Water flow, and with it erosion and sedimentation, lag behind meander form (figure 3.7). It takes a certain distance along a bend before helicoidal flow is fully developed. The adaptation length (λ_w) of main flow for morphology was introduced by De Vriend and Struiksma,1983 (equation 5). Flow adjusts quickly at first (in downstream direction) and then gradually approaches an equilibrium situation. The adaptation length is defined at 63% of the adjustment towards equilibrium (de Vriend and Struiksma, 1983). Discharge therefore influences both the amount (3.3.2) and location of erosion.

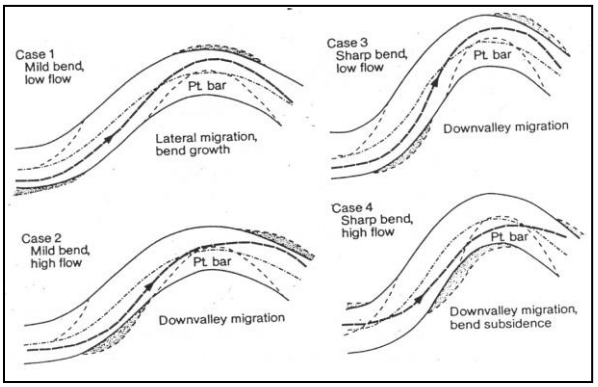

Figure 3.7: transverse profiles caused by stream paths during high water stage (solid line) and low water stage (dotted line), Chang (1988).

$$\lambda_w = \left(\frac{C^2}{2g}\right) h_0 \ , \ \ h_0 = \left(\frac{Q}{bC\sqrt{i}}\right)^{2/3} \qquad [5]$$

$$\lambda_s = \frac{1}{\pi^2}\left(\frac{b}{h_0}\right)^2 h_0 0.85\sqrt{\theta} \qquad [6]$$

*h_0 can be replaced by the h (flow depth) multiplied with a correction factor or just h; C = Chezy coef. (eq. 3); g = gravity (9.8 m/s^2); Q = discharge; b = flow width (90 m); i = water surface slope (6*10^{-4}); θ = Shields par. (eq. 2).*

Flow is guided by channel morphology, but on the other hand also sculpts morphology through erosion and sedimentation. Struiksma and Crosato (1989) determined that bed topography development also has a characteristic adaptation length (λ_s), shown in equation 6.

Adjustment lengths of flow and morphology in the Allier are related to discharge in figure 3.8. High discharges have long flow adjustment lengths and seek greater meander wavelengths (Dury, 1964). A large amount of flow momentum has to be redirected. With low discharges flow needs little distance to reach equilibrium with morphology (bend form). Morphology changes over a long distance with low discharges, because these discharges have less power to force sedimentary changes over a short distance. Morphological changes occur more directly with high discharges. Flow and morphology adjust simultaneously resulting in overall adjustment lengths of about 300 – 500 meters (figure 3.8).

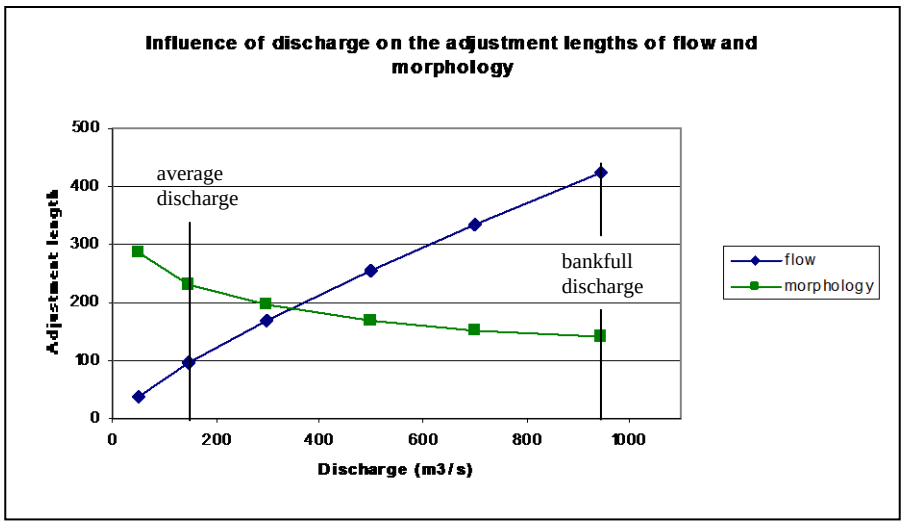

Figure 3.8: Adjustment lengths of flow and morphology as a function of discharge.

The ratio of the two adjustment lengths (λ_s/λ_w), the interaction parameter is important for the equilibrium river bed topography. Struiksma and Crosato (1989) modelled that with decreasing width, a river will deepen, damping will increase, the river will stabilize and there will be less pronounced bars.

3.4.2 Channel cross section

In a meander cross section, flow and morphology attempt to establish an equilibrium through (outer bend) erosion and (inner bend) sedimentation. An equilibrium situation can be represented by an ideal cross sectional slope of the inner bank (pointbar). The shear stress of lateral flow on sediment (equation 1), directed upwards along the pointbar slope, is opposed by gravitational force on sediment, working down the slope. Prayoyo and Struiksma (1985) determined the resulting pointbar gradient (α; equation 7) of an ideal cross section at the bend apex from equation 1:

$$\tan\alpha = 10.63\left(1-\frac{1.83}{C}\right)\frac{h}{r}\sqrt{\theta} \qquad [7]$$

α = angle between point bar slope and horizontal; C = Chezy coef. (eq. 3); h = flow depth; r = bend radius; θ = Shields par. (eq. 3).

The pointbar gradient is greatest with high discharges and the lowest at decreasing or low water (Lagasse et al., 1995). Cross profiles show the strongest asymmetry with rising stage, and decreasing asymmetry with falling stage due to erosion at the base of the pointbar (Anthony and Harvey, 1991). The relationship (equation 7) is however only valid at the apex of an ideal bend with constant radius and bed resistance. In nature this is never the case and effects of flow and sediment-transport generated upstream also have to be taken into account (Struiksma et al., 1985).

3.5 Bar characteristics and development

3.5.1 Bar morphology and structure

Bars are sedimentary structures that lie in or alongside a riverchannel. Bars characteristically have a length greater than or equal to the width of the river and a height comparable to the water depth (Kolkhuis Tanke, 1997). In this paper pointbars, alongside the river channel and riffles, crossing the river channel, will be examined (figures 3.9, 3.10).

Bar morphology

Pointbars are largely composed of distinguishable scroll bars. Scroll bars are most often long, arcuate or crescentic ridges, that lie approximately parallel to a pointbar and form the latest phase of accretion (among others Reading, 1996). Swales are troughs, caused by a lapse in sedimentation. They can be present along the inside margin of downstream scroll bar development (figure 3.9) or between phases of lateral scroll bar development (figure 3.10). In the first case swales are relatively short, wide and retain channel depth, still in usage during high discharges. Swales formed during lateral development are longer, narrower and have relief in the order of decimeters till about a meter in the Allier. Often lateral scroll bars and swales cannot be distinguished and are therefore described as a compound scroll bar.

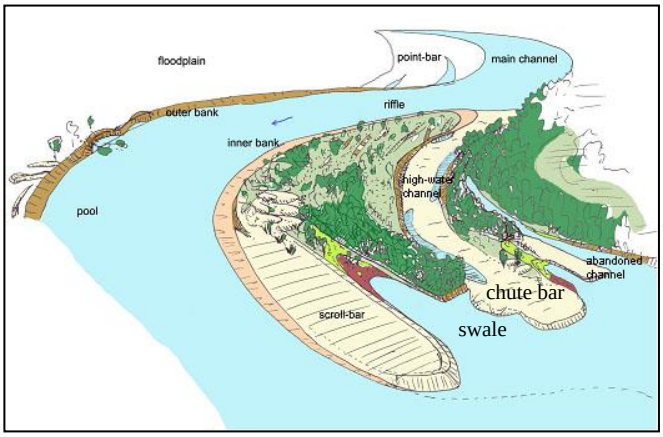

Figure 3.9: Point bar layout in the Volga river, Russia (de Kramer, 2001).

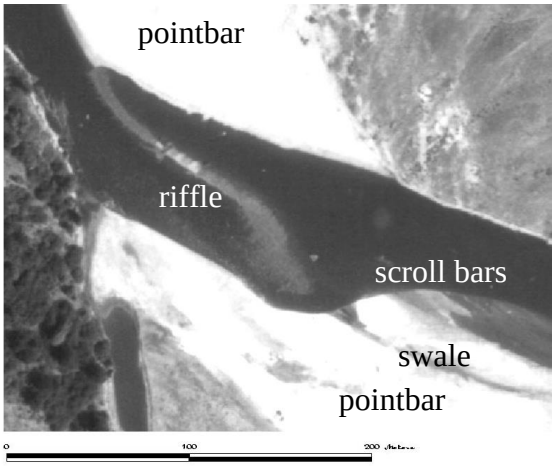

Figure 3.10: Riffle and pointbars near Chatel de Neuvre, Allier in 1975.

With high discharges a continuous sedimentation stroke crosses the channel (figure 3.10). This stroke gets interrupted by erosive crossing channels during low water conditions, allowing the development of multiple riffle bars. These erosive crossing channels can also cut across the downstream end of a pointbar. Additional bars that will be examined are chute bars that are often deposited in a downstream swale, after crossing the pointbar (figure 3.9) and counter pointbars that lie along sharp outer banks (3.5.3; figure 3.13).

Bars and scroll bars in particular, have a gently sloping stoss side and a steep lee side (figure 3.9). The steep lee side and bar flanks are formed by a combination of erosion, (undercutting) as well as sedimentation (slipface). The direction of scroll bars dips can vary considerably (Leclerc and Hickin, 1997) and can be related to local and temporary flow conditions.

Pointbar structure

Leclerc and Hickin (1997) found pointbars (consisting of sand and gravel) that were mainly built up by large-scale laterally accreted deposits with periodic channel fills located between surface scroll ridges (figure 3.11). Deeper deposits (lower point bar), formed with higher

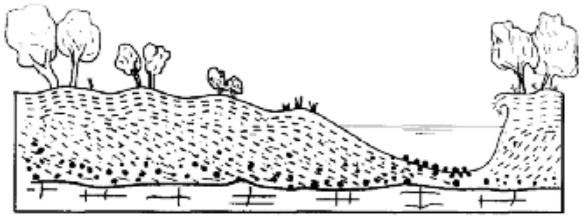

Figure 3.11: Pointbar structure (Nanson and Croke, 1992).

energy flows show non-continuous inclined strata (Bridge et al., 1995). Above the lateral deposits lie scroll ridge deposits overlain by vertically accreted deposits that preserve the underlying relief (Leclerc and Hickin, 1997). In downstream direction horizontal stratification was found and inclined stratification along some scroll bar ridges, pointing to downstream accretion.

3.5.2 Scroll bar development

When erosion takes place along the outer bank, the channel will widen and become more shallow, leading to flow separation and a greater flow resistance. Sedimentation takes place on the inside of the bend to counter-balance the erosion. Scroll bars are the result of sedimentation phases and their formation is controlled by channel bed dimensions. Sedimentation is however a discontinuous process and can lag behind outer bank erosion. This is related to factors, principally discharge, that determine the occurrence and intensity of erosion and sedimentation. A lapse between sedimentation phases is found in the form of a swale. The number of scroll bars and their size increase with the rate of bend migration (Reading, 1996). Scroll bars develop in the channel, expand or migrate in lateral and/or downstream direction, merge with the pointbar and become vegetated. Nanson and Hickin (1983) and Nijman and Puigdefabregas (1978) found no lateral accretion or motion of scroll bars towards the convex bank, even thought this is often seen as a prerequisite.

Bar development at flow separation

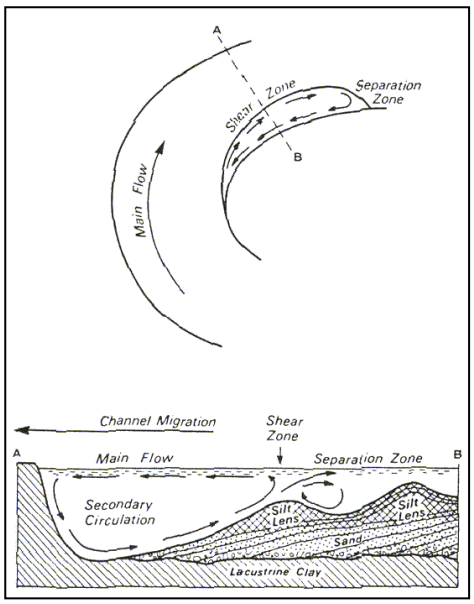

Nanson and Hickin (1983) proposed the initiation and development of scroll bars near flow separation in sharp bends (figure 3.12). Flow is concentrated in the outer part of the bend, where curvature is slightly lower than on the inside, reducing flow resistance (Leopold et al., 1960). On the border between the main flow and separation zone (figure 3.12) there is sediment availability (from the main flow) and a calm environment (separation zone), allowing deposition in the form of scroll bars. Secondary flow in the swale aides continued deposition of (suspended) sediment on the bar (figure 3.12; Nanson and Hickin, 1983).

Figure 3.12: The separation of flow in a river bend (Nanson, 1980).

Transformation of bar type

Sundborg (1956) found that transverse bars, that lie (perpendicular) across the channel, migrate downstream but there is also a component towards the inner bend. This is caused by faster migration near the thalweg. Bed load migrates in the form of transverse bars predominantly downstream but there is also a component towards the convex bank. A longitudinal (scroll) bar forms from a transverse bar, starting at the bend axis.

Bar development as result of sedimentary characteristics or vegetation
Pioneer vegetation can catch in sediment, initiating the formation of a (scroll) bar (Sundborg, 1956). Flow is diverted around vegetation and sedimentation can occur in calm water behind the vegetation where flow expands. Vegetation succession consequently stabilizes the underground enabling the area of sedimentation to expand and the development of a bar.

Nanson and Hickin (1983) mention sediment characteristics as a factor in scroll bar development. Water velocities vary from high near the thalweg, to low near the convex bank. Corresponding to this range of velocities are grain sizes that settle at certain points along the velocity gradient. Bi-modal sediment will be deposited in two separate clusters along the velocity gradient, that can initiate bar the formation in longitudinal direction.

3.5.3 Counter pointbar development

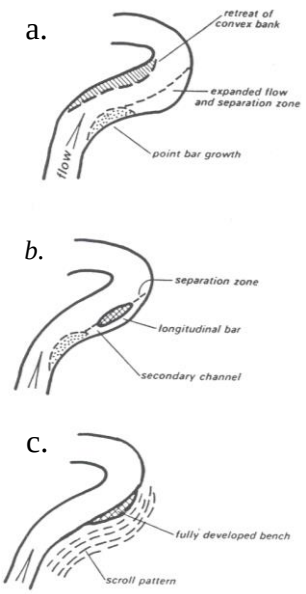

Under certain conditions counter pointbars can develop along the outer bank of a meander. They are associated with tight meanders, bend radius less than 2.5, (Thorne, 1992) and cohesive banks (Andrle, 1994). Rapid downstream migration is also important an important factor (Nanson and Page 1983). Wolfert (2002) describes the development of concave pointbars as an extreme inversion of scroll bar form to concave (Wolfert, 2002).

Flow is directed to the upstream part of a sharp inner bend, causing erosion (figure 3.13 a). Flow expands behind the upstream pointbar, and in some cases a counter current develops (Andrle, 1994) leading to sedimentation (longitudinal bar figure 3.13 b). Continued sedimentation extends the longitudinal bar towards the bank, often leaving a secondary channel along the margin (Nanson and Page, 1983).

Figure 3.13: Counter pointbar (bench) development (Nanson and Page, 1983).

4. Methods

Data and observations were acquired during research and fieldwork for three main purposes:

1. to *describe* morphology and how it changes in space and time,
2. to *correlate* changes in morphology to factors that are expected to influence these changes and
3. to *analyse* morphology, getting insight into the conditions and processes that led to its formation.

The basis of this research was formed by a series of aerial photographs made in the period 1954 - 2002 (4.1). These photographs gave a planar view of meanders and how they developed in time. Bend radii were determined (4.1.1) and the location, direction and amounts of channel migration were quantified (4.1.2). Measurements were used for *description* and *correlation*. On a smaller scale the characteristics and development of morphological units (bars and channels) and other elements along the river channel (vegetation and man-made structures) were *described* and used for *analyses* (4.1.3). Levelling and dGPS equipment was used to determine the elevation and (basic) planar form of morphological entities (4.2) in the period 1995 - 2003. These measurements added more detail, on a smaller time and spatial scale, to the *description* of riverbed and floodplain morphology. Additional field observations (4.3) such as tree age, relative sediment size and sedimentary structures completed the *description* of morphological units together with sketches and photographs. The *analyses* of these field observations and (small scale) aerial photography revealed conditions during the development of the morphology, including the presence of vegetation, flow velocity and flow direction and more. At a larger scale, discharge data (4.4) and bend radii were *correlated* to changes in pointbar dimensions to determine their influence on this process.

4.1 Aerial photographs

Aerial photographs, made in the period 1954 - 2002, were acquired from the *Institute Geographique National*. The photo intervals are generally less than eight years (this is exceeded once at Chemilly - Château de Lis). The scale of the photo's varies from approximately 1:50,000 to about 17,000 (with the top of the photo's directed to the north).The aerial photographs were scanned and subsequently georeferenced with the aid of ground control points (predominantly road crossings) from a 1:25,000 map. The resulting geometrically corrected images have an error of less than 10 meters, determined using the location of trees that are recognizable on multiple images.

4.1.1 Determining bend radius

The planform morphology of a meander (size and shape) can be described by one or multiple circles. Circles have been fit over aerial photos to determine bend radii (figure 4.1). The outer bank was principally used to determine bend radius. This lies closest to the thalweg, the center of flow that guides erosion and deposition. The radius of a circle was determined near the point of maximum curvature at the bend axis. To determine the relative bend radius (3.3.2), the width of the river was determined at the points of inflexion between bends, where the river margins are usually well defined.

Determining the curvature from aerial photo's was done manually in ArcView GIS. A circle was made progressively smaller until it fit and the bend radius could be determined. Using this method, the circle covers the greatest part of the bend when it fits.

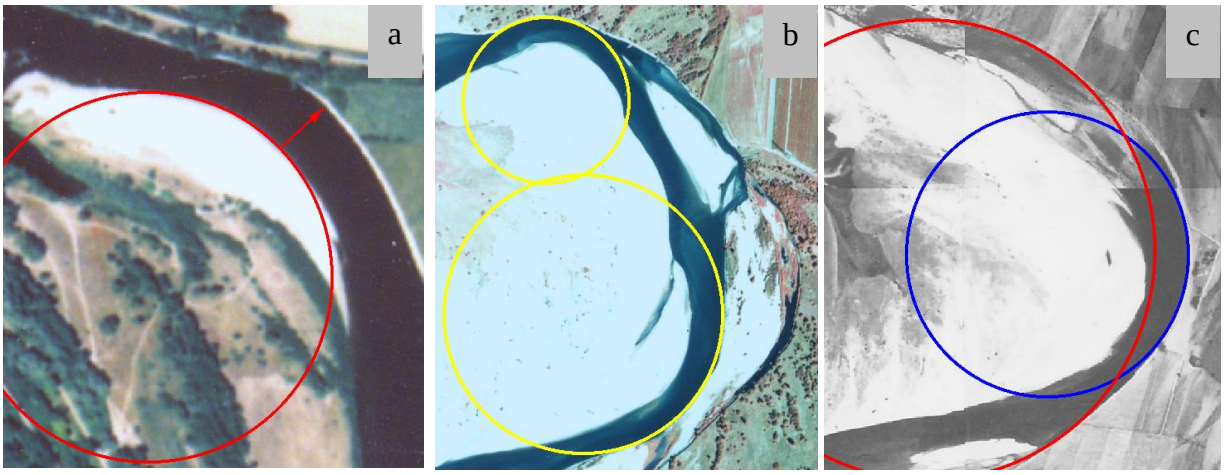

Figure 4.1: Determining bend radii; a. bend with kink where the inner bend radius is determined to which the width of the channel is added. b. compound bend represented by two circles. c. bend with a radius for maximum (blue) and overall (red) curvature.(aerial photographs a: St. Loup 2002, b,c: Château de Lis 1997, 1960)

River bends are ideally represented by a circle, but in practice this was most often not the case. The more accurate a circle fit, the smaller it became, describing only a small part of the bend. Overall circles were fit along the outer bend, as far as possible in up- and downstream direction until bend curvature decreased or changed direction (figure 4.1 c). In many cases circles additional to one at the maximum curvature, were used to describe compound bends (b). When a kink lies within a bend (due to a dike or resistant bank), the inner bend radius was used to determine the bend radius (a). The river width was added to the inner bend radius to allow the comparison of these bends with "normal" meander forms.

4.1.2 Channel migration: downstream and lateral sedimentation/erosion.

Extents of erosion and sedimentation

The change in the riverbed location through time was quantified through lateral and downstream sedimentation and erosion, determined from aerial photographs. Distances (m) were measured to quantify changes in the location of pointbar (sedimentation) and channel (erosion). The distances were measured in two dimensions, parallel to channel flow direction (downstream) and perpendicular (lateral) and averaged to annual values.

In a meandering river downstream and lateral direction change continuously due to channel migration. The downstream axis was determined by drawing a line between the beginning and end of the active (not fully vegetated) point bar. The downstream end was defined as the tip of the point bar or the end of the first mature scroll bar. The upstream end of the pointbar was found at an upstream extension or where the curvature of the bend changed near the riffle. To measure the lateral change between two situations, first the maximum lateral extent of the pointbar in both cases was determined (figure 4.2). This was measured from a line that represents the average downstream direction of the two situations. The lateral change (sedimentation or erosion) of a pointbar was determined by subtracting the maximum lateral extent of the final from the initial situation. The location of the maximum lateral extent usually changed in time, such as in figure 4.2 where it moved downstream. The lateral change is therefore a measure of change in the overall form of the pointbar. There were locations where sedimentation and erosion took place at higher rates. The same procedure was used to determine the downstream direction, measured from a line that lies in the lateral direction.

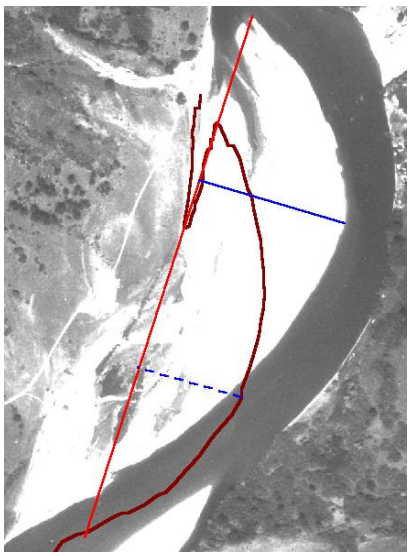

Figure 4.2: Determining lateral change (sedimentation or erosion). Two situations are visible: the brown contour line marks the initial outline of the pointbar, while the pointbar on the aerial photo marks the final situation. The average downstream direction of the two situations is marked by the red line and perpendicular to it lie the measured lateral extents in blue. The dotted line is the initial lateral extent while the final lateral extent is marked in a solid blue line. (aerial photograph: Châtel de Neuvre, 1968)

Lateral erosion was measured as the distance between waterlines from two situations (different years) where they lie furthest apart (figure 4.3). This distance was taken perpendicular to the tangent of the bend or the flow direction (an average of the two situations). Downstream erosion was determined by the downstream limit of erosion that is sometimes visible as a protuberance. The direct distance between two of these points from different years was taken.

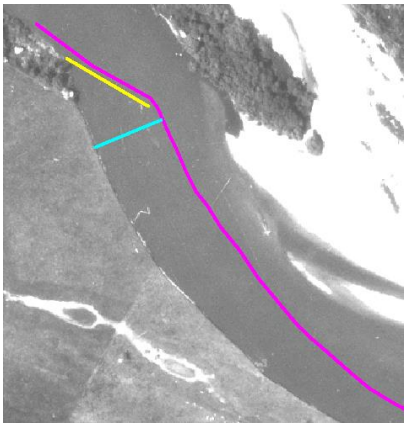

Figure 4.3: Determining outer bend erosion. Two situations are visible: the purple contour line marks the initial outer bend, while the channel edge on the aerial photo marks the final situation. (Lateral) erosion is the greatest distance between the outer bend waterlines perpendicular to the waterlines (light blue). Downstream erosion is the distance along the initial waterline that a protuberance has moved (yellow). Note that lateral and downstream erosion directions are not perpendicular. (aerial photograph: Beauregard, 1980)

Apart from steady and continuous pointbar growth, some complications were encountered when measuring sedimentation and erosion. Between two situations the downstream tip of a pointbar became stable and vegetated, while sedimentation continued laterally, slightly further upstream along the pointbar. The growth before stabilization was taken into account and not just the absolute change between the initial and final situation. Islands that formed in the channel alongside the pointbar that have a form that suggests lateral sedimentation (convex) were also included in sedimentation amounts. The extent of the pointbar was measured with a fluctuating waterline as margin. Although the aerial photographs were made during summer low waters, amounts of lateral sedimentation amounts from 1992 onwards were corrected to an average waterlevel using an average pointbar gradient of 0.033. For the correlation with discharge, the values of (lateral and downstream) sedimentation and erosion were corrected for bend radius. The observed values were divided by expected values, based on bend radius, to exclude its influence when correlating with discharge. This results in dimensionless parameters for meander migration. The relation between sedimentation and erosion and bend radius was similarly corrected for the number of days with high discharge (above 550 m^3/s).

Areas of erosion and accretion

Areas of outer bend (floodplain) erosion and the centers of these areas (centroid) were calculated using ArcMap GIS. These values were determined for Châtel de Neuvre (all years, excluding the cutoff in the early 1990's) and for Chemilly and Beauregard (second half of the bend) in the 1990's. The measurements represent amounts of erosion amounts (bank height is constant) and where it was concentrated. The downstream movement of the focus of erosion was determined as an angle about the bend axis (figure 4.4). The angle was measured between the center of an eroded area and the initial location of the bend apex.

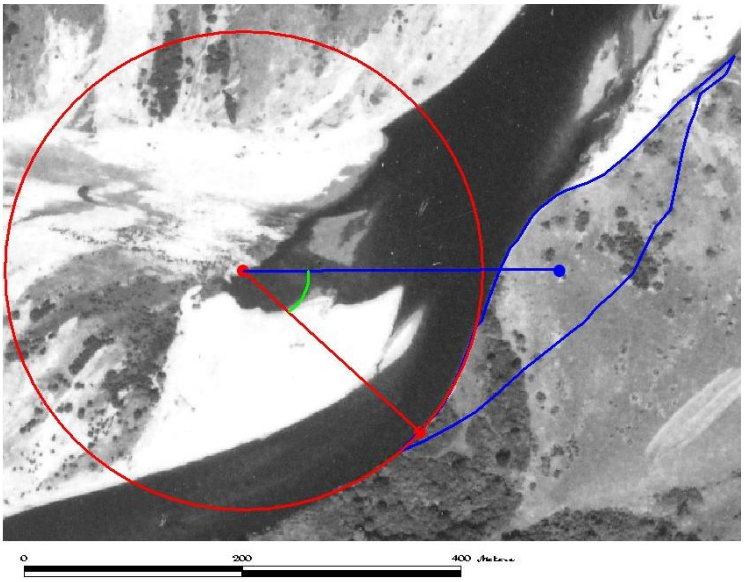

Figure 4.4: The rotation of concentrated erosion around the bend axis. The red dot on the circle markes the bend axis (maximum curvature), while the blue dot lies in the center (centroid) of the eroded area. Note that only erosion of the overbank is taken and not sediment in the channel.

Areas were also determined of accreted units that were added to a pointbar laterally or in downstream direction. Pointbars that migrated as a whole or changed form were not included in calculations because erosion affected the planar development of the pointbar. Measurements were taken mostly over short periods in the 1990's, when the form of the pointbar remained stable (no erosion), while sedimentation units in the form of bars were added. Examples of longer periods with solely pointbar expansion were found at St.Loup (1968-1975, 1985-1993) and Chemilly (1954-1960).

4.1.3 Morphological description

The analyses of aerial photographs was done on the basis of morphological units, including vegetation and man-made structures, that are guiding factors in and the result of river processes. Morphological units were recognizable and described on aerial photographs through their form/orientation, location and colour/texture. The description of a morphological form included its dimensions (width and length) and characteristics such as curvature (of a bar for instance), orientation (whether a dike lies parallel or perpendicular to the main flow direction) and continuity (the extent to which a riffle is interrupted by channels or a kink in a bank that reveals a resistant section). The form of a morphological unit is also determined by its perimeter and its absolute and relative location in the overall structure of a river. Observations with respect to location included how bars were spaced and if intermittent swales were present, the distance between (strokes of) trees and the riverbed and (counterpoint)bar development alongside dikes. The darkness of colours on aerial photographs showed relative water depths and sediment moisture conditions, where dark shades were associated with water (abundance). The combination of colour with texture allowed the distinction vegetation types, through the recognition of tree crowns and lighter coloured undergrowth with no texture.

4.2 Levelling, GPS and dGPS

Levelling and dGPS measurements were made between 1995 and 2003 to determine the location, form and elevation of morphological entities. The location and dimensions of bars and channels were precisely determined, but also the location of the banks in years when aerial photographs were unavailable. Elevation measurements added an extra dimension to morphology from which height/depth and (pointbar) gradient were derived.

Levelling profiles, made in 2003 for this research, were compared to earlier profiles made by Wilbers and de Kramer in 1995, 1996 and 2002. For each bend an average of seven profiles were levelled approximately perpendicular to the channel. The location of the profiles is shown in a recent aerial photo of every bend (figures 6.9, 7.10, 8.11, 9.11, 10.11). The leveling profiles are shown in cross sections with a downstream view direction and a low waterline.

With a GPS the location of the levelling apparatus was recorded. This was used as control for levelling measurements taken from a fixed point (nail in tree). GPS measurements were also used to make contours of the (slightly variable) waterline bordering the pointbar, to determine changes in pointbar form. The locations of field observations (4.3) were also recorded using a GPS. dGPS measurements were made for the Chemilly – Château de Lis area by TU Delft. Measured profiles covered the whole pointbar, with the emphasis on areas with high relief and actively changing areas.

Levelling inaccuracies were mainly found in the x y plane. The reading of the levelling rod was done with an accuracy of within a centimetre (height), that leads to an error in the measured distance of one meter. In an x y plane, angles had to be measured using a compass, which made inaccuracies of about two degrees (scale on compass) possible. GPS measurements have a greater inaccuracy than levelling. The GPS averages values the unit receives, calculating an error which amounted to about 4 meters. There is however also an absolute error caused by the transmission of the signal between the satellite and GPS. The advantage of GPS measurements is that the accuracy is constant while with levelling errors can accumulate when moving the levelling apparatus. dGPS measurements have an accuracy within 2 cm in height and location.

4.3 Field observations

Field observations and descriptions were made to analyse morphology and understand the processes behind them. These were often recorded on photographs or in sketches. High water flow directions were deduced from: the orientation of morphologic features (troughs, scroll bars, chute bars etc), sediment plumes that lie behind obstacles (usually vegetation), vegetational debris that is “stuck” at the upstream side of tree trunks and the imbrication of sediment (pebbles). An indication of water depth and flow velocity at a certain location was given by the sediment size and the presence or absence of young vegetation. Profile pits gave a sequence of development through layers of sediment, with varying sediment size and structures, that characterize flow conditions that were present. The age of trees on the pointbar was determined with the aid of a drill that retrieved a core on which age rings can be counted. Tree age gives an indication of the conditions (stable underground, enough moisture, little sedimentation etc) that were needed for the development of the tree.

4.4 Discharge

Discharge was used in this research to determine its influence on meander migration (erosion and sedimentation). Stage and discharge, with a few exceptions, were measured or averaged on a daily basis. This data was available from stations at Moulins and Châtel de Neuvre and from the *Division Hydrométrie et Données Diren Centre Service de Bassin Loire-Bretagne*. Here the cross section of the riverbed remains constant in time and water levels were correlated to discharge.

5. Allier discharge

Figure 5.1 shows a direct relationship between waterlevel and discharge at Moulins and the polynomial function that best describes the relationship (equation 8). Additional (sub-) relationships can be distinguished above and below the regression line, especially prominent near the higher discharges with long recurrence intervals (marked in red; figure 5.1). The stage-discharge relationship has been revised in the period of 32 years.

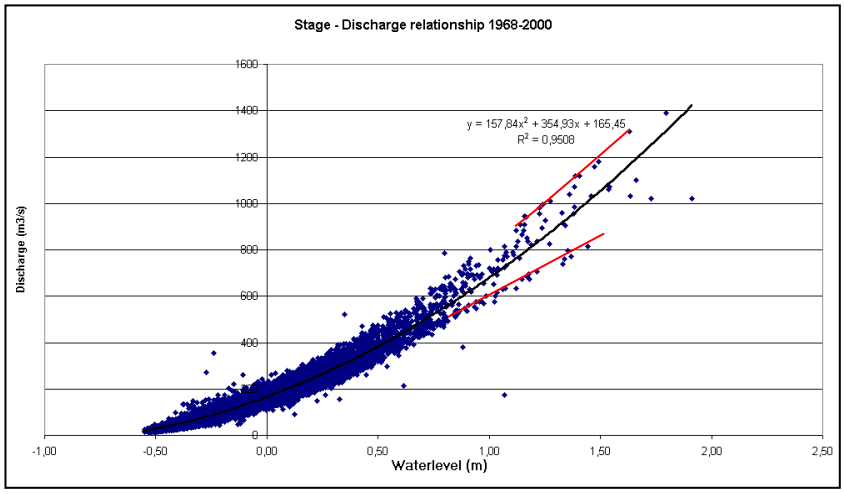

Figure 5.1: Stage discharge relationship and regression (including two additional sub-relationships marked in red). Discharge is placed as unknown variable (y) that is determined by the known waterlevel (x), even though waterlevel is dependent on discharge. The waterlevels were measured at Moulins.

$$Q = 157.84h^2 + 354.93h + 165.45 \quad [8]$$

A flow duration curve was constructed to determine the distribution of waterlevels in time at Moulins (figure 5.2). The occurrence frequency of waterlevels above zero show a constant exponential decrease with increasing waterlevel (straight gradient with logarithmic scale). Waterlevels higher than 1.3 meters show a relative decrease in frequency. This is caused by an increasing flow width which makes increases in waterlevel relatively smaller. The relative large increase in flow width is related to the cross sectional form of the river and marks the waterlevel or discharge at which the channel is filled and water enters the floodplain.

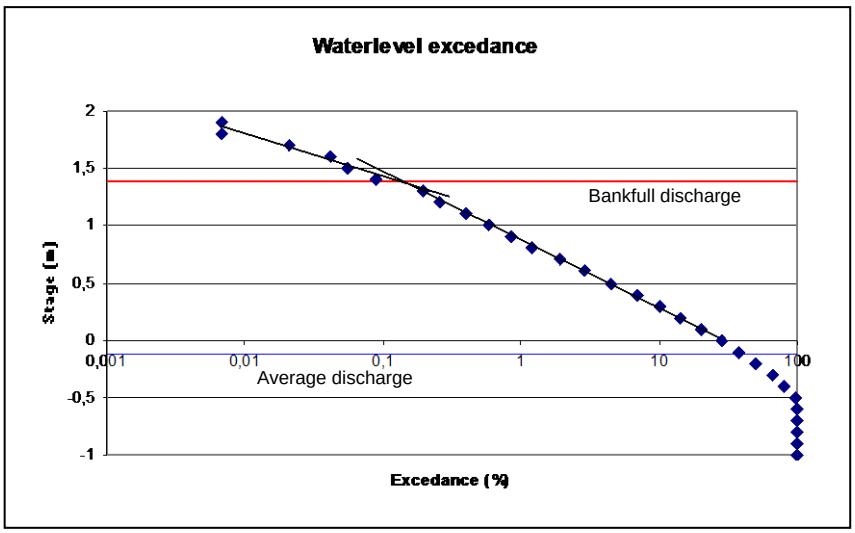

Figure 5.2:Waterheight excedance on a daily basis between 1960 and 1989, Moulins.

Like various other authors De Kramer (1998) assumed that meander migration in the Allier takes place with high discharges. He found that bend radius correlated best with meander migration velocity (erosion) using waterlevels higher than 0.8 m (this was only slightly better than with lower waterlevels). These waterlevels, just below the edge of the channel,

correspond to discharges that cause the greatest morphological changes (3.3.2). In the Allier, however, annual meander migration, indicates that the threshold for erosion is not very high.

Three values have been chosen to describe discharge, representing different time-scales. They are: average discharge, significant discharge (days with waterlevel exceeding 550 m^3/s) and maximum discharge. Average discharge is a long term index, using the whole range of measured discharges. The significant discharge represents a short time scale ranging from more than a week to a couple of days, to no days at all. The maximum discharge of a year is measured on a single day that represents that year. Where the time scales of discharge and erosion / sedimentation match (single day, a few days or years), the best correlation is expected. This gives information about the (discharge) conditions under which meander migration takes place.

6. Meander and pointbar development case 1: St. Loup

6.1 Meander development 1960 - 1993

1960

In 1960 the pointbar of St. Loup showed two phases of lateral scroll bar development (figure 6.1; 1,2). At the downstream end of the pointbar two extending scroll bars were present (1). The inner bar (left) was slightly larger due to sediment deposition at the end of a chute channel, that was positioned along a stroke of vegetation. Near the pointbar axis younger scroll bars were present (2), where the youngest one (island) was also part of the upstream riffle (blue). Bar morphology was therefore influenced by lateral sedimentation and erosive crossing channels. Older phases of scroll bar development were depicted by swales that contained water and vegetation (3).

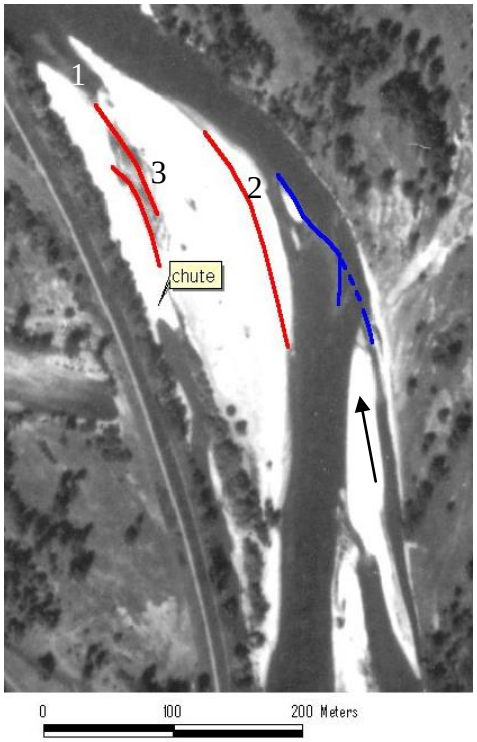

*Figure 6.1: **1960** aerial photo; underwater bar margin in blue, scroll bar contours in red.*

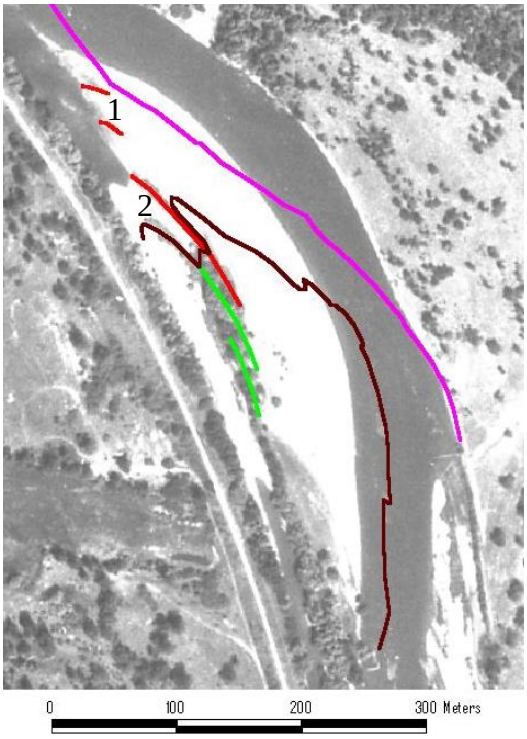

*Figure 6.2: **1968** aerial photo; scroll patterns in red; bars from 1960 in green, the 1960 inner bank in brown and the outer bank in purple.*

1968

In the period between 1960 and 1968 outer bank erosion in downstream direction allowed downstream pointbar expansion (figure 6.2). At the downstream end of the pointbar the shoreline advanced onto the pointbar through swales (1) that occurred downstream from each other (in 1960 swales occurred laterally next to each other, figure 6.1). The swales separate about 20 meter wide scroll bars. Vegetation in swales, already seen in 1960 (figure 6.1 (3)), continued its development downstream, along the edges of the two scroll bars seen in the 1960 shoreline (figure 6.2 (2)).

1975

Between 1968 and 1975 the pointbar grew downstream while barely being eroded at the upstream end (figure 6.3). Three major scroll bars were present at the downstream end of the pointbar. The oldest two were about 20 meters wide (1,2), while the youngest (3) was slightly

wider, showing a new phase of accretion. Vegetation developed along the inner shoreline from 1968 (4), distinguishing scroll bars of about 25,10, and 20 meters wide (old to young).

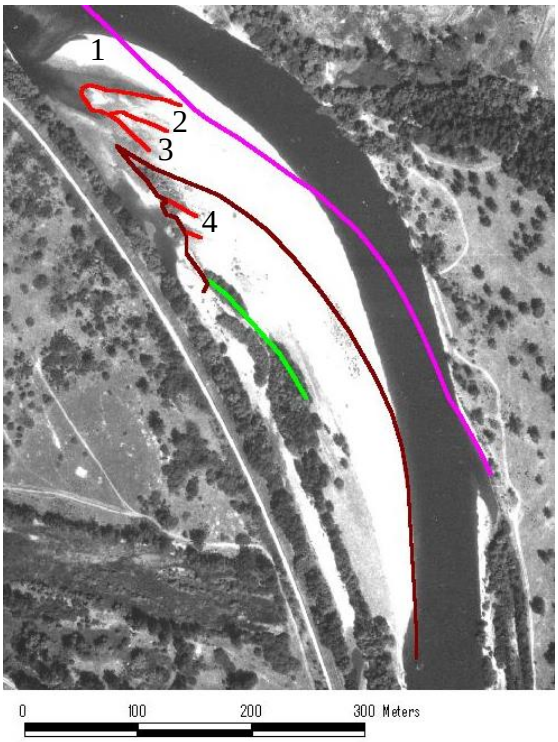

*Figure 6.3: **1975** aerial photo; scroll patterns in red and from 1968 in green; the 1968 inner bank in brown and the outer bank in purple.*

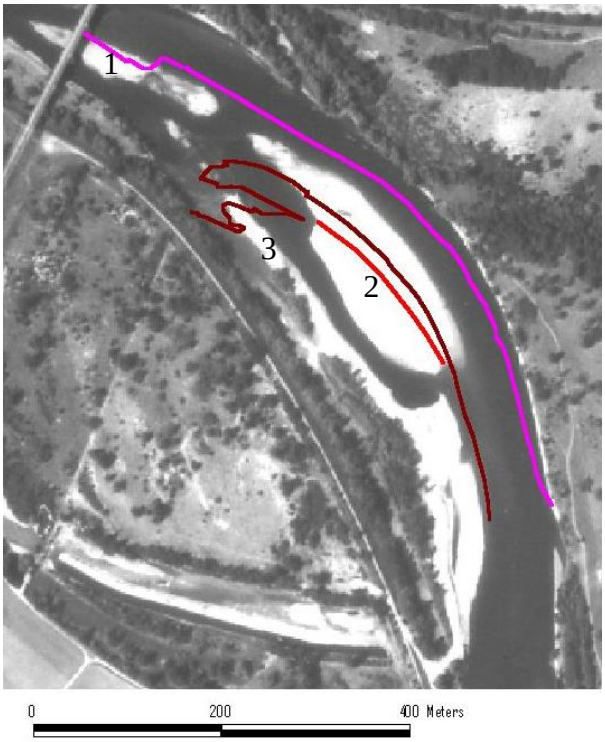

*Figure 6.4: **1980** aerial photo; scroll patterns in red; the 1975 inner bank in brown and the outer bank in purple.*

1980

In 1980 high water levels partially covered the pointbar that predominantly expanded in downstream direction (figure 6.4). Two islands made up a large part of the pointbar (1,2). The downstream island (1) had a width of about 25 meters, while the upstream island (2) included a swale whose extension was already visible in 1975 (figure 6.3 between bars 1 and 2). The inner strip of the point bar (3) was about 18 meters wide and coincided with the scroll bars 2 and 3 from 1975 (figure 6.3). The high water distinguishes relief on the pointbar (scroll bars) through partial flooding (of swales).

1985

Between 1980 and 1985 the pointbar merged to a single body and flow became concentrated in the outer part of the bend (figure 6.5). Lateral development occurred at the upstream end where a scroll bar of nearly 20 meters wide was recognised (1). In the downstream extension of the pointbar a riffle was present. The downstream island, that developed behind a bridge pillar, and the end of the pointbar, were about 20 meters wide (2). Moving upstream the pointbar width doubled to just over 40 meters and remained fairly constant (3).

1993

Lateral erosion occurred in the upstream half of the bend between 1985 and 1993, accompanied by lateral sedimentation (figure 6.6; 1) that started in 1985 (figure 6.5; 1). In the area of lateral sedimentation, two scroll bars could be recognized, between 15 and 20 meters wide (1). Strong lateral migration also enabled the development of swales, found as a wide stroke of vegetation (2) and two stagnant pools, 25 meters apart (3).

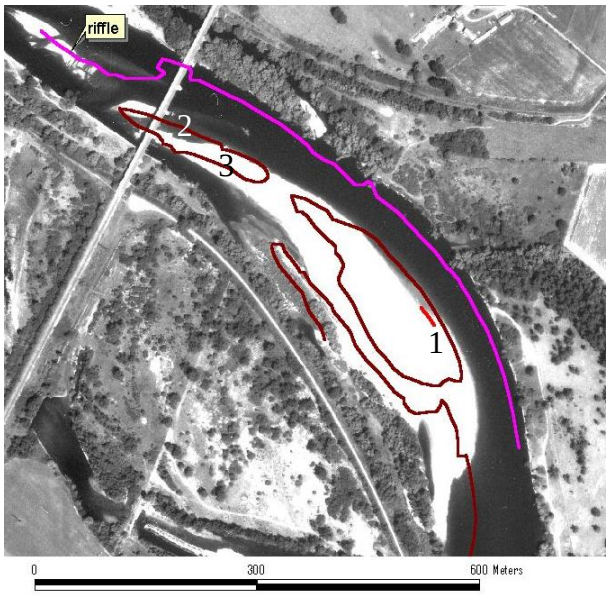

*Figure 6.5: **1985** aerial photo; scroll patterns in red; the 1980 inner bank in brown and the outer bank in purple.*

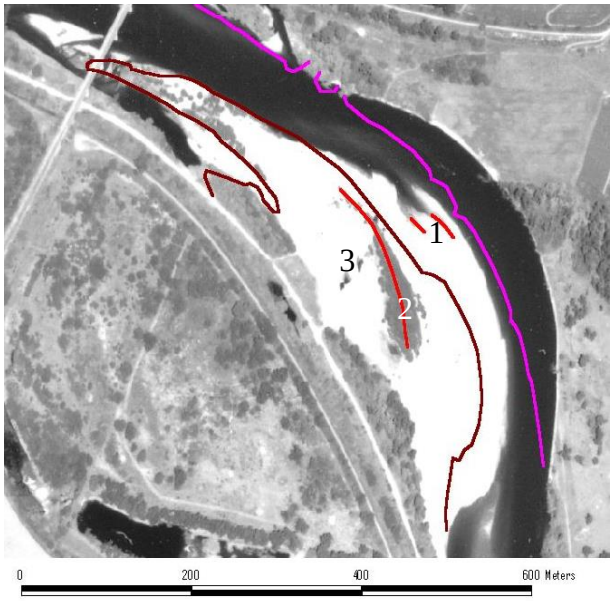

*Figure 6.6: **1993** aerial photo; scroll patterns in red; the 1985 inner bank in brown and the outer bank in purple.*

6.2 Meander development 1993-2003

6.2.1 Outer bend erosion

Between 1993 and 1995 the outer bend eroded up to 70 meters along the downstream half of the bend (figure 6.7). Erosion was less in the period 1995-1996, during which the bend moved outwards only 15 meters.

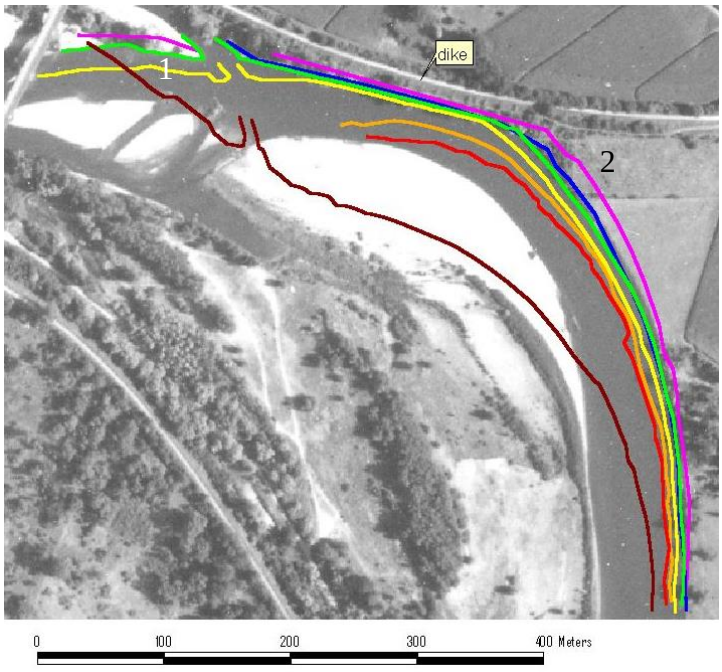

Figure 6.7: 2000 aerial photo with the outer bank marked from: 1993 (brown), 1995 (red), 1996 (orange), 1998 (yellow), 2000 (green), 2002 (blue), 2003 (purple).

After the channel came into contact with the dike, between 1996 and 1998, flow became concentrated along the dike, causing maximum erosion where the river turned away from the dike. Between 1998 and 2000, erosion downstream of an old channel (1) reached 20 meters, but became less in later years. Erosion also took place at the upstream end of the dike (2). Annual erosion amounted to about 5 meters with the exception of the period 2002-2003, where maximum erosion was nearly 15 meters. Erosion at the upstream end of the dike (2) was larger than further upstream, causing this stretch of river to straighten in north-south direction oblique to the dike. Helicoidal flow and lateral erosion decreased throughout time.

6.2.2 Pointbar sedimentation

The location of low-water shorelines along the pointbar, in the period 1993-2003, are shown in figure 6.8. Cross sectional profiles across the pointbar and riverbed and their locations are

shown in figure 6.9. The development of the pointbar and scroll bars, between 1995 and 2003, was also registered by a photo series made by J. de Kramer (figures 6.10a,b).

Upstream pointbar development
The upstream half of the pointbar was fairly inactive and covered with vegetation. It was in a advanced state of development. Sedimentation and morphological changes on the pointbar are small, apart from some chute splays at the upstream tip (figure 6.9).

Cross section 1 shows a riffle in the riverbed, at the upstream end of the pointbar (figure 6.9). The thalweg lies on the inside of the bend (left bank), while near the outside another channel was developing. On the pointbar lie various steep levees (x = -65; more were visible in the field) along chute channels that emerge from the vegetated pointbar and enter the main channel just downstream from the cross section.

Cross section 2 (figure 6.9) shows the whole pointbar and riverbed, that changed little through time, apart from modest lateral sedimentation on the left bank of the channel. The channel profile changed from asymmetric in 1995 (outer bend) to symmetric, with a bar that became symmetric in time (2003; riffle). The curvature of the upstream part of the bend decreased because of the downstream progression of the maximum curvature and the influence of the dike on flow (see section 6.3.1). The decrease in curvature and weakening helicoidal flow caused the change in channel profile from asymmetric to symmetric.

Cross section 3 lies near the beginning of the actively accreting pointbar (figure 6.9). The profile from 2003 shows an asymmetric profile, while in 2002 a knick point was found near a distance of -15. In 2002 helicoidal circulation had not yet fully developed, otherwise the knick point would have been removed. In 2003 there was a convex pointbar profile with two vague plateaus (x = -50 and -80) that show the first signs of scroll bar development.

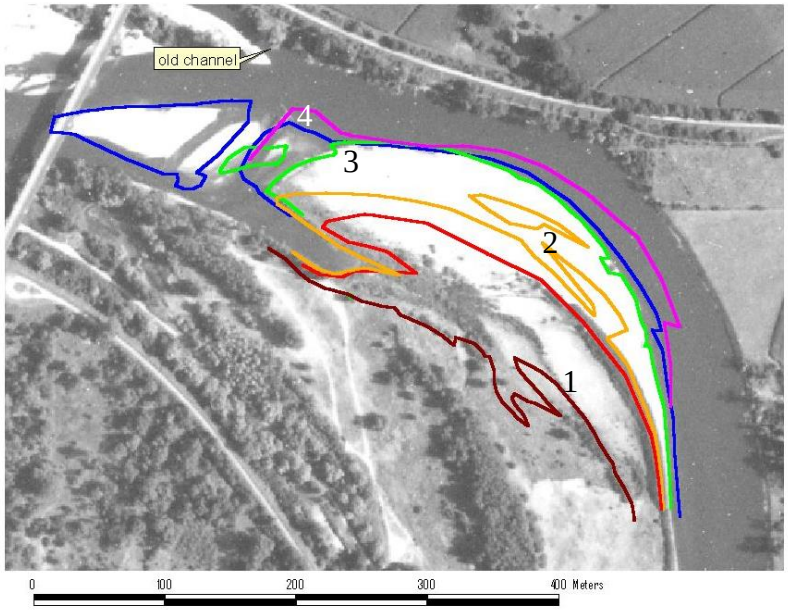

*Figure 6.8: **2000** aerial photograph with added inner bend shorelines from: 1993 (brown), 1995 (red), 1996 (orange), 1998 (green), 2002 (blue), 2003 (purple).*

Scroll bar development
Different phases of downstream and lateral pointbar expansion occurred through the development of scrollbars (figure 6.8). In the period 1993-1994 the youngest phase of scroll bar development (1) migrated downstream, until its form was delineated by a stroke of trees (figure 6.8). Between 1995 and 1996 lateral scroll bars developed, 10-15 meters wide in the form of an island and peninsula (2). These distinct bars and (submerged) swales developed because of an increase in space, created by strong lateral erosion between 1993 and 1995 (6.2.1).

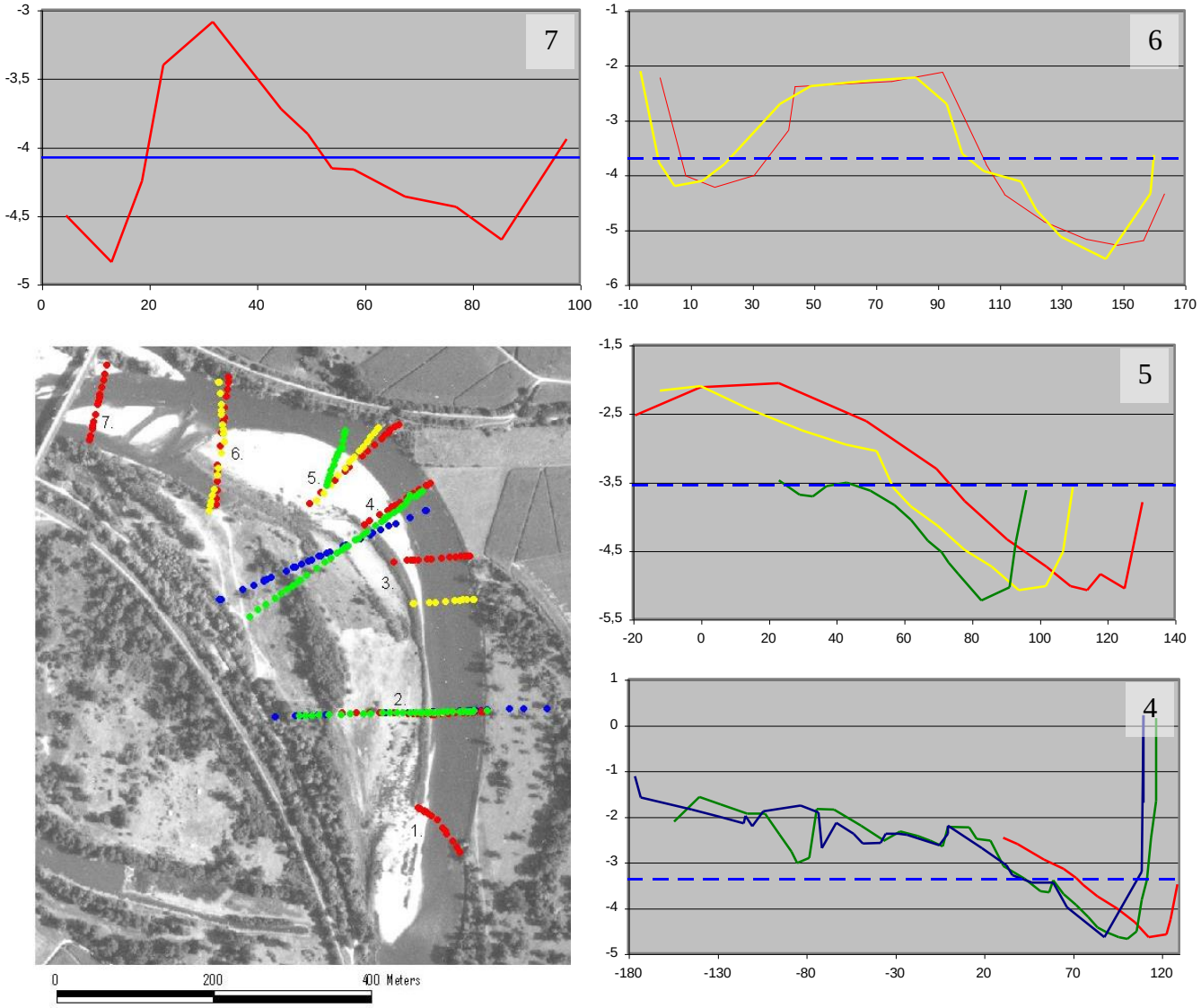

Figure 6.9. The location of profiles from 1995 (blue), 1996 (green), 2002 (yellow) and 2003 (red) with the aerial photo from 2002 on the background. The numbered profiles are displayed around the location map. On the x and y axis are height and distance, both in meters. Heights are related to a fixed point (nail in tree). Distances are related to a zero point where the profiles are closest together or in the case of profile 3 the outer bend was taken as zero point.

Scroll bars are separated by swales, that lie parallel to the shoreline and hold pioneer vegetation (1995, 1996, 1997; figure 6.10a). Between 1996 and 1997, the pointbar developed predominantly laterally (figure 6.10b), until the outer bank was fixed by revetments.

Cross section 4 (figure 6.9) shows the peninsula (x = 60) seen in figure 6.8 (2). The bar developed near the point of maximum erosion, starting out as a level platform in 1995 and becoming steeper and more pronounced the following year, attaining a height of about 25 cm. Two older scroll bars (x = -35 and 0), had heights of 20 and 40 cm and became more symmetric in time. Relief further onto the pointbar was formed by high waters that were directed by (strokes of) vegetation. In the period 1996 – 2003, the cross-sectional slope of the pointbar surface increased from 0.024 to 0.027.

Cross section 5 shows the morphological development of the riverbed near the 1996 apex and in later years near the transition of erodable outerbank to revetments (figure 6.9). The 1996 scroll bar (x = 40) corresponds to the 20 meter wide island from figure 6.8 (2). Note how the relief of the scroll bars from 1996, particularly the island, was visible in the shoreline from 1998 (figure 6.8). Just after the channel encountered outer bank revetments, a narrow scroll bar (less than 10 meters wide) still developed, visible in the 1998 shoreline (figure 6.8; 3). The bar presence in 1998 indicated that lateral sedimentation lagged behind erosion, which stopped earlier, in 1997 (figure 6.7).

Pointbar development opposite of a protected bank

After the outer bank became artificially fixed, lateral accretion along the inner bank decreased since 1998 and scroll bar development ceased (figure 6.8). Erosion along the revetment in up- and downstream direction created new room for sedimentation of the opposite bank. Sedimentation in downstream direction occurred, together with local minor lateral erosion (figure 6.10a).

In cross section 5, the channel asymmetry decreased in time (figure 6.9). The gradient of the pointbar increased from 0.031 to 0.034 in the period 1996-2003, and lost its convex profile. The channel started to slightly erode the inner bend, creating a knick point in the profile, visible in 2002 and (less clear) in 2003. This was a small and temporary change in morphology related to variations in discharge. In 2003 a bar was visible in the outer part of the channel that results from low flow velocities in the corner where eddy's can also form.

Cross section 6 shows an immature scroll bar in the 2002 main channel that was removed in 2003. The two channels are slightly eroded the island, making its edges steeper and concave (similar to cross-section 5, 2002). The revetments caused the thalweg to be redirected inwards and no energy was used detaching and transporting material from the outer bend. The channel was fairly symmetric, compared to cross-section 5 (2003), along the straight channel. The form of the bar was slightly asymmetric, with its highest part along the channel. Helicoidal flow was disturbed along the protected bank, limiting the inward transport of sediment and causing sedimentation to be concentrated near the channel.

At the end of the point bar a bulge developed opposite from an old channel in 2002 and 2003 (figure 6.9; 4). Flow in the channel decelerated because of an increased flow width near the end of the point bar and old channel, enabling local sedimentation along the inner bend. The pointbar was crossed by erosive channels at its downstream end (figure 6.8; figure 6.10a). The pointbar was expanding downstream, along the protected outer bank and channel next to it.

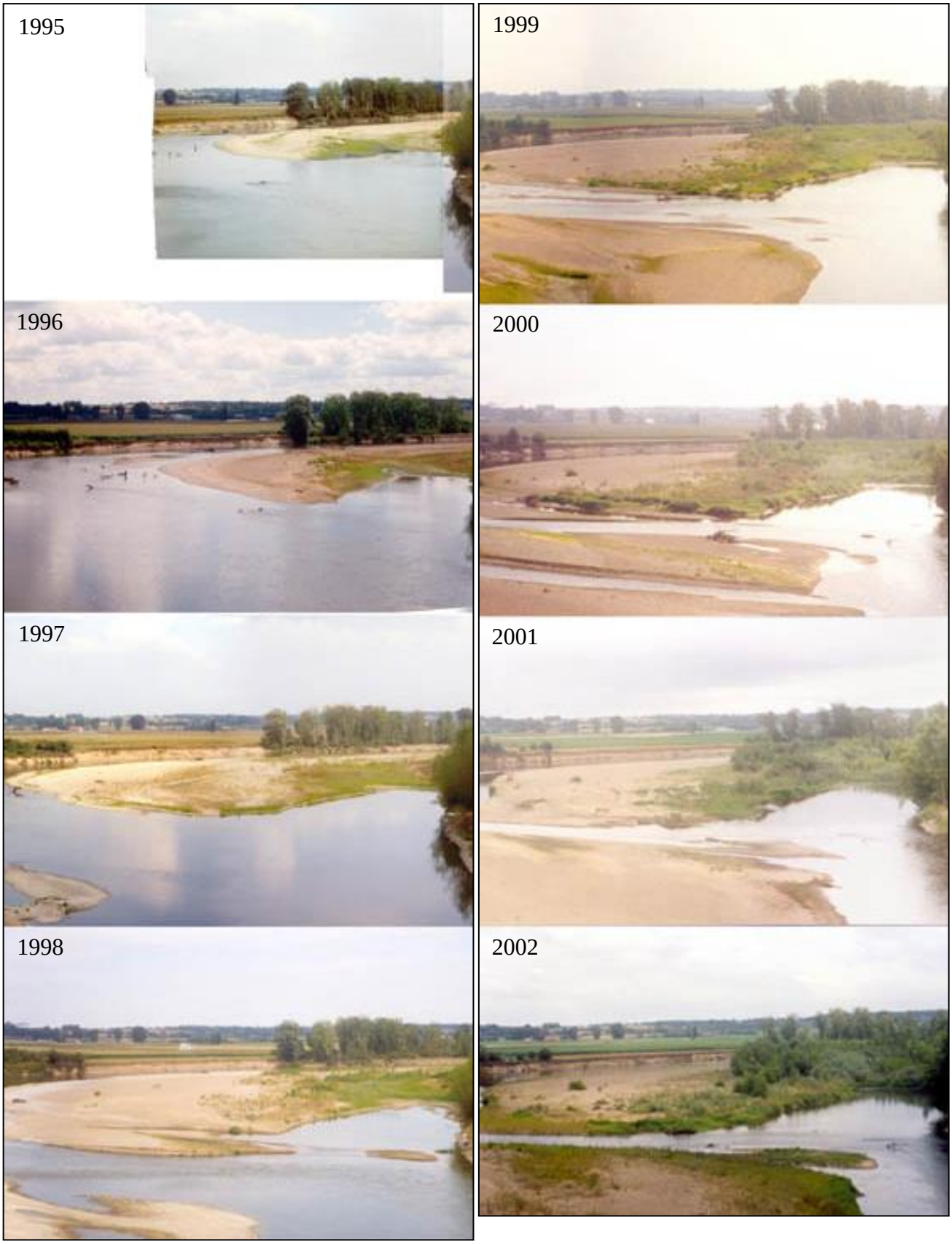

Figure 6.10a: Meander development between 1995 and 2002 at the St. Loup bend (photo's J. de Kramer). Picture taken from the bridge downstream of the pointbar in ESE direction.

Figure 6.10b: Meander overview St. Loup in 2003. Picture taken from the bridge downstream of the pointbar in ESE direction.

The swale, behind the point bar, held stationary water that had a waterlevel equal to that of the downstream riffle to which it was connected. Cross channels developed because the waterlevel gradient across the pointbar was greater than that between the outer bend and the downstream riffle. Vegetation played an important role in their stabilization, catching in sediment, and steepening of banks, limiting erosion to the edges (figure 6.10a,b).

In cross section 7 a bar, just visible beneath the shoreline (maximally 15 meters wide) was recently added to the downstream section of the pointbar. A similar bar was seen in figure 6.10b at the left bottom of the picture. The bar was slightly assymmetric (steep on the inside of the bend) caused by weak helicoidal flow that has developed in the last part of the bend.

6.3 Overall meander change

The bend radius at St. Loup increased since 1960, due to downstream meander migration (figure 6.11). Incoming and outgoing flow were forced in downstream direction by the resistant western bank (similar to Lagasse et al, 1995). From 1980 lateral development started to dominate, initiated by the development of vegetation on the pointbar, that forced flow outwards (figure 6.6). This caused a decrease in maximum bend radius, increasing the curvature over a shorter stretch of river. Since 1997 meander development was directed downstream (and a small extent upstream; figure 6.8, 6.11) by revetments on the northern bank. An angle developed in the outer bend were the revetments started and along the inner bank curvature increased.

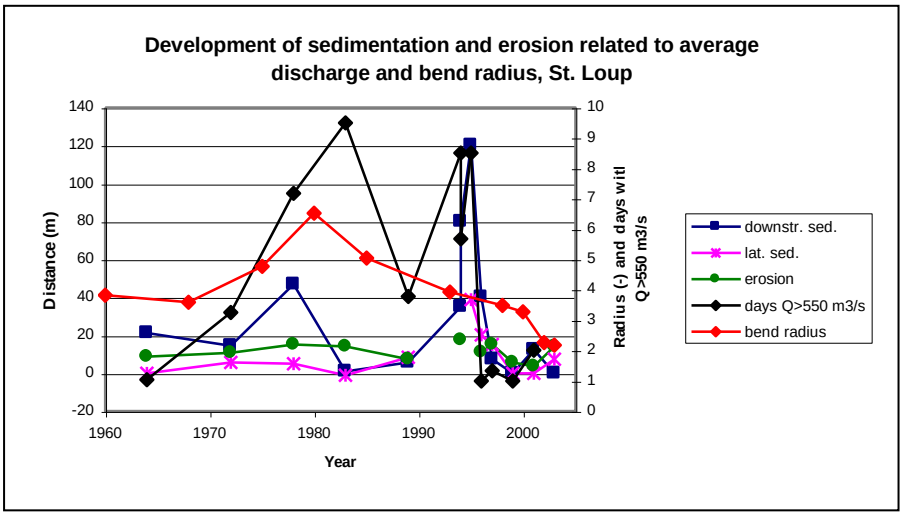

Figure 6.11: Annual pointbar development (sedimentation and erosion) and factors average discharge and bend radius in time.

7. Meander and pointbar development case 2: Châtel de Neuvre

7.1 Long term meander history

1960

The 1960 aerial photograph of the Châtel de Neuvre pointbar (figure 7.1) can be divided into two sectors (separated by orange lines). The upstream half of the pointbar was dominated by chute processes. Paths of concentrated sedimentation (1,2) crossed through vegetation (including strokes of trees formed during earlier lateral sedimentation). The downstream end of the pointbar was characterised by lateral sedimentation, containing an extending scroll bar complex separated from the surrounding land by a large swale (3).

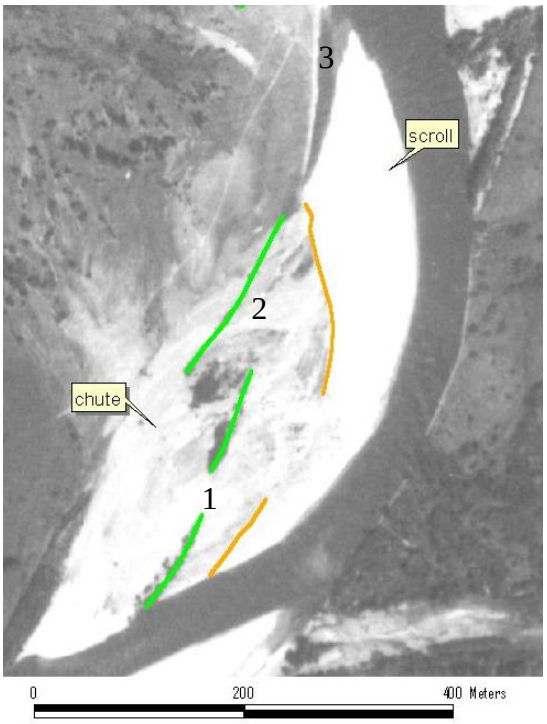

*Figure 7.1: **1960** aerial photo; old vegetated scroll contours in green, and the boundary between scroll and chute processes in orange.*

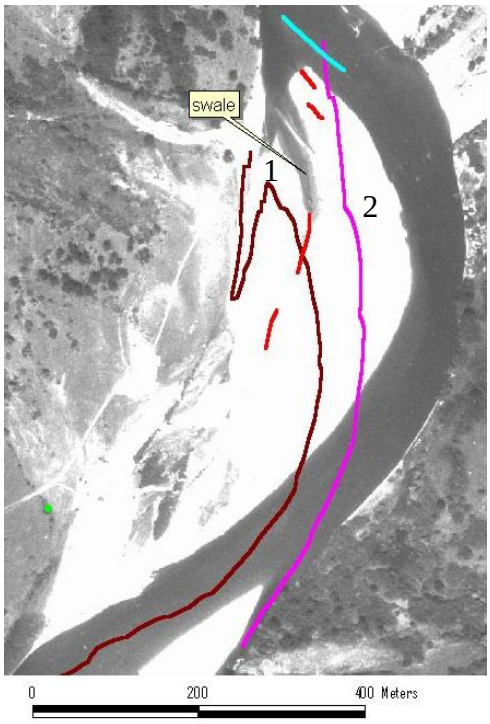

*Figure 7.2: **1968** aerial photo; scroll patterns in red, underwater bar in blue and from 1960: inner bank in brown and outer bank in purple.*

1968

Between 1960 and 1968 erosion expanded and developed the downstream part of the meander. The pointbar extended downstream (figure 7.2; 1) before an additional scrollbar complex was added laterally (2). The lateral complex also expanded downstream creating a large swale along its side. At the downstream end of the pointbar there were various bars (marked in red, 10 to 20 meters wide), including a sedimentation stroke under water (blue). A through extended onto the point bar, moving inwards and not following a path parallel to the 1960 shoreline. The path wasmore characteristic for a chute channel that crossed the pointbar.

1975

Between 1968 and 1975 the meander continued to expand in downstream direction, developing a complex nature (figure 7.3) characteristic for a rotational bend (figure 3.3). An additional (new) point bar developed at the upstream end of the lengthening “Châtel de Neuvre” bend. At the downstream end of the main pointbar scroll bar development progressively moved upstream (1 to 3) towards the bend apex. Bars 1 and 2 were about 30

meters wide, while bar 3 and the youngest bar were about 20 meters wide. The second bar connects with the riffle that crosses over to the beginning of the opposite pointbar.

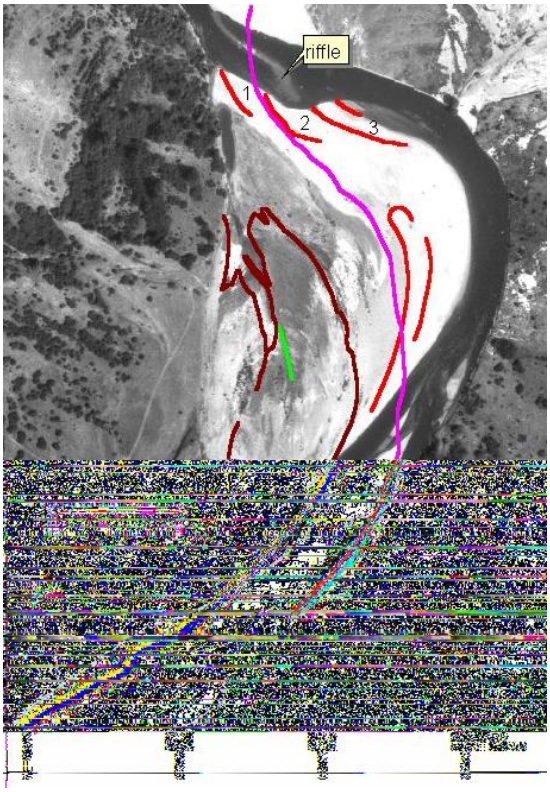

*Figure 7.3: **1975** aerial photo; scroll patterns in red, vegetation stroke in green and from 1968: inner bank in brown, outer bank in purple.*

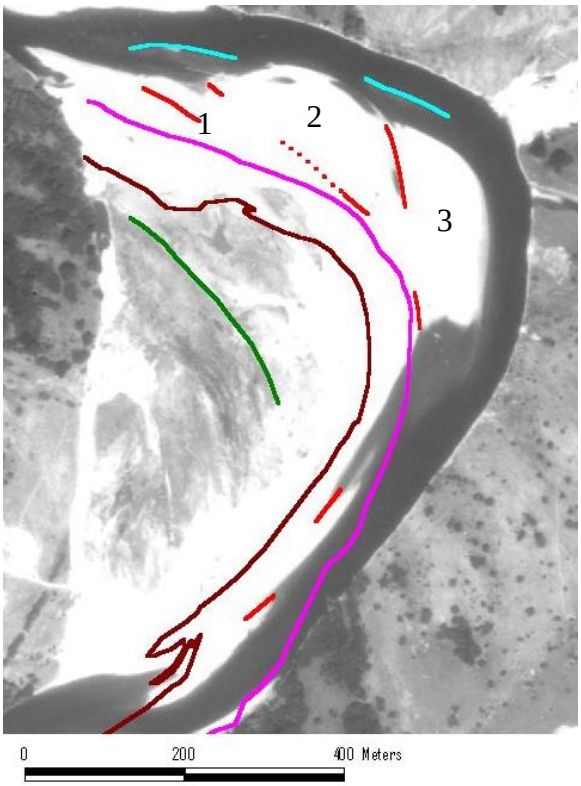

*Figure 7.4: **1980** aerial photo; scroll patterns in red, underwater bars in blue, vegetation stroke in green and from 1975: inner bank in brown, outer bank in purple.*

1980

While the downstream half of the meander kept expanding scroll bar development continued to move upstream (figure 7.4). Since 1975 complexes 1 (bars 1,2) and 2 (bar 3 and the youngest bar) expanded and a third was added. Underwater bars line the pointbar at the downstream ends of complexes 2 (nearly 20 meters wide) and 3. The newly developed point bar from 1975 developed downstream through two scroll bars of about 20 meters wide.

1985

Between 1980 and 1985 the channel upstream of "Châtel de Neuvre" cut-off two consecutive sharp and short bends (figure 7.5; 1: immature pointbar, 2: upstream pointbar in orange). With high water flow took a straighter path with less resistance, using the swale behind the upstream pointbar from 1980. The downstream bend expanded in the first and last part of the bend (3,4). Meander migration in the upstream part occurred with the presence of sharp upstream bends, while downstream migration occurred mainly after the cut-off, when the course of the channel was straightened. In upstream part of the bend scroll bars were visible due to water turbulence that reflected sunlight (figure 7.5b). Three bars, over 10 meters wide, were present on the downstream end of the pointbar, one already attached. A bar extended upstream, becoming part of the riffle that crossed towards the opposite bank.

1992

Between 1985 and 1992 the channel attempted to re-establish the bends that were cut-off in 1985 (figure 7.6). Lateral migration dominated because of the sharp bend at the upstream end of the cut-off where flow enters the bend obliquely (figure 7.5a; 5). The new pointbar was remoulded, showing scroll patterns from before the cut-off (green) and a new phase of scroll bar development (red) at the downstream end (the youngest bar was about 20 meters wide).

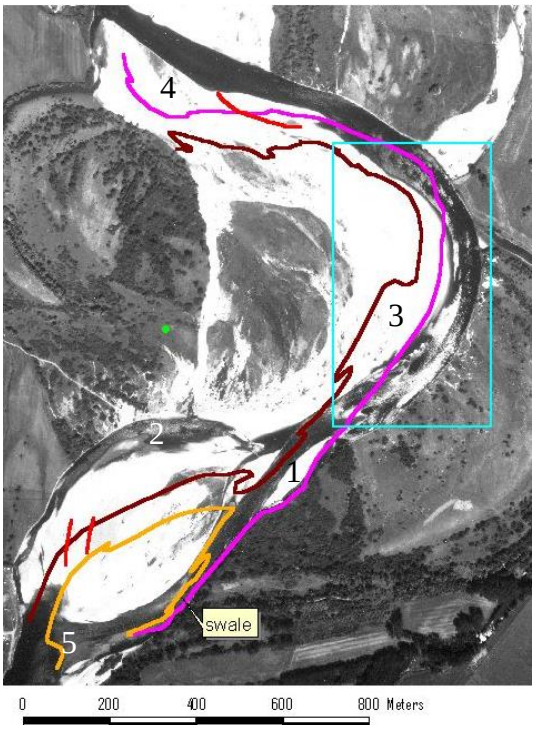

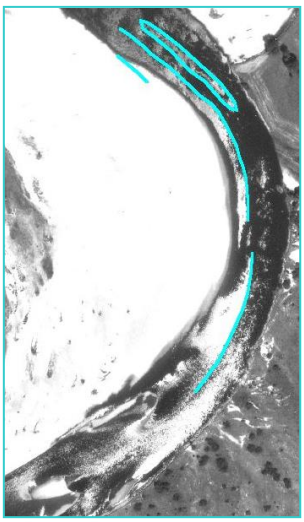

*Figure 7.5a: **1985** aerial photo; scroll patterns in red, and from 1980: inner bank in brown and of the upstream pointbar in orange, outer bend in purple.*

*Figure 7.5b: **1985** aerial photo insert from figure 7.5a with channel bars.*

*Figure 7.6: **1992** aerial photo; scroll patterns in red, vegetational patterns in green and from 1985: inner bank in brown and the outer bank in purple.*

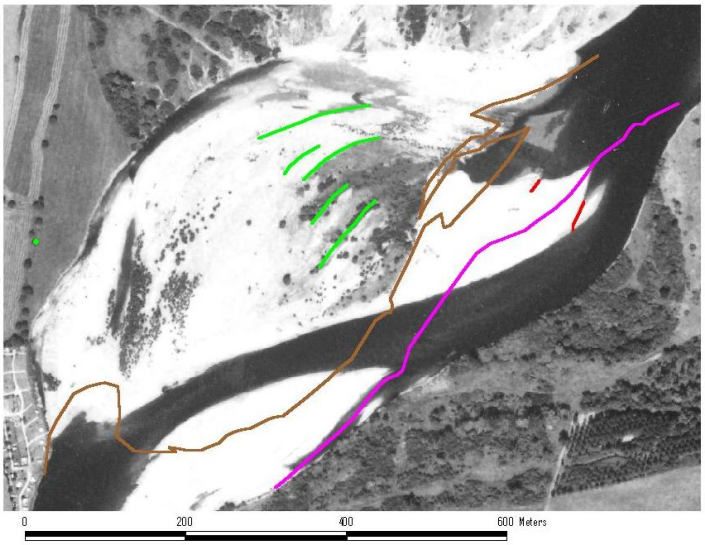

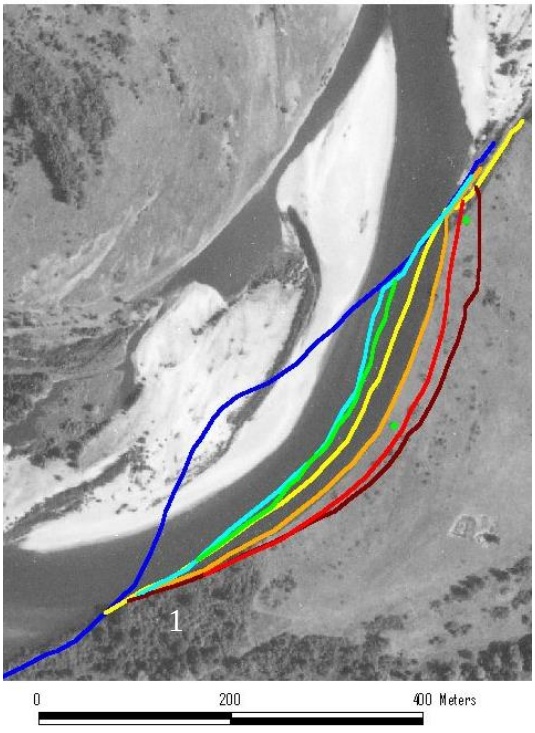

*Figure 7.7: **2000** aerial photo with outer banks from 1992 (dark blue), 1995 (light blue), 1996 (light green), 1998 (yellow), 2000 (orange), 2002 (red) and 2003 (brown).*

7.2 Meander development between 1992-2003

7.2.1 Outer bend erosion

Erosion between 1992 and 1995 was concentrated downstream, moving the downstream margin about 215 meters, while lateral erosion amounted to a maximum of 105 meters (figure

7.7). Maximum and downstream erosion were about 15 meters in the period 1995 – 1996. Downstream erosion, between 1996 and 1998, was 95 meters while lateral amounted to 20 meters. Between 1998 and 2000, erosion (maximum of 25 meters) occurred along the whole bend and not just in the downstream part. The bend was located downstream of resistant vegetation (trees; figure 7.7; 1). In the periods 2000 – 2002 and 2002 – 2003, 20 meters downstream erosion occurred and 20 and 30 meters laterally.

7.2.2 Point bar sedimentation

Between 1992 and 1998 the pointbar developed predominantly in downstream direction (figure 7.8). This was the result of a strong downstream flow component coming from a straight upstream stretch since the cut-off (figure 7.5 a). Recently deposited and unvegetated sediment was readily eroded at the upstream end and accreted at the downstream end of the pointbar.

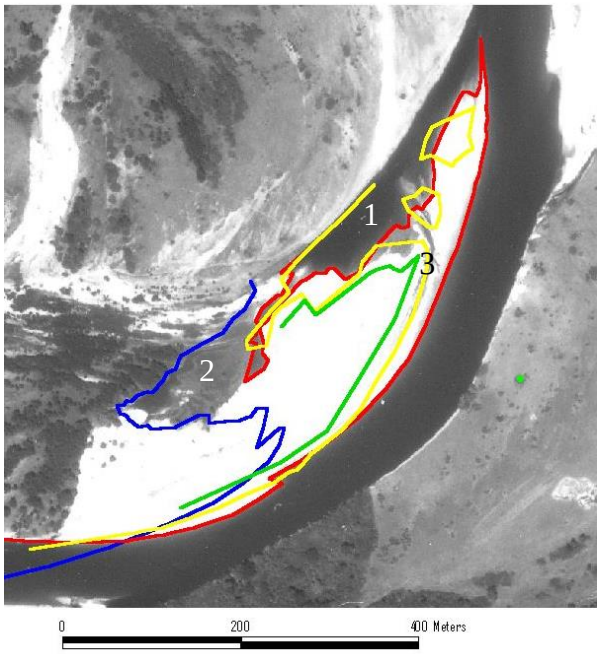

*Figure 7.8: **1998** aerial photo with inner banks from 1992 (blue), 1995 (green), 1996 (yellow), and 1998 (red). The 1995 and 1996 shorelines were based on levelling by Wilbers and de Kramer.*

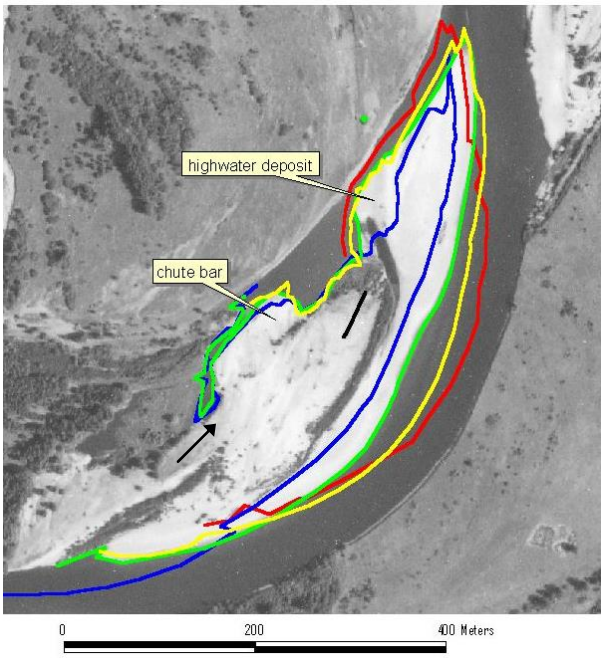

*Figure 7.9: **2000** aerial photo with inner banks (pointbar) from 1998 (blue), 2000 (green), 2002 (yellow) and 2003 (red).*

A swale developed as result of the quick downstream development of the bend (sedimentation had trouble keeping up; figure 7.8; 1). Sedimentation occurred along the main channel, but also in the swale behind the pointbar. Sedimentation occurred at the end of the cut-off channel (from 1985), that was in use during high discharges in the early 1990's (figure 7.8; 2). In the late 1990's a similar a similar process occurred in the form of a chute bar (figure 7.9). Water flowed across the pointbar (arrow figure 7.9) in a unvegetated depression (figure 7.10). Flow diverged when it entered the deep swale, allowing its sedimentary load to settle (figure 7.11). A third source of sediment in the swale was a crossing channel (figure 7.8; 3). It crosses the narrow pointbar to benefit from an increase the waterlevel gradient, as opposed to flowing along the long pointbar (similar to St. Loup, section 6.2.2). The channel started out as a lateral swale, the upstream part was nearly parallel to the shoreline, and ends crossing the pointbar draining water and releasing sediment. The highwater deposit marked in figure 7.9 and the sediment plume in at the end of figure 7.8 (3), resulted from crossing channels. The high water deposit expanded substantially due to the concentration of flow in crossing channels that lie along a stroke of trees (figure 7.12). The channels cannot cross further upstream. In

1998 the bars separated by crossing channels in 1996 were incorporated into the main pointbar.

Figure 7.10: Chute channel on the foreground with on the background sediment plumes (that originate from the main channel) within a stroke of poplars a stroke of poplars.

Figure 7.11:At the end of a chute a bar develops, where flow enters the swale.

The development of cross-section 1 (figure 7.13) showed that the major swale (x = -300) was accreting on the left due to the abandoned channel (figure 7.8; 1) and on the right from the main channel. The pointbar near cross-section 1 (figure 7.13; 1) consisted of two scroll bar complexes in 1995. These bars were distinguishable through vegetation (figure 7.10). In 1997 vegetation established along the edge of the two bars in a swale (figure 7.8; 2). The stroke of poplars (swale) caught in sediment and its roughness led to the concentration of flow in a channel along its margin (figure 7.12 and 7.13; 1 x = -140). On the inside of the stroke of trees (left) sedimentation occurred in fairly calm water allowing a total of about 85 centimetres increase in height, or an average of 10 centimetres per year (figure 7.13; 1). On the outside a new bar developed as the channel migrated laterally.

Figure 7.12: Looking downstream through a crossing channel along stroke of poplars (left) and with the main channel on the right.

Cross-section 2 (figure 7.13; 2) lies just downstream of the vegetated part of the pointbar and shows two main bars, only narrower and steeper than in cross-section 1. Behind the vegetated stroke flow diverged, allowing sedimentation, but locally erosion also occurred along crossing channels. This resulted in the formation of two bars, the youngest about 35 meters wide and 45 cm high and the older about 30 meters wide and 55 cm high.

Length profile 3 (figure 7.13) shows the downstream lengthening of the pointbar (70 meters) and the changing nature of the crossing channels on the left. Bars of about 65 cm in height were present between crossing channels. They were remoulded in time and no bars from 1996 could be recognized in 2003. The bars from 1996 varied in width, with narrow, deep channels in between. In 2003 the bar width varied less (about 25 meters), while the troughs are larger. The downstream end of the pointbar (right of length profile 3) increased in height nearly a meter (just over 10 cm per year). Downstream from the vegetation where channels cross the

pointbar (left of profile 3) sedimentation was less. The closer to the vegetation, the deeper the channels and the more outspoken the topography.

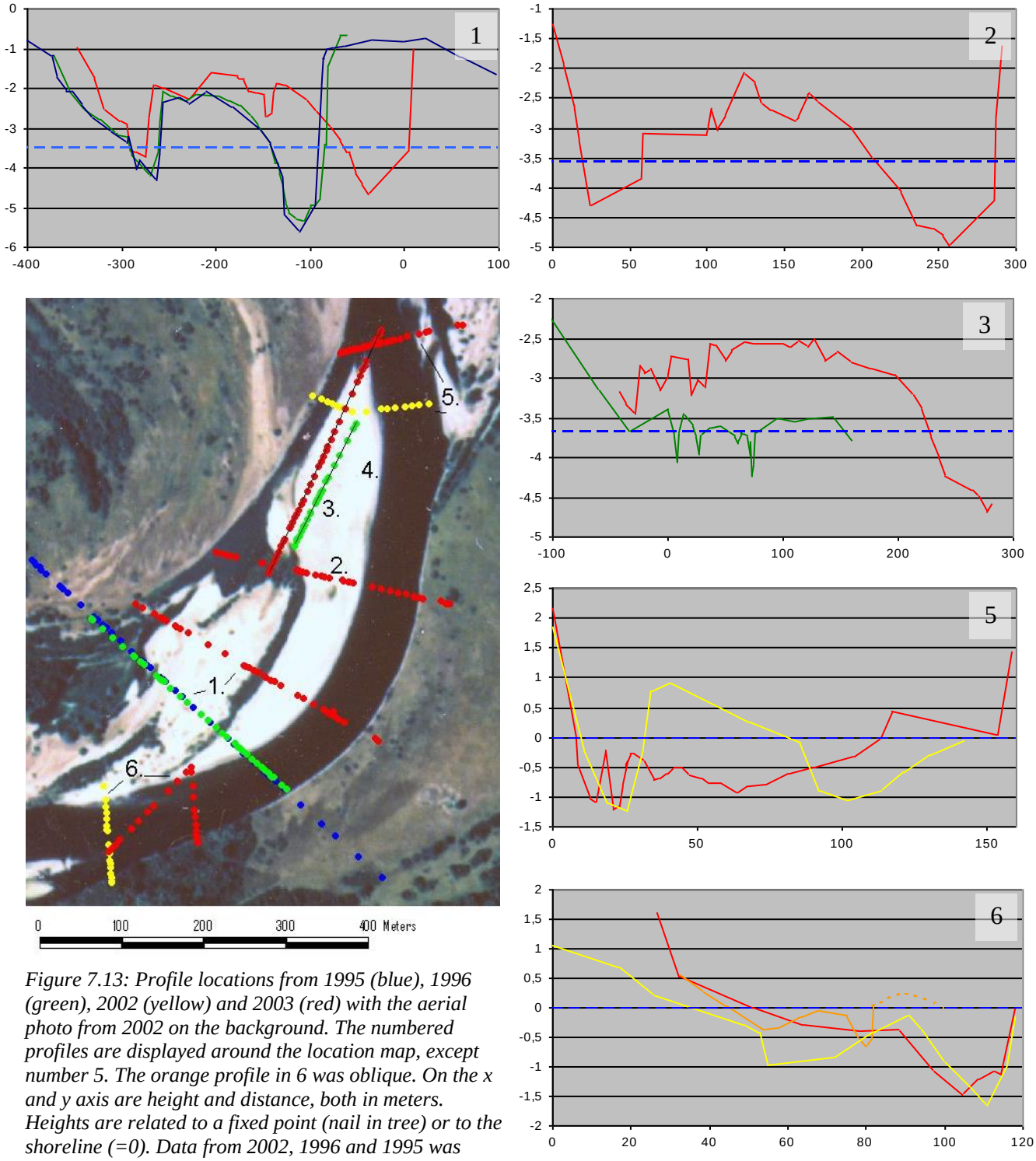

Figure 7.13: Profile locations from 1995 (blue), 1996 (green), 2002 (yellow) and 2003 (red) with the aerial photo from 2002 on the background. The numbered profiles are displayed around the location map, except number 5. The orange profile in 6 was oblique. On the x and y axis are height and distance, both in meters. Heights are related to a fixed point (nail in tree) or to the shoreline (=0). Data from 2002, 1996 and 1995 was adapted from de Kramer and Wilbers. Levelled heights from 1996 were corrected to fit measurements from other years, assuming that overbank heights, maximum waterdepth and waterlevel remain constant.

Between 1998 and 2003 (figure 7.9) the pointbar had reached a maximum downstream extent and continued expanding in a lateral direction. This coincided with the outer bend moving beyond a stretch of resistant vegetation (figure 7.7; 1) and increased lateral erosion. The upstream bend had also increased its curvature since the cut-off, directing flow towards the eastern bank of "Châtel de Neuvre". Sedimentation occurred between the main channel and the crossing channel along the trees in figure 7.13 (1), creating a new scroll bar (the right one of the three in 2003).

Near the bend apex two scroll bars were present near the 2003 shoreline (figure 7.13; location 4). The bars could only be discerned at their tips, where they were about 10 cm high, while their main body had merged with the pointbar. At the tip of the pointbar a series of bars was present (figure 7.13; 5). The bars increased in height (21, 95, 100 cm) and steepness with age and development (right to left). In 2002, slightly further upstream, the pointbar was steepend by the main channel, where the channel asymmetry changed, concentrating flow near the inner bend. The erosive nature of the end of the pointbar was absent in 2003 due to the outward migration of channel, away from the point bar.

Cross section 6 (figure 7.13) shows the crossing of flow at the upstream end of "Châtel de Neuvre". The upstream cross section from 2002 (yellow) shows a major bar in the center of the channel, that was an extension from the upstream pointbar (figure 7.13). This bar grew and emerged from the water in 2003 (oblique orange profile). In the field it was visible that low discharge flowed through the wider of the channel (left of the major bar). With high discharges water also flowed across the pointbar and through the swale (deepest part on the right, not levelled in the 2003). An additional bar was present in the oblique orange profile. This bar separates low discharges that were predominantly concentrated in the narrow channel on the right and higher discharges that flowed mainly in the wider depression on the left. In the downstream profile flow was concentrated near the outer bend leaving a plateau on the inner bend that lies in the extension of the complex of bars that formed the riffle. In the outer part of the channel a small ridge was found that formed between the trees that were eroded from the bank and obstruct flow along the outer margin.

7.3 Overall meander change

Initially the bend at Châtel de Neuvre decreased its bend radius from more than 5 to about 2.5 in 1980 (figure 7.14). It was not confined by resistant banks and developed a rotational character (figure 3.3). In 1985 the radius increased, related to downstream erosion following the cut-off of the upstream bend (figure 7.5a).

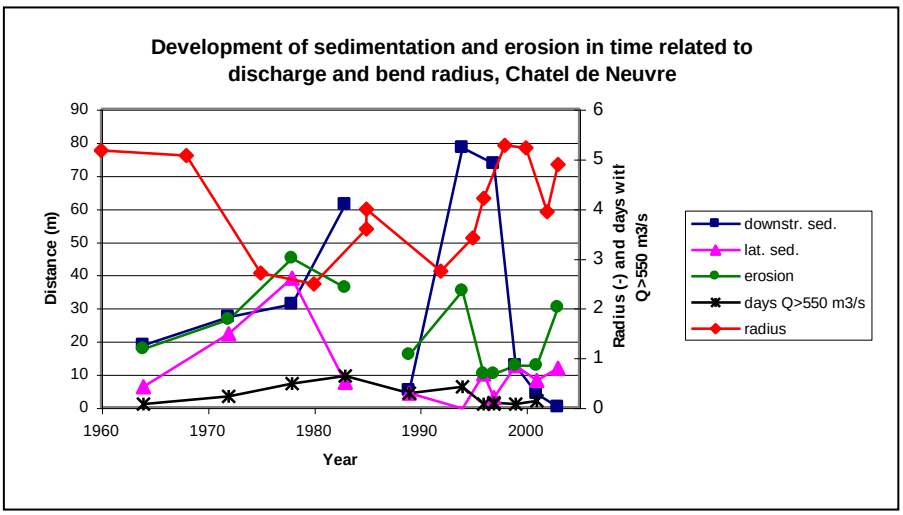

Figure 7.14: Annual pointbar development (sedimentation and erosion) and factors average discharge and bend radius in time.

In the 1990's, the new meander developed in downstream direction, because of the straight entrance of flow into the bend, along the cutoff. This caused an increase in bend radius from 2.7 to more than 5. Lateral development followed since 1998, slowly decreasing bend radius. The change in development was related to the (downstream) length that the pointbar and channel acquired, along which helicoidal flow developed (section 3.4.1). A resistant forested reach along the outer bend was also surpassed allowing lateral expansion (figure 7.7; 1).

8. Meander and pointbar development case 3: Chemilly

8.1 Long term meander history

1954

In 1954 multiple phases of scroll bar development existed on the pointbar (figure 8.1). The oldest phase (1) consisted of three bars, about 45 meters wide, near the downstream end of the pointbar (a younger bar, about 20 meters wide, was present in the channel alongside the pointbar). The following phase of sedimentation was concentrated further upstream (2), depositing two bars of about 35 meters wide. The youngest scroll bars in 1954 formed under water, along the whole pointbar (3). Two separate ridges merged into a large bar (about 30 meters wide) in the downstream part of the bend.

1960

Dominant lateral outer bank erosion created room for lateral sedimentation, expanding the pointbar from the 1954 submerged bank(s) (3), that could still be recognized in the 1960 waterline. The downstream lengthening of the pointbar resulted from sedimentation and low water levels (narrow channel near crossing). The waterline (brown) and swales (green) from 1954 provided a habitat for various strokes of trees. Diverging sediment splays on the pointbar were oversplay and chute deposits. High discharges overshot the upstream bend, diverge, slow down and release sediment. Chute deposits developed similarly, only flow was initially concentrated (along the pointbar edge), reaching further onto the pointbar.

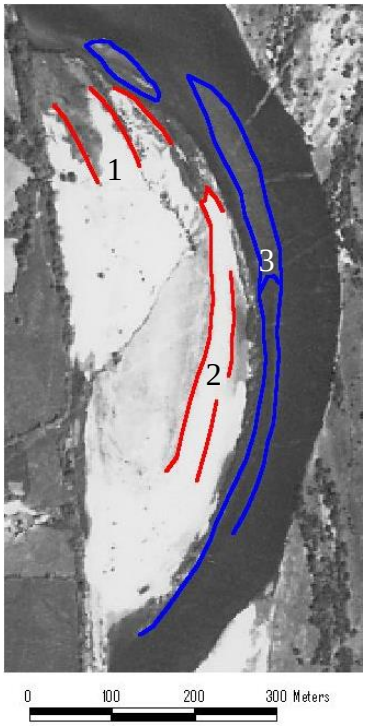

*Figure 8.1: **1954** aerial photo; scroll bars above water in red and underwater in blue.*

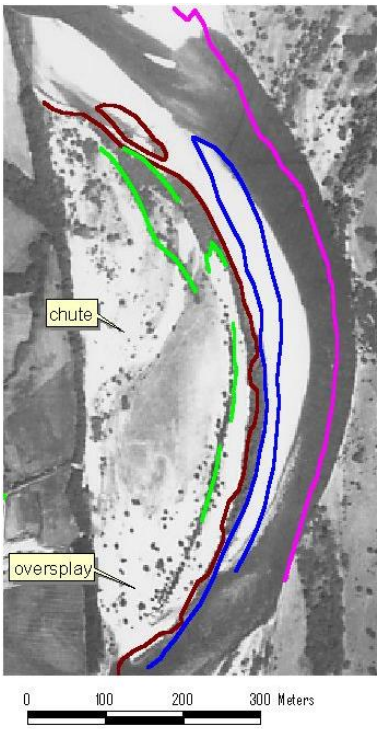

*Figure 8.2: **1960** aerial photo; from 1954: scroll bars in blue and green, inner bend waterline in brown, outer bend margin in purple.*

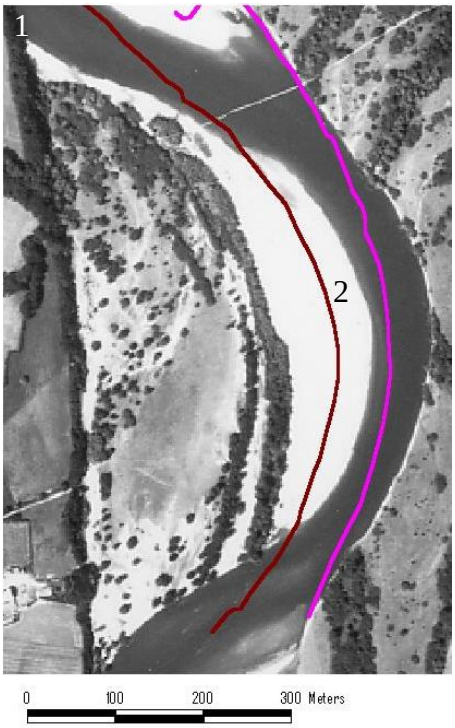

*Figure 8.3: **1967** aerial photo; 1960 inner bend waterline in brown, outer bend margin in purple.*

1967

Between 1960 and 1967 lateral meander migration led to an increased bend curvature. A scroll bar of nearly 30 meters wide was added (2), bordered by a swale that coincided with the 1960 waterline. The bend downstream of "Chemilly" eroded upstream along a revetment (1).

1978

The laterally migrating bend came into contact with a revetment on the right, between 1967 and 1978 (figure 8.4). The bend preceding "Chemilly" was later straightened and stabilized, related to the construction of a bridge about 500 meters upstream. The straightening of the channel caused flow to enter the "Chemilly" bend obliquely, cutting this bend off too. The old (1) and new (2) channel both carried water (figure 8.4), the new channel developing a new meander pattern with low discharges. The cut-off also led to a new area of chute deposits (3).

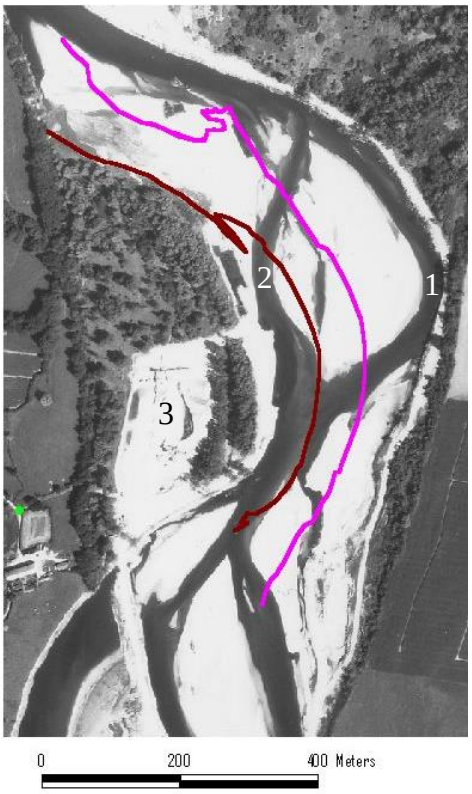

*Figure 8.4: **1978** aerial photo, showing "Chemilly" and the upstream, cut-off bend; 1967 inner bend waterline in brown, outer bend waterline in purple.*

1980

Flow concentrated in the cut-off channel that slowly migrated outwards, while the abandoned channel got filled with sediment from the upstream end (figure 8.5). The straightening of the meander increased the channel gradient and caused large downstream pointbar expansion. The pointbar downstream of "Chemilly" has also been cutoff as result of upstream changes.

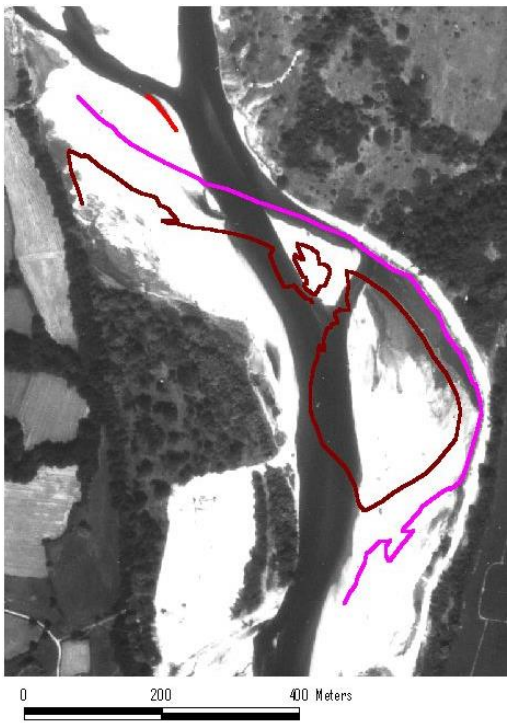

*Figure 8.5: **1980** aerial photo; scroll bar in red, 1978 inner bend waterline in red, outer in purple.*

1985

Between 1980 and 1985 the meander at Chemilly developed laterally and downstream (figure 8.6). The downstream margin of the youngest phase of lateral growth was marked by a swale (red). Channel curvature increased in an attempt to reestablish the situation from before the cutoff. Flow patterns that covered the pointbar are shown in an insert (figure 8.6). At the upstream end of the pointbar flow was nearly parallel to the channel, while at the downstream end plumes varied somewhat in direction, resulting from local topography and vegetation.

1992

Prominant lateral erosion caused the "Chemilly" bend to increase in curvature and shorten in length (figure 8.7). The downstream bend showed similar development, but at its upstream end (its downstream end was constrained by revetments). With high discharge flow crossed the downstream pointbar (through the dotted line), detaching a series of scroll bars that

became narrower moving outwards (1). On the main pointbar scroll bars of over 20 and nearly 40 meters wide were found, the younger and narrower bar extending downstream under water.

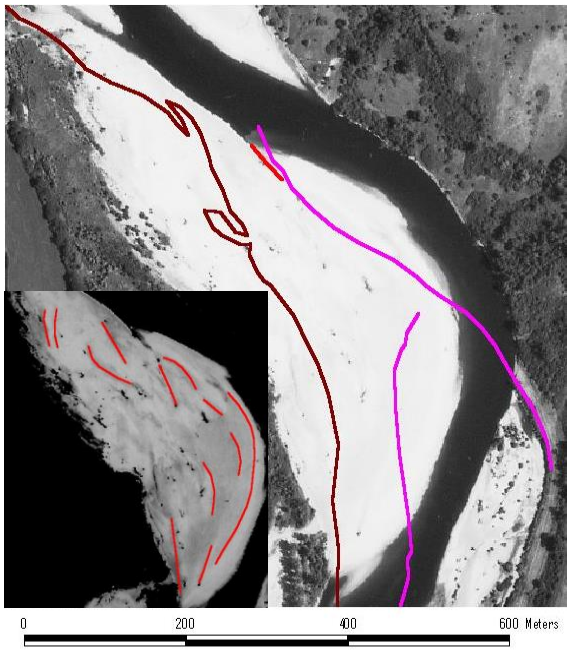

*Figure 8.6: **1985** aerial photo; swale in red, from 1980: inner bend waterline in brown, outer in purple. Insert picture shows flow/sediment patterns.*

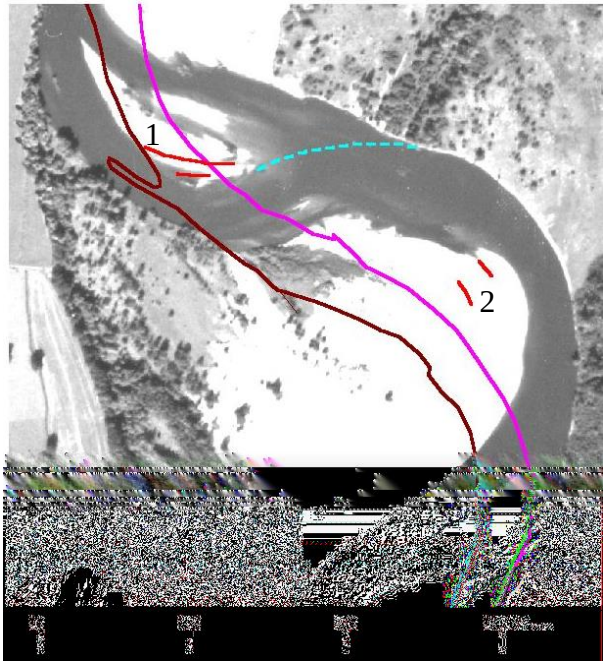

*Figure 8.7: **1992** aerial photo; scroll patterns in red, the location of the outerbend before cutoff in dotted blue, and from 1985: inner bend waterline in brown, outer in purple.*

8.2 Bend development between 1992 and 2003

8.2.1 Outer bend erosion

Between 1992 and 2003, lateral erosion occurred expanded the bend in north north-eastern direction (figure 8.8). Initially, between 1992 and 1995, erosion was high, totalling over 150 meters. Later, erosion rates amounted to about 15 meters per year. The downstream bend showed little net change although periods of sedimentation and erosion/cutoffs occurred (1), depending on the direction of incoming flow (from “Chemilly” bend).

8.2.2 Sedimentation

Conform with erosion the pointbar initially expanded rapidly in north north-eastern direction, before slowing down since 1995 (figure 8.9). In the late 1990’s the lengthening bend at Chemilly started developing a compound nature with an additional bend at the upstream end (2). In 1997 a scroll bar had developed (1), that extended underwater towards the opposite bank in upstream direction. Its form shows similarities with a (crossing) riffle.

The downstream part of the bend was characterized by varying cross sections, from typically outer bend (asymmetric) to wide (symmetric) riffle-like cross sections (figure 8.10; 1). The steep inner banks (two upstream profiles) and the bar on the left bank (downstream cross-section) were formed by chute deposits, deposited here after crossing the pointbar.

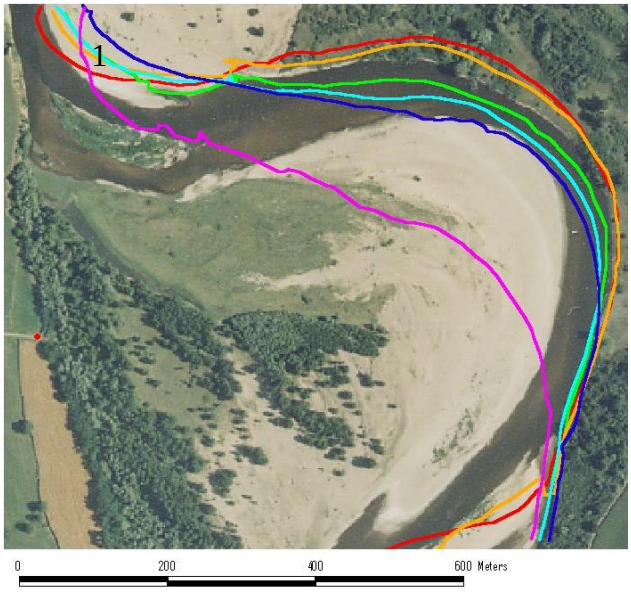

*Figure 8.8: **2000** aerial photo with waterlines from 1992 (purple), 1995 (dark blue), 1997 (light blue), 1998 (green), 2002 (orange), 2003 (red).*

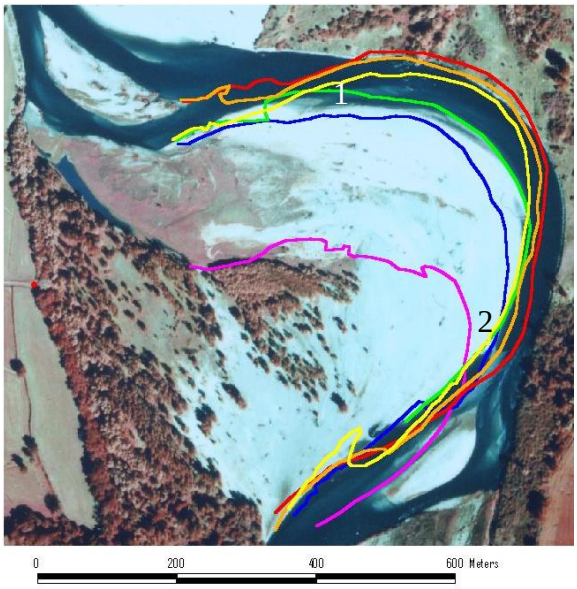

*Figure 8.9: **1997** aerial photo with waterlines from 1992 (purple), 1995 (dark blue), 1998 (green), 2000 (yellow), 2002 (orange), and 2003 (red).*

Cross section 2 over the riffle and the upstream part of the bend showed flow crossing from left to right (figure 8.10). In 2002 flow was concentrated on the inside (left) of a wide channel. In 2003 the thalweg had moved to the right bank while riffle bars (x = -25) developed on the inside. The development of the upstream bend (figure 8.9; 2) allows the development of scroll bars together with riffle bars (figure 8.12; 2, x = -40, -80). The oldest scroll bar and swale (x = -80) extended downstream, maintaining a height of about 15 cm, to cross section 3, (x = -45). Cross section 3 (figure 8.10) shows a bar that extended downstream from a channel that crossed the shallow riffle. The bar was symmetric increased in height temporarily, before slowly moving outwards and disappearing in downstream direction.

Figure 8.8 shows the periodically advancing and retreating waterline of the pointbar downstream of "Chemilly" (1). Figure 8.11 shows islands and bars that developed along the pointbar and in the channel. Through chute cut-offs these bars were isolated from the downstream pointbar and partially ended up on the opposite bank. In 1995 and 1997 an island was present consisting of two main bars, the top one (directed SW), about 60 meters wide and the bottom one (directed south) about 35 meters wide. The bottom part of the island had the most vegetation (see also figure 8.9), despite being the youngest part. This part was located furthest from the main channel and was therefore less exposed to flow. In 2000 the island was partially eroded, while the part that remained was added to the pointbar in 2003 (figure 8.10). The cutoffs occurred because two sharp bends were a short distance apart. High discharges could not adjust to the new bend over the short distance and partially crossed the downstream pointbar.

Cross section 4 shows three bars with channels in between (figure 8.10). The core of the channel bar was directed inwards, until it was cut-off from the main pointbar (green). The channel bar from 2002 had asymmetry that indicated flow crossed it moving southwards. This asymmetry was caused by flow circulation from the "Chemilly" bend that reached downstream. Along the short distance between the bends opposing helicoidal flow could not yet develop in the cut-off bend. Further downstream, helicoidal flow had developed in the downstream bend, showing channel and bar asymmetry in the opposite direction. Between

2002 and 2003 the channel bar was eroded along the new channel and remolded to symmetric or slightly asymmetric in the opposite direction (figure 8.10). Further onto the “Chemilly” pointbar lie two similar bars and abandoned channels.

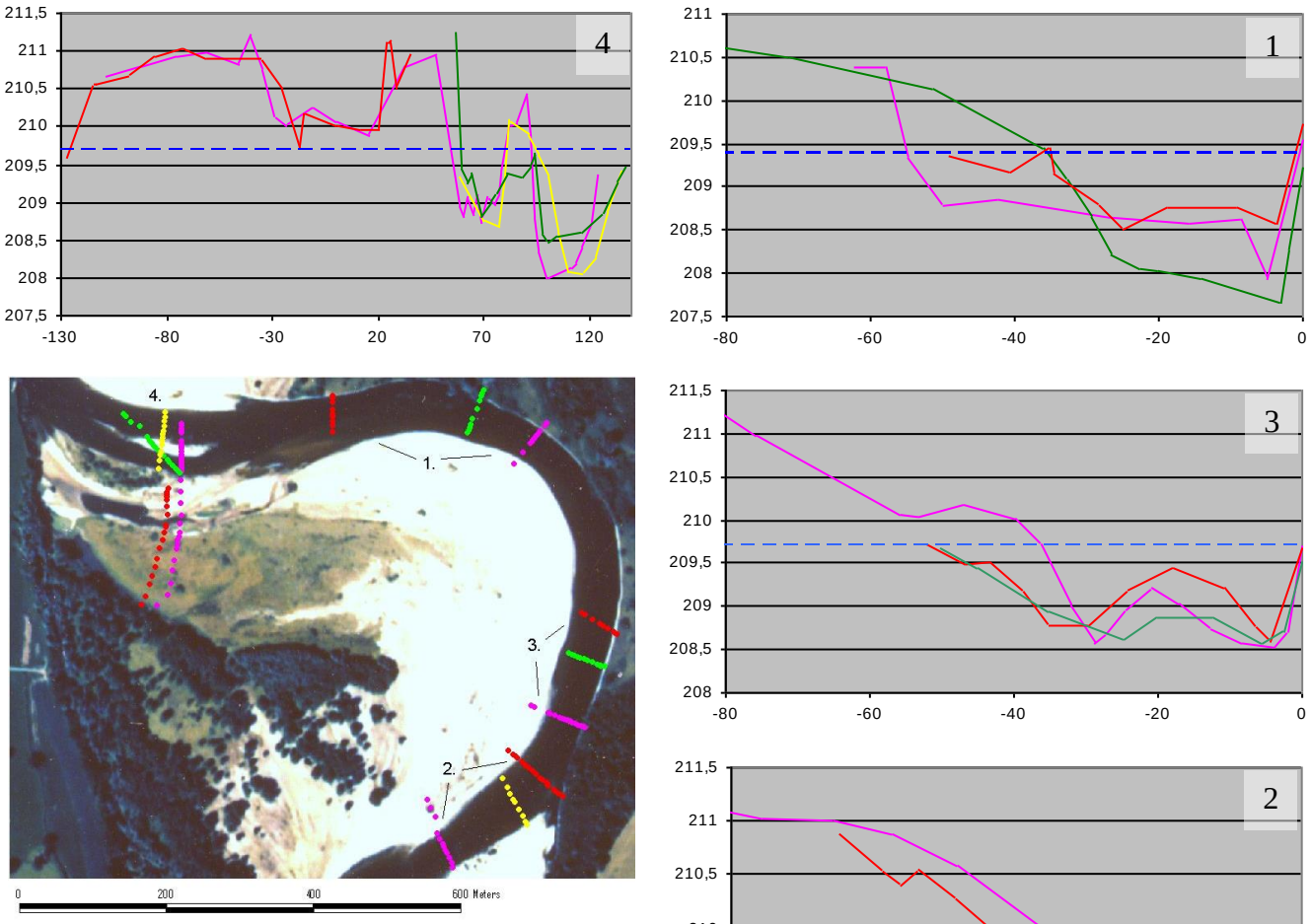

Figure 8.10: Profile locations from 2002 (yellow) and 2003: upstream in purple, middle/oblique in green, downstream in red, with the aerial photo from 2002 on the background. The numbered profiles are displayed around the location map. On the x and y axis are height and distance, both in meters. Heights are related to the French national 0 point. Distances are related to the position of the outer bend (zero point) and in the case of profile 4 to the point where the profiles are closest together.

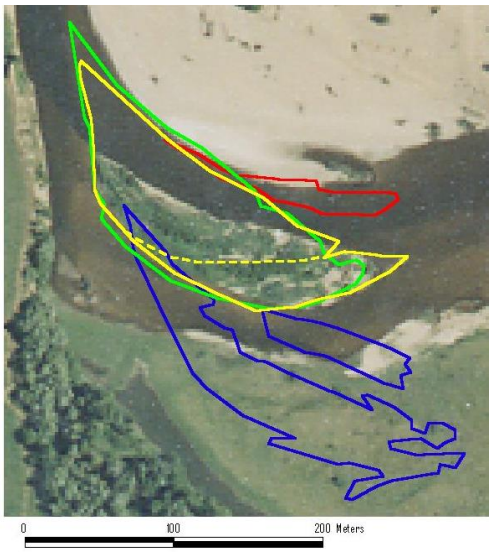

*Figure 8.11: **2000** aerial photo with waterlines from 1992 (blue), 1995 (green), and 1997 (yellow) and 2002 (red).*

8.3 Overall meander change

Bend radius decreased between 1954 and 1978 through dominant lateral migration. The bend at Chemilly was subsequently cut off just like the bend upstream from it. The bend initially changed its direction of propagation to downstream. In the 1980's lateral development dominated again and gradually changed to rotational development (figure 3.3). The bend radius decreased rapidly at first, before becoming stable at values below 2.5 (figure 8.12). Fluctuations in bend radius occurred because the focus of erosion varied (related to varying discharge or bank resistance).

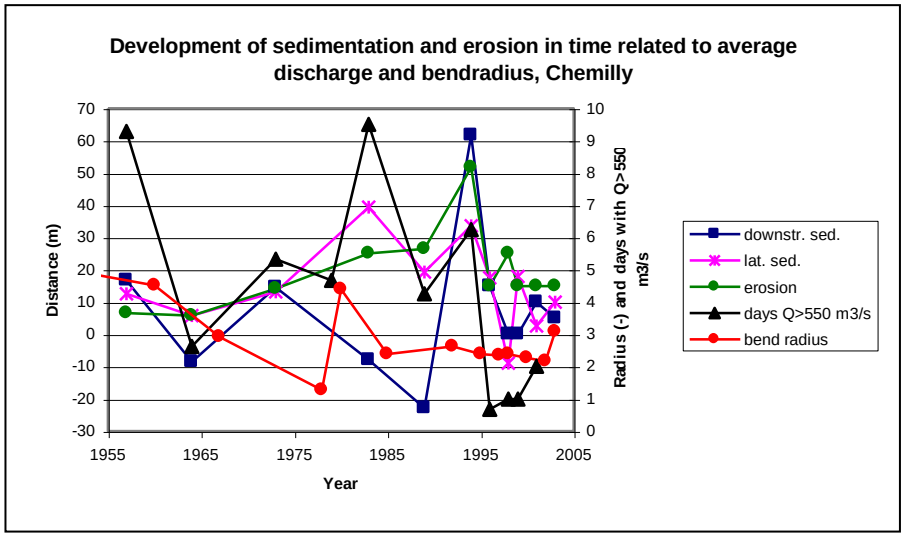

Figure 8.12: Annual pointbar development in time related to discharge and bend radius.

9. Meander and pointbar development case 4: Château de Lis

9.1 Long term meander history

1954

In 1954 the meander at Château de Lis was developing as a compound bend (figure 9.1). Scroll bars, 20 - 25 meters wide, formed at the downstream end of the pointbar (1). The youngest bar (complex) had not yet reached the downstream margin of the poinbar. The meander at Château de Lis was closely followed by a bend that was constrained by a dike (2). Two asymmetric bars (3) were formed by weak helicoidal flow in the beginning of the downstream bend, but were also part of the riffle where flow crossed to the left bank. The (downstream) pointbar had to develop in the direction of the (scroll)bars because near the downstream end the dike limited meander expansion.

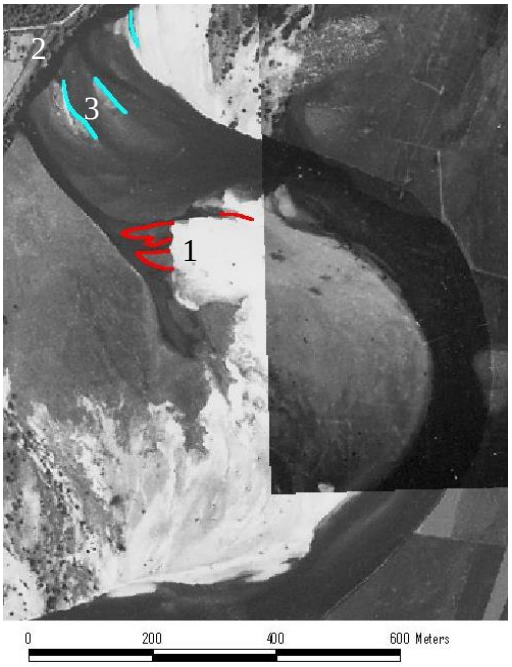

*Figure 9.1: **1954** aerial photo; scroll bar contours in red and riffle/scroll bars of the downstream bend in blue.*

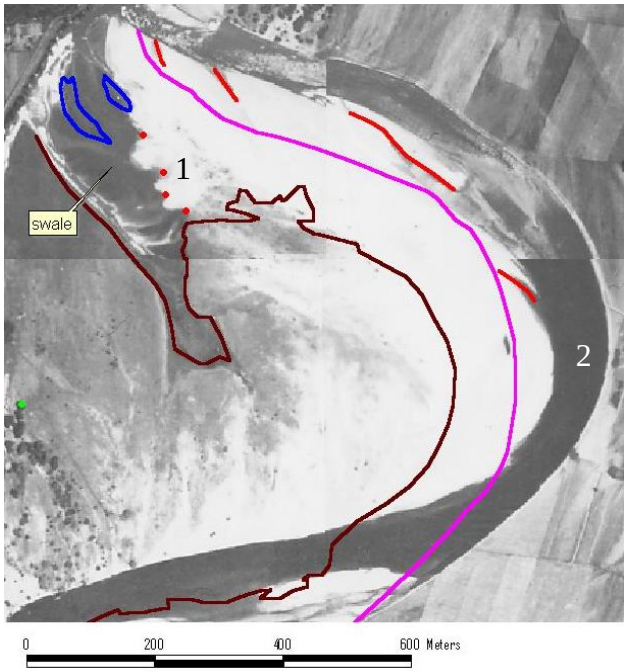

*Figure 9.2: **1960** aerial photo; scroll bar contours in red, and from 1954: shoreline in brown, outer bend margin in purple, and channel bars in blue.*

1960

Between 1954 and 1960 the meander expanded laterally and downstream (figure 9.2). The downstream expansion of the pointbar left a large swale alongside. The former riffle and its bars (from 1954) were included into the pointbar and swale at Château de Lis. The oldest phase of sedimentation consisted of rounded bars at the margin of the swale (1). After downstream sedimentation reached the end of the pointbar, sedimentation was concentrated further upstream towards the maximum curvature of the bend (2).

1967

The compound bend expanded laterally in the second part of the bend (figure 9.3). In the downstream part of the bend, bars developed across the channel (1). With low water flow meandered within the bend, moving in- and outwards (arrows) between the (riffle)bars. With high water flow followed the large bend along the outer scarp. The swale from 1960 was filled with vegetation. The two riffle/scroll bars from1954 were recognizable in the topography from 1967, sparsely vegetated and lined with higher vegetation. The bars kept

their form, while the smaller one moved slightly to the NE, towards the former downstream pointbar (figure 9.1).

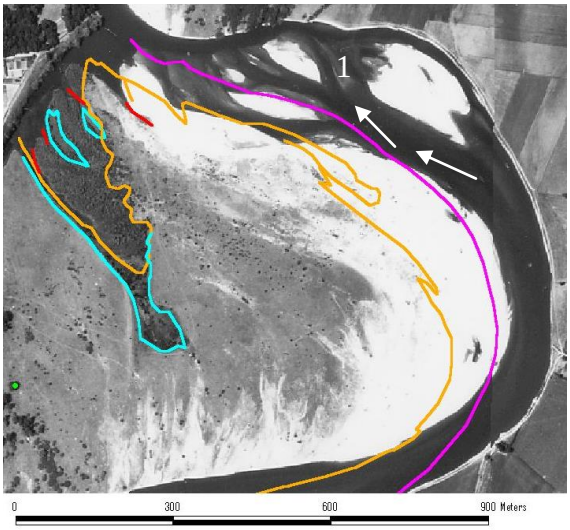

*Figure 9.3: **1967** aerial photo; scroll bar contours in red, and from 1960: shoreline in orange, outer bend margin in purple, and the 1957 shoreline and channel bars in light blue.*

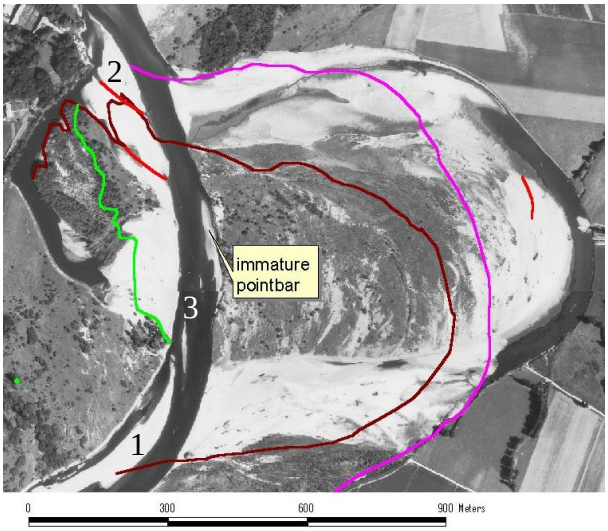

*Figure 9.4: **1978** aerial photo; (scroll) bar contours in red and from 1967: vegetation edge in green, inner shoreline in brown and outer bend margin in purple.*

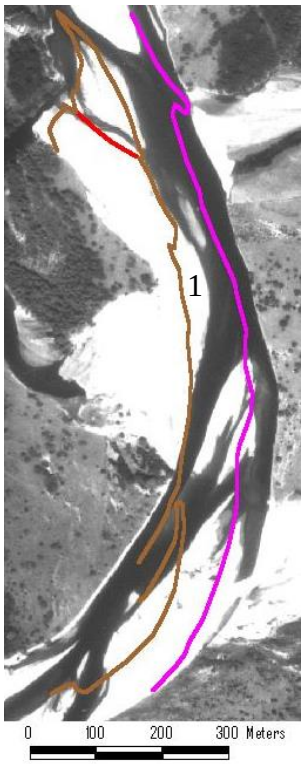

*Figure 9.5: **1980** aerial photo with 1978 scroll bar contours in red, inner shoreline in brown, and outer bend margin in purple.*

1978

Between 1967 and 1978 the bend continued to grow laterally and eventually got cut off (figure 9.4), in the same period as the bend at Chemilly. The bend was straightened along the forested swale from 1967 (green). Two narrow pointbars developed in weak bends at the up- and downstream end (1 and 2) of the former pointbar. The upstream bend (1) was followed by a riffle (3), including two bars, that crossed to an immature pointbar on the eastern bank. Topography in the abandoned loop was exposed (apart from the upstream end) revealing the last phase of accretion (red) that occurred next to the deepest part of the bend (maximum curvature).

1980

The bend upstream of "Château de Lis" was cut off, redirecting flow coming into the bend (flow switched to the right channel at the bottom of figure 9.5). The downstream component of flow moved sediment from the "upstream" pointbar downstream (figure 9.4; 1) to a new location (figure 9.5; 1, opposite from the eroded immature pointbar). A bar, nearly 20 meters wide, formed the new accretion phase of the young pointbar.

1985

Between 1980 and 1985 the meander grew in lateral direction (figure 9.6) and approached a form similar to that before the cut-off. Sedimentation initially occurred laterally near the upstream end (1) and subsequently moved downstream (2; demarcated by a swale in green). At the downstream end bars were about 20 meters wide above water, with swales in between (red), and underwater (blue).

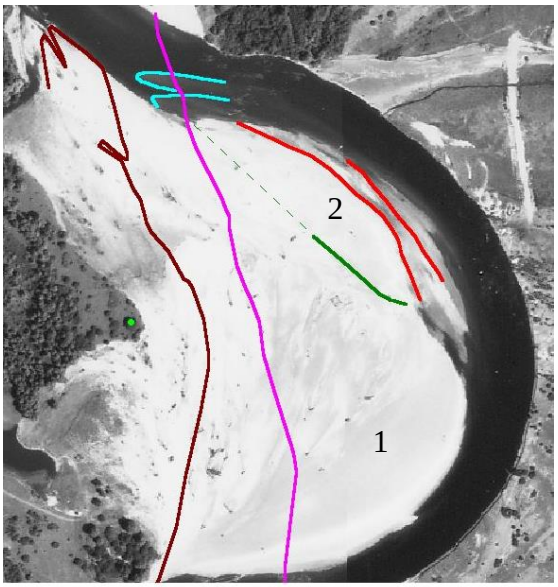

*Figure 9.6: **1985** aerial photo; scroll patterns in red, underwater bars in blue, a swale in green; from 1980; inner shoreline in brown, and outer bend margin in purple.*

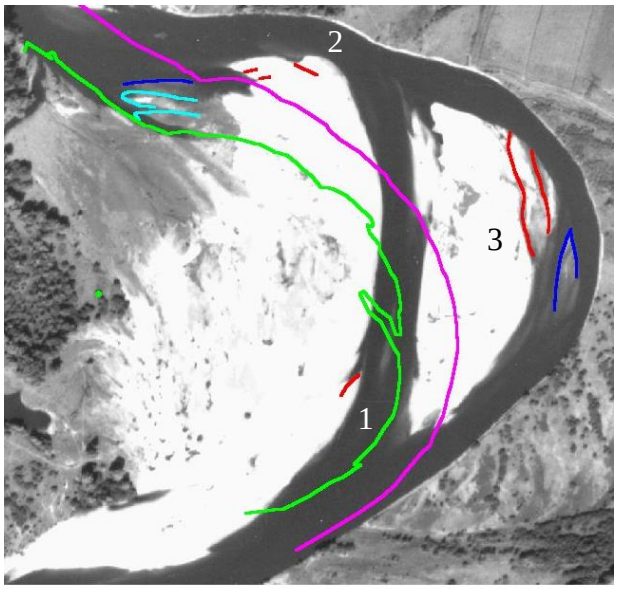

*Figure 9.7: **1992** aerial photo; scroll patterns in red underwater bars in dark blue; from 1985; inner shoreline in green, underwater bars in light blue, and outer bend margin in purple.*

1992

In 1992 the bend was partially cut-off due to the increasing length of the bend (figure 9.7). The thalweg was located on the outside of the channel at the beginning of the bend (1), followed by a straight stretch of channel and moved outwards again near the downstream end of the compound bend (2). On the inside of these "bends" pointbars developed. At the downstream end of the pointbar, bars in blue developed before the cut-off, and scroll bars in red, ranging in width from 15 to 25 meters, after the cut-off. The abandoned part of the pointbar (3) had bars of 35 and nearly 20 meters wide, while a new bar was developing underwater before the cut-off.

9.2 Bend development between 1992 and 2003

9.2.1 Outer bend erosion

After the cut-off from (before) 1992, erosion occurred in the two bends (figure 9.7; 1, 2) and was strongest in the downstream bend that had the greatest curvature. Between 1995 and 2003 the channel near the upstream bend eroded the outer bend till the maximum extent of 1992, before the cut-off (figure 9.8; 1). Since 1998, erosion occurred only in lateral direction, upstream from the resistant bank along the elevated agriculture land. The change to lateral migration changed the form of the upstream bend, causing flow to move inwards at the beginning of the downstream bend. In 2000 this development caused a chute cut-off at the downstream bend (figure 9.9). In the period 1992 – 2003, the downstream bend grew larger due to lateral and downstream erosion.

9.2.2 Sedimentation

Sedimentation occurred in three zones (figure 9.9). At the upstream bend an immature pointbar from 1995 grew and migrated downstream till it got bound by the chute cutoff in 2000. On the pointbar scroll bars of about 10 meters wide were present (in 1995, 1997) and on its inside a swale was extended.

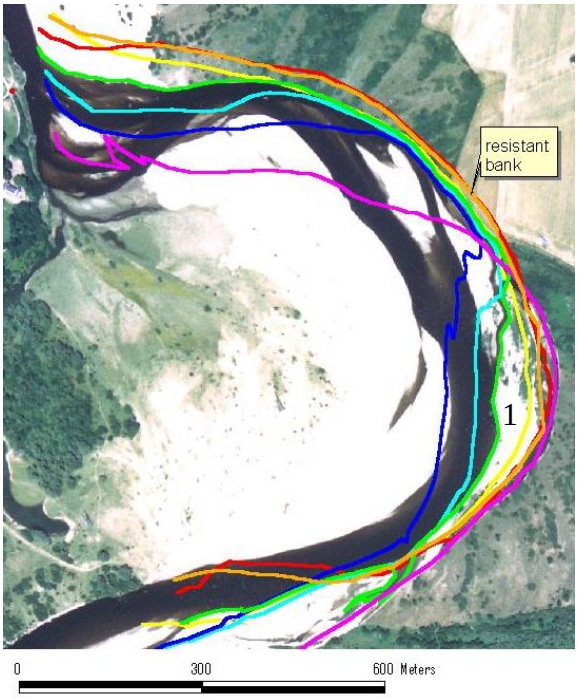

*Figure 9.8: **1998** aerial photo with outer bend margins from 1992 (purple), 1995 (dark blue), 1997 (light blue), 1998 (green), 2000 (yellow), 2002 (orange), 2003 (red).*

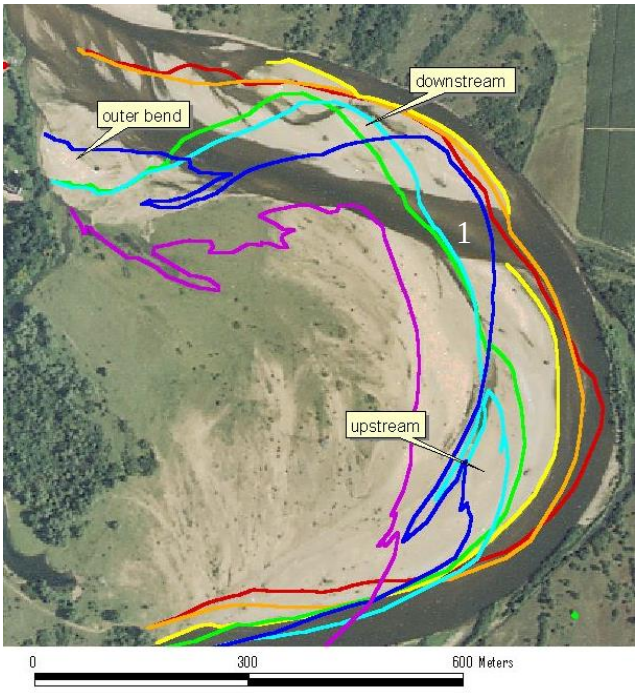

*Figure 9.9: **2000** aerial photo with shorelines from 1992 (purple), 1995 (dark blue), 1997 (light blue), 1998 (green), 2000 (yellow), 2002 (orange), 2003 (red).*

Cross section 1 in figure 9.11 gives an overview across the pointbar from the highest part, where chute processes occur, to the abandoned chute channel and the most recent phase of lateral accretion. In 2003 a scroll bar was visible, over 10 cm high and nearly 20 meters wide, that was already present in 2002. The channel migrated outwards, abandoning the chute cutoff from 2000 that was only used with high discharges. In the middle of the abandoned channel riffle bars were present (figure 9.9; 1).

A symmetric channel profile became more asymmetric and scroll bar development initiated near the bend apex between 2002 and 2003 (figure 9.11; cross section 2). On the pointbar two bars (x = -110, -160), about 40 meters wide, could be distinguished in 2002 and an additional one in 2003 (partially covering the low bar from 2002). The bars had grown in height and inwards, while sedimentation has partially closed a swale (x = -190).

In the downstream bend sedimentation occurred in a WNW direction (figure 9.9). At the end of the straight stretch of channel, between the partial bends, a riffle was present, where flow moved to the outside of the downstream bend (figure 9.10). The riffle from 1995 (orange) was connected to scroll bars (red) on the western and eastern bank (the two bars on the east belong to a narrow, underdeveloped pointbar). The riffle was only intermittently dissected by crossing channels. In 1997 the riffle and scroll bars moved downstream and inwards, due to the sharpening of the upstream bend. The riffle was used with low water, while with high discharge flow had already crossed to the outer bend behind the underdeveloped pointbar. The inward channel migration created space for the pointbar on the eastern bank, that included the 1995 riffle into its body. In both 1997 and 1998 the riffle on the west bank was connected to the youngest phase of scroll bar development.

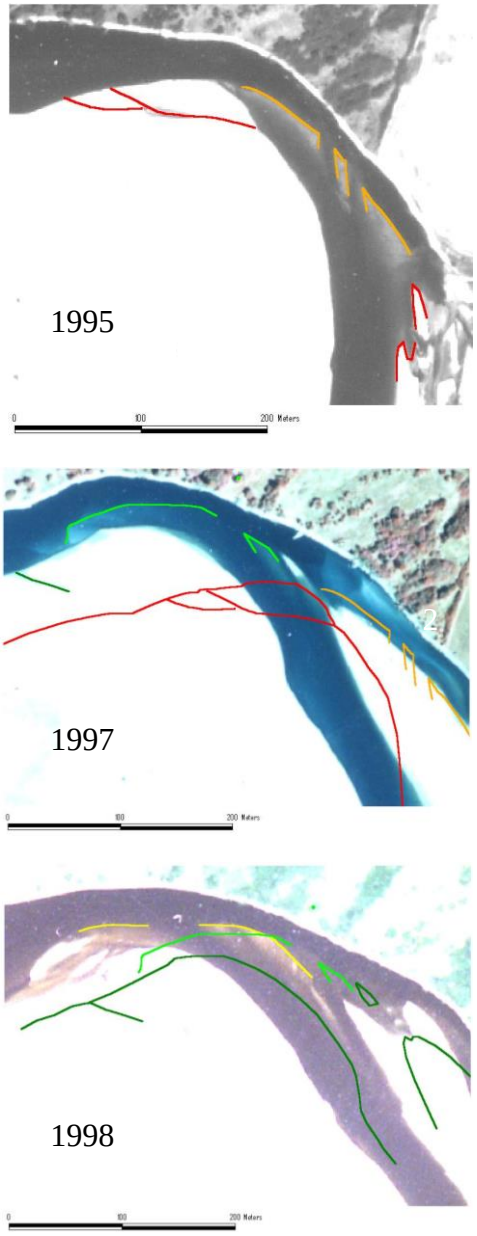

Figure 9.10: aerial photos with bars and shorelines from 1995 (orange and red), 1997 bars and swale (light and dark green) and 1998 bars (yellow).

Flow crosses from left to right at the beginning of the "Château de Lis" bend (figure 9.11; cross-section 3). The upstream channel had a symmetric cross-section with a riffle bar that showed great similarities with the bars to the right, that belonged to the upstream pointbar. The thalweg was on the right and a bar on the left in the downstream profile. The middle cross-section, from 2002, showed an even narrower and more asymmetric profile. This situation moved downstream in the period 2002-2003 beyond the downstream profile from 2003.

Between the bends the channel became characteristic for a riffle, even though the thalweg remains on the outside (figure 9.11; cross section 4). Bars on the inside belonged to the last phase of scroll bar development before the cut-off from 2000 (figure 9.9).

Bars were present on the inside of the sharp outer bend that followed the "Château de Lis" pointbar (figure 9.12). Figure 9.12 a shows counter pointbars from 1995, that developed during two phases of accretion (1,2). Initially the bars formed in the sharpest part of the corner (1), before bars were added upstream and became larger (2). Other bars developed as scroll bars and through chute cutoffs ended up in the outer bend, similar to the situation in 1954 (figure 9.3) and at Chemilly (figure 8.11). Two scroll bars were attached to the pointbar on the northern bank in 1992 (3). The bars were isolated from the pointbar in 1997; the moved downstream and their form was slightly changed. In 1995 the upper bar was still joined with the pointbar, while the bottom bar was submerged in the channel (not eroded). In 1997, erosion removed part of the counter pointbars from 1995 and in 1998 the bar complex in the channel was partially eroded (figure 9.12 b). In later years the bars were added to the southern bank (at the downstream end of the "Château de Lis" meander) and the outer part of the sharp meander was filled with sediment.

Periodic cutoffs occurred because two sharp bends were a short distance apart and high discharges crossed over the downstream pointbar (see also section 8.2.2). Channel relocation (northwards) ensured that bars between the initial and eventual channel remained intact and were barely eroded. The southern channels were abandoned and filled with sediment.

The downstream part of the Château de Lis pointbar had little curvature. The upstream profile showed an asymmetric profile with bar development, while further downstream a riffle profile (with a bar in the middle) was present just before the crossing of flow (figure 9.11; cross section 5). The inner bank was steep as a result of channel erosion and sediment transported

by high discharges through the abandoned channel and across the pointbar. Sedimentation occurred at the highest point, before water entered the outer bend channel.

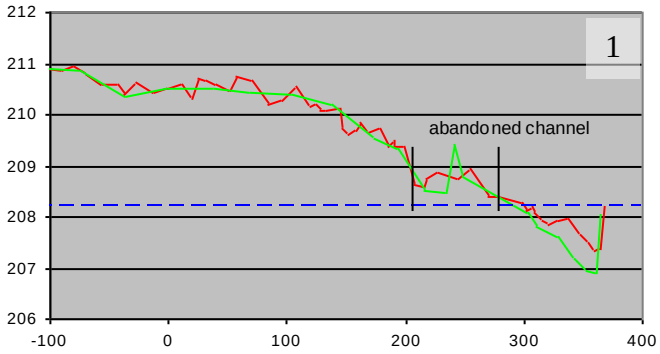

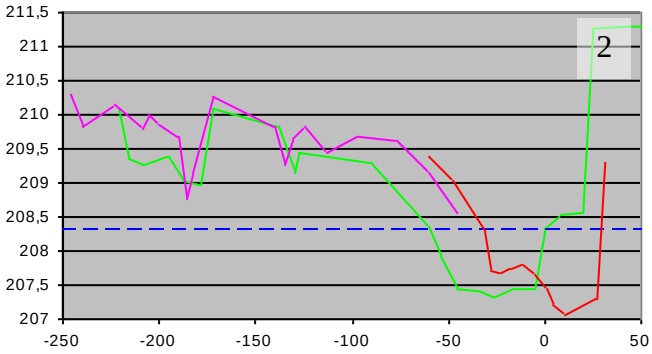

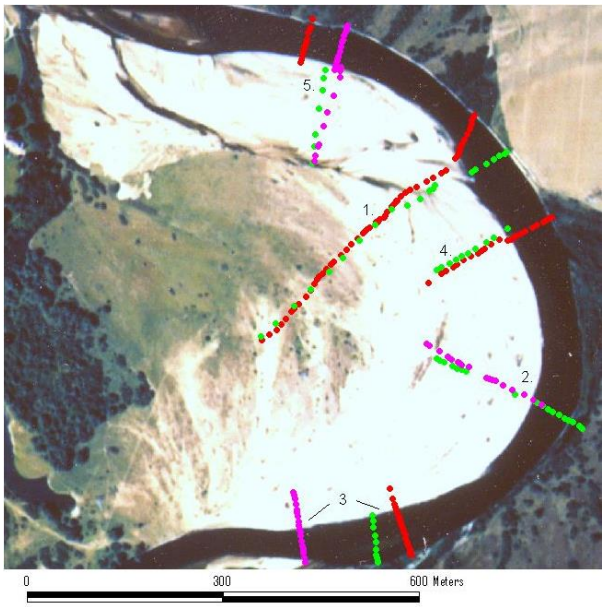

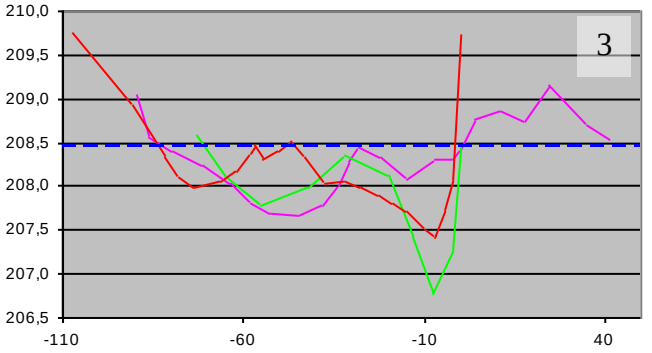

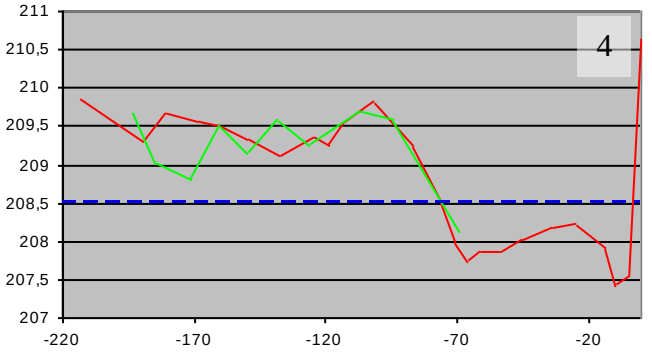

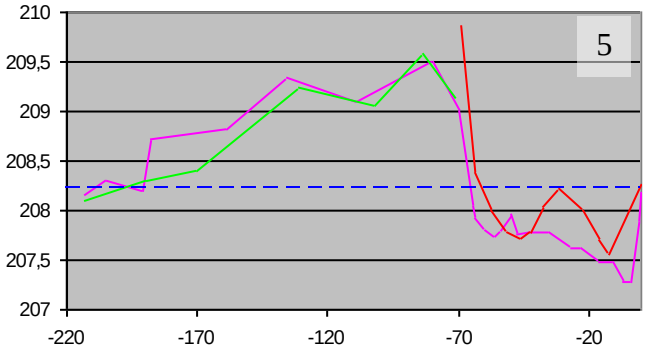

Figure 9.11: ***2002*** *aerial photo with the location of cross sections from 2002 (green) and 2003 (purple and red). The numbered profiles are displayed around the location map. On the x and y axis are height and distance, both in meters. Heights are related to the French national 0 point. Distances are related to a zero point where the profiles are closest together or in the case of profile 3 and 5 the outer bend was taken as zero point.*

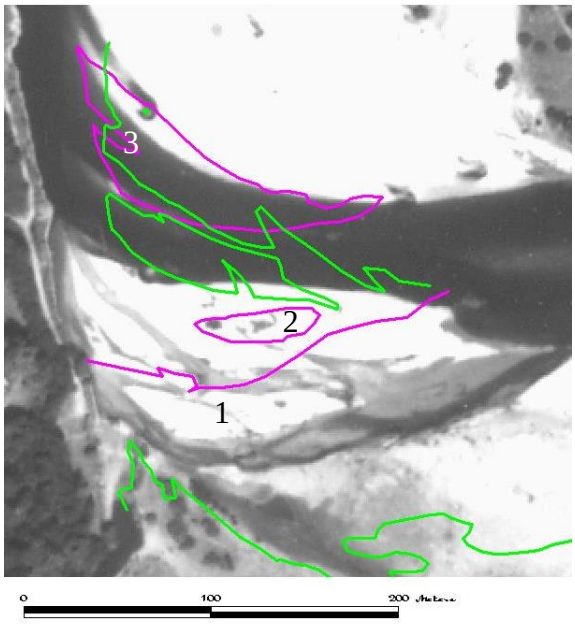

*Figure 9.12a: **1995** aerial photograph with bars and shorelines from 1992 (green) and 1997 (purple).*

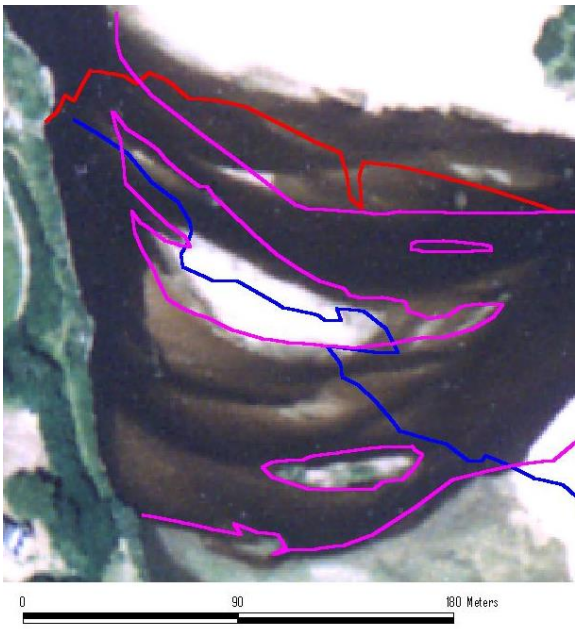

*Figure 9.12b: **1998** aerial photograph with bars and shorelines from 1997 (purple), 2000 (blue) and 2003 (red).*

9.3 Overall meander change

The bend at Château de Lis expanded laterally and downstream, increasing its radius, until it was cutoff in the late 1970's (figure 9.13). After the cutoff lateral development continued, decreasing the bend radius. In the early 1990's a chute cutoff occurred, causing the development of a compound bend. Erosion was concentrated at the downstream bend, while at the upstream end a less sharp bend developed. Between the two compound bends, the pointbar showed lateral retreat between 1995 and 1997 (figure 9.10). A cutoff of the downstream pointbar before 2000 straightened the second part of the "Château de Lis" bend. This was only temporary as the upstream bend expanded laterally, increasing its radius and directing flow outwards into its old channel (figure 9.10).

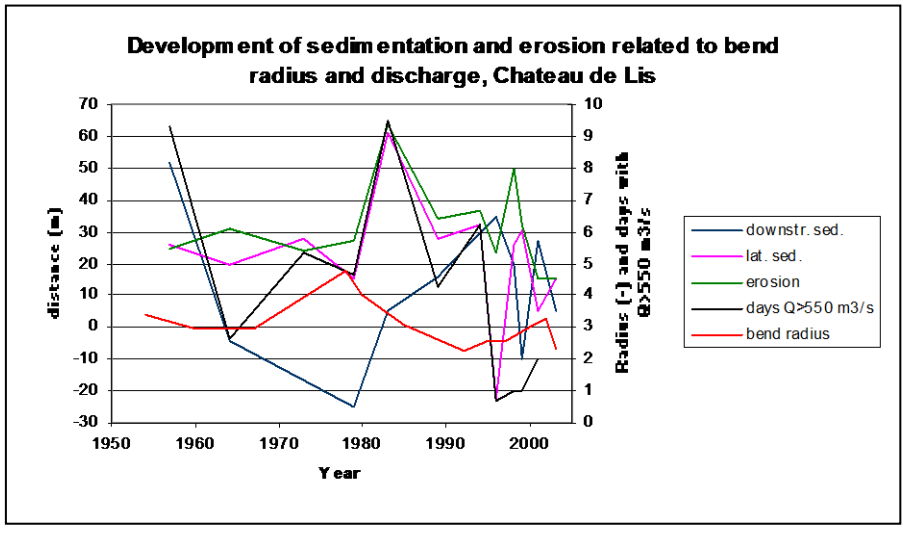

Figure 9.13: Annual pointbar development (sedimentation and erosion) and factors average discharge and bend radius in time.

10. Meander and pointbar development case 5: Beauregard

10.1 Long term meander history

1957

In a part of the Allier that had a dominating braiding pattern (section 2.3), a meander at Beauregard, started to develop (figure10.1). Incoming flow was directed towards the south-western bank causing erosion (purple). On the opposite bank a pointbar, 20 to 30 meters wide, slowly developed. Trees grew on the pointbar near the waterline revealing that sedimentation amounts were limited. At an upstream protuberance the main flow let go of the bank causing turbulence, behind which the pointbar developed in calmer water.

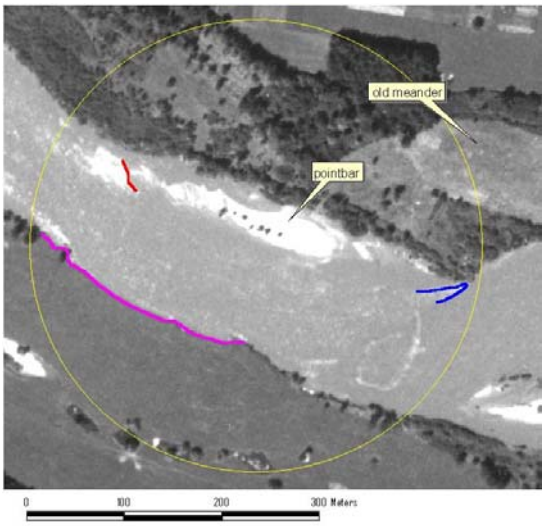

*Figure 10.1: **1957** aerial photo: "Beauregard" bend, encircled in yellow, eroded bank in purple, bar contour in red and flow turbulence in blue.*

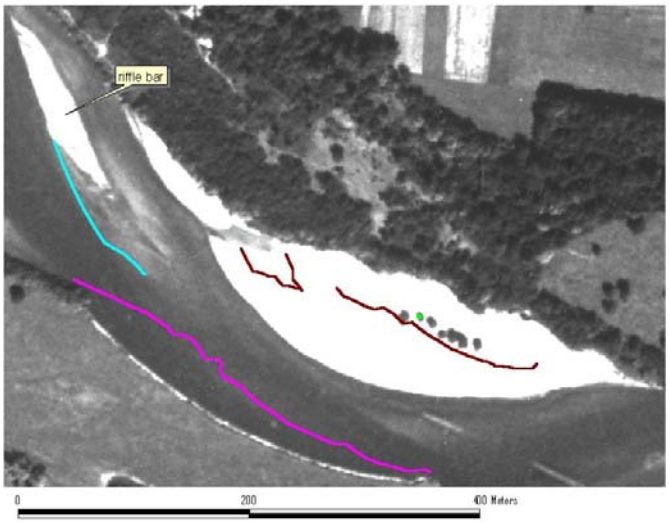

*Figure 10.2: **1963** aerial photo; underwater bar in light blue and from 1957: inner bank in brown and outer bank in purple.*

1963

The pointbar expanded in downstream and lateral direction to a great extent when compared to the limited amount of erosion in these directions (figure 10.2). Lateral expansion was the result of the development of helicoidal flow and an asymmetric profile that allowed space for sedimentation of the inner bend. Downstream sedimentation attached a 20 meter wide bar to the pointbar, but also occurred near at the riffle bar (25 meters wide). With an increasing bend size, the riffle bar was added to the pointbar.

1967

Between 1963 and 1967 flow at the downstream end of the bend was diverted to a southern channel (figure 10.3). The riffle topography in the abandoned northern channel was partially preserved in the form of stagnant pools (1) and an indented shoreline (2). The bend expanded with the lateral accretion of a bar attached to the point bar (red) and an island a little further downstream (3), about 25 meters wide.

1971

The bend continued to expand downstream (figure 10.4). Lateral sedimentation was concentrated near the downstream, underdeveloped, end of the pointbar. The island from 1967 (figure 10.3; 1) was attached to the pointbar, opposite from the location of maximum erosion. On the upstream end a bar just over 10 meters wide developed. The downstream end of the bar, marked by a swale at the shoreline coincided with the beginning of the outer bend.

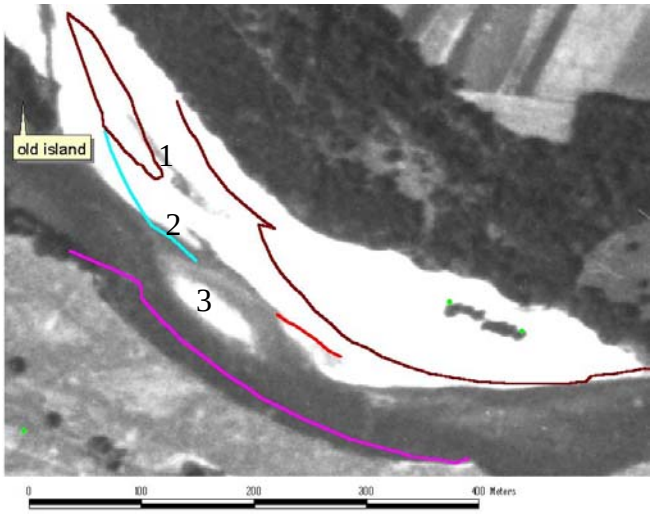

*Figure 10.3: **1967** aerial photo; scroll contour in red, and from 1963: underwater bar in light blue, inner bank in brown and outer bank in purple.*

1975

Between 1971 and 1975, outer bank erosion and pointbar accretion occurred along the whole bend, including the upstream part. (figure 10.5). At the upstream end of the bend the thalweg was reflected inwards before crossing back to the outer bend at a riffle (insert). This flow pattern allows the development of an upstream bar of about 25 meters wide (1). Bars further downstream (2), about 20 meters wide, show an older phase of scroll bar development.

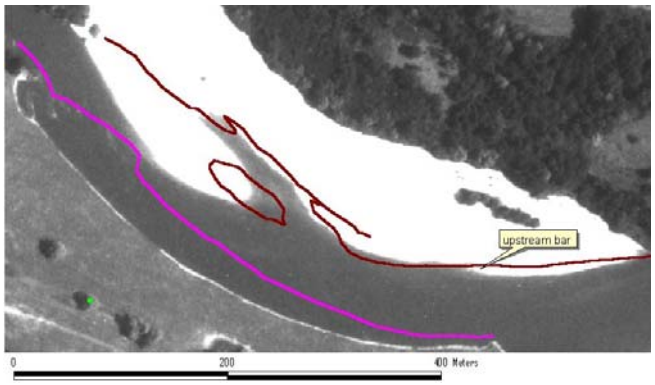

*Figure 10.4: **1971** aerial photo; the 1967 inner bank and scroll patterns in brown and the 1963 outer bank in purple.*

1980

Erosion and sedimentation were mainly concentrated in downstream direction (figure 10.6). The riffle bar from 1975 was located just in front of the (1980) pointbar. The nearly 20 meter wide bar was remoulded slightly to a scroll bar (blue), with a swale between it and the forested bank. Halfway down the pointbar a major scroll bar of nearly 25 meters wide was present (1), while at the upstream end a remnant of the upstream bar from 1975 was visible (2).

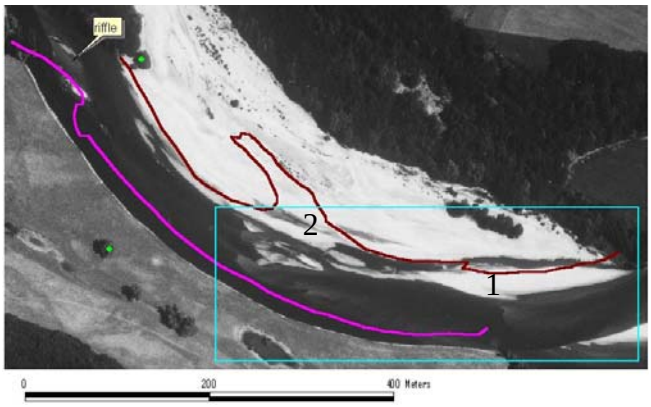

*Figure 10.5: **1975** aerial photo: the 1971 inner bank in brown and outer bank in purple. Insert shows 'high contrast' channel in with the thalweg marked with blue arrows.*

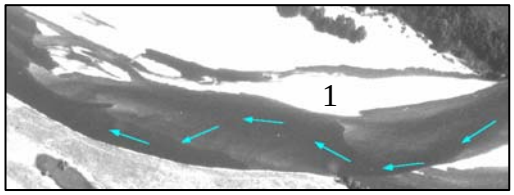

1985

Between 1980 and 1985 the pointbar grew notably in laterally, but mostly in downstream direction, while outer bank erosion was limited (figure 10.7). Various scroll patterns (swales) were visible as dark contours and a vegetated stroke. The swale from 1980 can be extended in later scroll patterns (1). A scroll bar developed halfway through the bend, while at the end of the pointbar a riffle-like bar was added. It had an upstream extension and along its edge (right) a channel was abandoned.

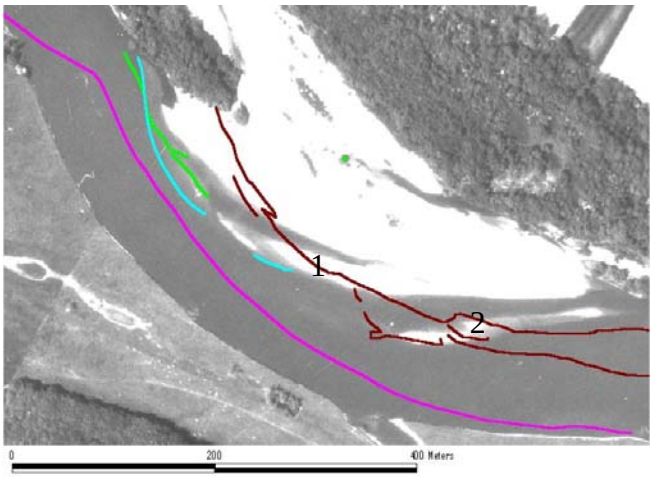

*Figure 10.6: **1980** aerial photo; (scroll) bars in blue and from 1975; inner bank and scroll bar contours in brown, outer bank in purple and riffle bar in green.*

1993

Pointbar development between 1985 and 1993 was limited to the downstream end, consisting of two scroll bars that are partially obscured by high water levels (figure 10.8). On the pointbar older phases of scroll bar development were recorded by vegetation (green) that developed in swales. The scroll bar from 1980 lied within a vegetation stroke and expanded downstream (1981) before a new lateral phase was added (1982). Two bars were added in 1983 and 1984 with a lateral and downstream component. Vegetation most likely developed with low and constant discharges, in the spring of 1982 and 1984 (similar to St. Loup, figure 6.6; 2).

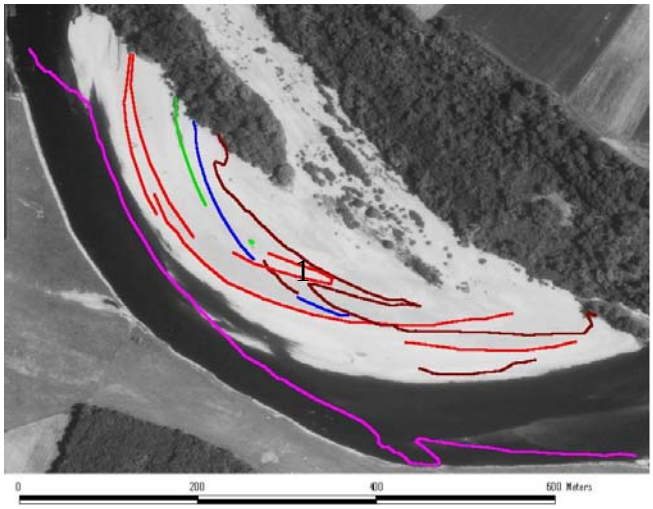

*Figure 10.7: **1985** aerial photo; scroll contours in red; from 1980: inner bank in brown, outer bank in purple and underwater bars in blue.*

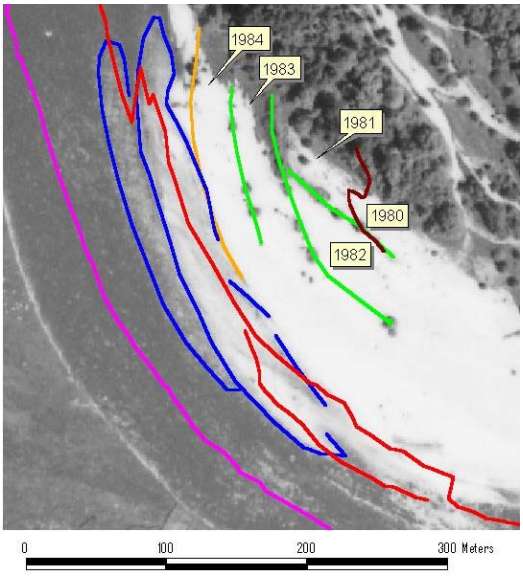

*Figure 10.8: **1993** aerial photo; vegetation (scroll) contours in green and underwater scroll bars in blue; from 1985: inner bank in red, scroll pattern in yellow, and outer bank in purple; 1980 inner bank in brown.*

10.2 Meander development between 1993-2003

10.2.1 Outer bend erosion

Resistant outer bank material divided the bend in two (figure 10.9; between 1 and 2). Two dents are found in the bend (1,2), where the flow ran into and moved away from the resistant bank. The stretch of channel, along the resistant bank, was straight and becoming becoming longer in time. The highest amounts of erosion were found near the downstream end of the bend (3), increasing from about 5 to 10 meters per year while moving downstream in time.

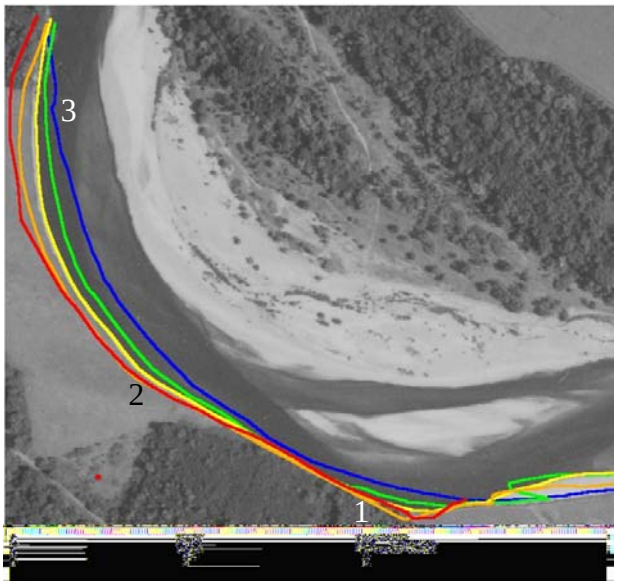

*Figure 10.9: **2000** aerial photo with outer banks from 1993 (blue), 1998 (green), 2000 (yellow), 2002 (orange), 2003 (red).*

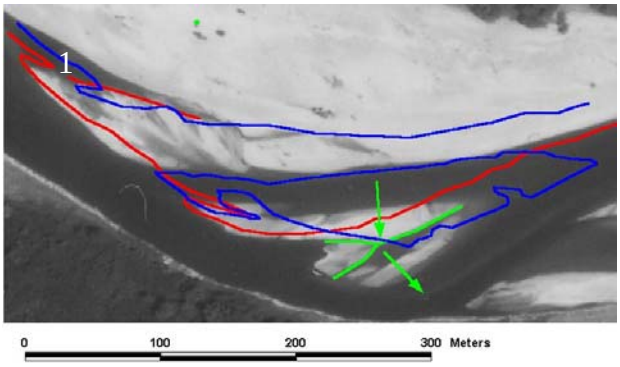

*Figure 10.10 a: **1998** aerial photo with scroll patterns marked in green; bars and shorelines from 2000 (blue) and 2002 (red).*

Figure 10.10 b: A photograph from 2003 of the scroll patterns visible in figure 10.10a.

The dent at the upstream end of the resistant bank (1) was sharpening and slowly eroding upstream, in south-eastern direction. The sharp bend and the direction of incoming flow (low sinuosity) allowed the occurrence of chute cut-offs (figure 10.10).

10.2.2 Point bar sedimentation

Bars that made up a cut-off island, in the upstream part of the bend (1998) showed a change in sedimentation direction eastwards (figure 10.10). Erosion could only make room for sedimentation in this direction because of the resistant bank. The cut-off island grew in size and migrated inward, towards the pointbar. The northward expansion was enabled the decreasing size of the “cut-off” channel that also migrated northwards. In 2003, the downstream end of the high water channel was located in a former swale (1).

Various bars were present in the channel at the upstream bend (figure 10.11; cross section 1). The distance between bar crests increased with age in the downstream profile from 23 to 29 (channel bars) till at least 30 meters (to the adjacent crest on the pointbar that was partially eroded by the chute channel). The upstream profile showed riffle bars that were asymmetric in opposite directions. The bars formed a short transition between the upstream part of the “Beauregard” bend, that migrated upstream and the bend upstream from it, that had a low sinuousity and expanded in downstream direction.

Along the straight resistant part of the bend a transition from an outer bend to a wider riffle was visible (figure 10.11; 2). Initially there was a deep channel on the outside (left) and three distinct bars on the inside, with 15 and 30 meters in between. In 2003 the channel became wide and developed a profile characteristic for a riffle, with multiple channels (chute channel at x = 110 m). Further along the resistant bank (cross section 3), the channel was even wider (65 meters with low discharge). Flow has crossed to the inner bank and (riffle) bars developed in the middle and outer part of the channel. Helicoidal flow was disturbed near the abrupt change in flow direction at the beginning of the resistant outer bank (figure 10.9; 1). Along

the following straight path flow moved inwards (reflected of the outer bend), forming an immature bend in the opposing direction similar to figure 10.5 (insert). Flow moved towards the outer bend again at the end of the straight stretch, where the downstream bend commenced. A riffle crossed between the resistant bank and the downstream part of the bend (figure 10.11).

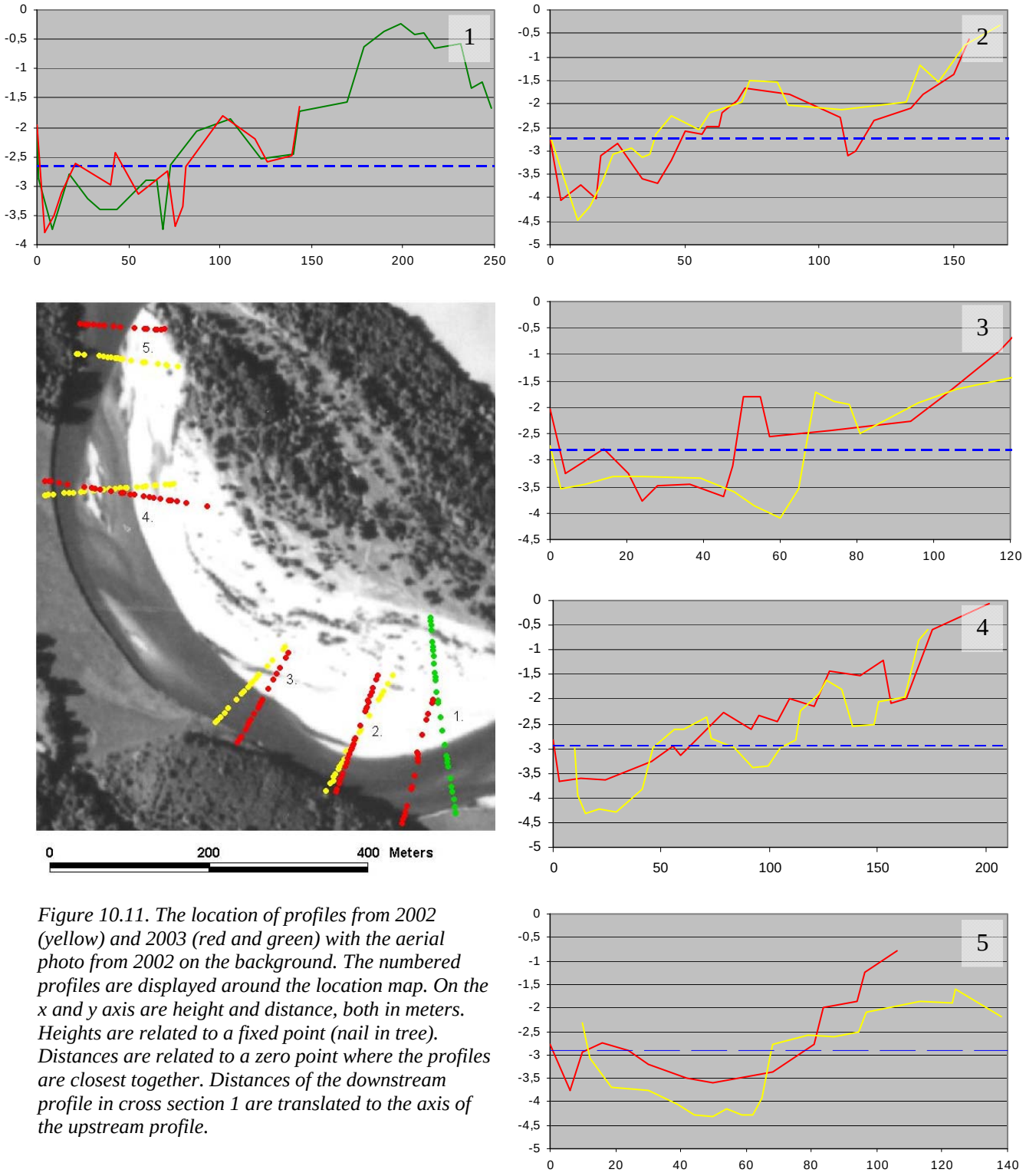

Figure 10.11. The location of profiles from 2002 (yellow) and 2003 (red and green) with the aerial photo from 2002 on the background. The numbered profiles are displayed around the location map. On the x and y axis are height and distance, both in meters. Heights are related to a fixed point (nail in tree). Distances are related to a zero point where the profiles are closest together. Distances of the downstream profile in cross section 1 are translated to the axis of the upstream profile.

In the period 1993-1998 there was initially a phase of downstream pointbar expansion (figure 10.12; 1), followed by lateral development (2,3). Underwater bars from 1993 (blue) moved

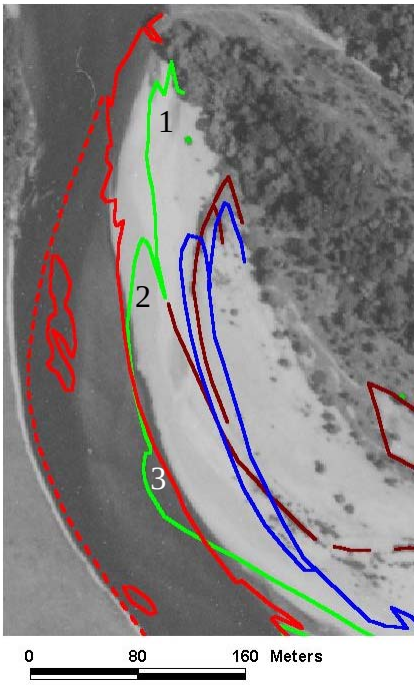

*Figure 10.12: **2000** aerial photo with vegetation patterns in brown; bars from 1993 in blue and inner banks from 1998 (green) and 2002 (red), with a dotted riffle margin.*

downstream and inwards slightly, where vegetation (brown) developed along their edges. A swale from 1998 (on the inside 2) also coincided with later vegetation patterns that occurred in its extension. In the period after 1998 downstream sedimentation dominated and a riffle developed along the bend.

Near the axis of the downstream bend an asymmetric profile developed, especially in 2003 (figure 10.11; cross section 4). The distance between scroll bars from that year increased from 24 to 32 and 43 meters (bars at x = 55, 80, 110 and 150) with age, moving onto the pointbar. The bars also became less asymmetric and higher. Scroll bar development in 2002 was effected by high water channels that cut across the point bar.

Near the downstream edge of the pointbar flow crossed to the inner bank (figure 10.11; cross section 5). In 2003 a bar had already developed along the left bank, belonging to the downstream pointbar. Its development was aided by the abundance of trees in the channel, whose roughness directed flow inwards. The scroll bar was only slightly asymmetric because helicoidal flow in this stage of the new bend was weak or absent.

10.3 Overall meander change

The meander at Beauregard was unique in a river section that had a more braiding character. Its continuous presence was related to a change in flow direction (bank resistance), that caused centripetal forces and lateral motion. In the period between 1957 and 1993 the relative bend radius increased from about 4 to 6 (figure 10.13). The increase in bend radius, that lengthened the bend. was caused by meander expansion that mainly occurred at the downstream end. The upstream part of the bend was not eroded because flow had a stable straight entrance into the bend from a stretch of river with low sinuousity.

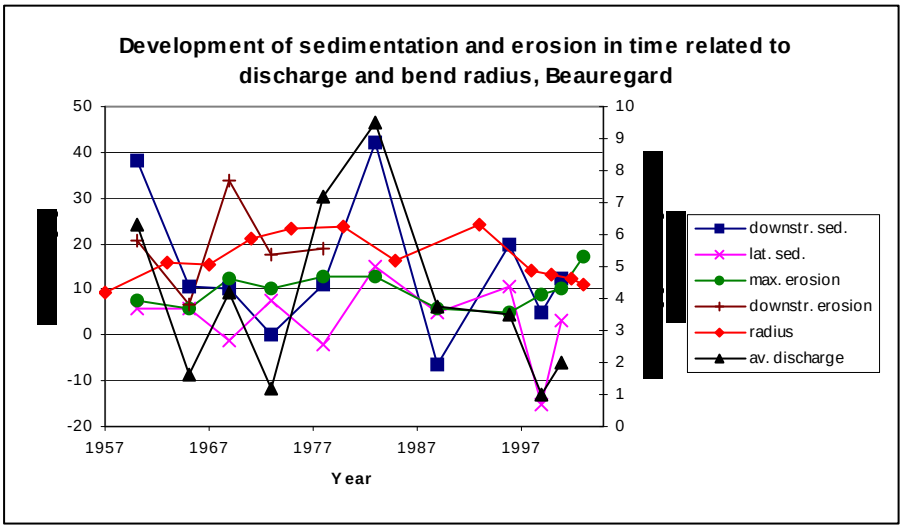

Figure 10.13: Annual pointbar development (sedimentation and erosion) and factors average discharge and bend radius in time.

After 1993 the bend has been divided by a resistant bank, developing a compound bend. The lateral component of erosion in the downstream bend strengthened. This was a result of strengthening helicoidal flow in the lengthening bend and the presence of a resistant forest near the downstream end of the bend (figure 10.9). This caused the increase of curvature in this part of the bend (figure 10.13). The radius of the upstream bend decreased because of upstream erosion that caused the dent to sharpen.

The large bend (low curvature) ensured enough room for the development of scroll bars and intermittent swales that allowed scroll bars to be distinguished. Scroll bar width varied between 15 to 30 meters (figure 10.14 and 10.11; 2,4). Occasionally bars were narrower (figure 10.4; upstream bar) when there was a lack of room for sedimentation caused by a resistant outer bank. Scroll bars were wider with low bend radii and narrower with large bend radii (figure 10.14).

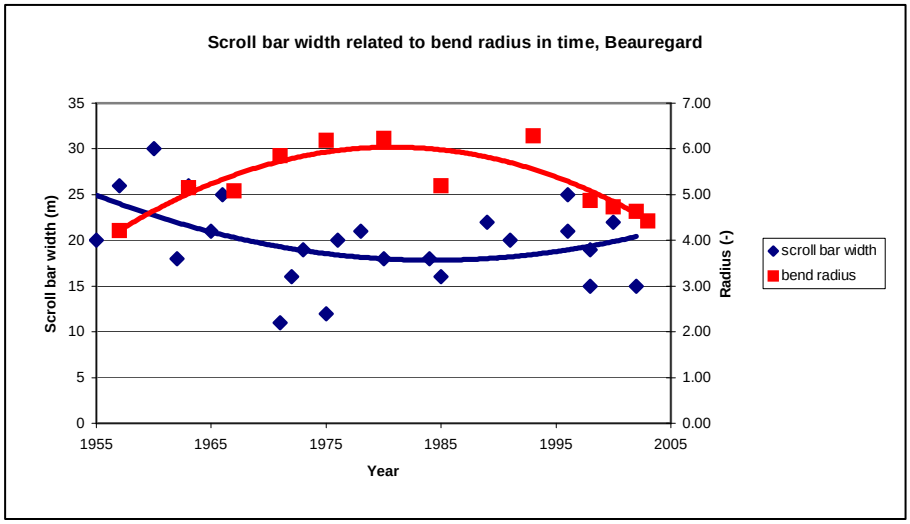

Figure 10.14: Scroll bar width and bend radius development in time, including polynomial trendlines.

11. Influence of discharge on meander development

11.1 Relation discharge – meander development of individual bends

Three variables were used to relate discharge to sedimentation and erosion, namely: maximum discharge, days with discharge above 550 m^3/s and average discharge (chapter 5). The number of days with discharge above 550 m^3/s was used as the main variable in this report. It covers the range of discharges capable of substantial sediment transport well (section 3.3.2 and chapter 5). De Kramer (1998) also found that meander migration correlated best with bend radius when corrected for the amount of days with discharges above 550 m^3/s.

For all individual bends the amount of days with discharge higher than 550 m^3/s was correlated with erosion and (lateral and downstream) sedimentation (figure 11.1 a-e). Regression (direction and form) and correlation (strength) of linear relationships were analysed. Statistically significant correlation was determined on the basis of explained variation (R^2) based on an a-select F distribution (with about 12 data points, R^2 values greater than 0.35 are significant with 5% uncertainty). All bends showed increasing linear trends, where large amounts of erosion and sedimentation corresponded to longer periods of high discharge (especially clear with higher correlation).

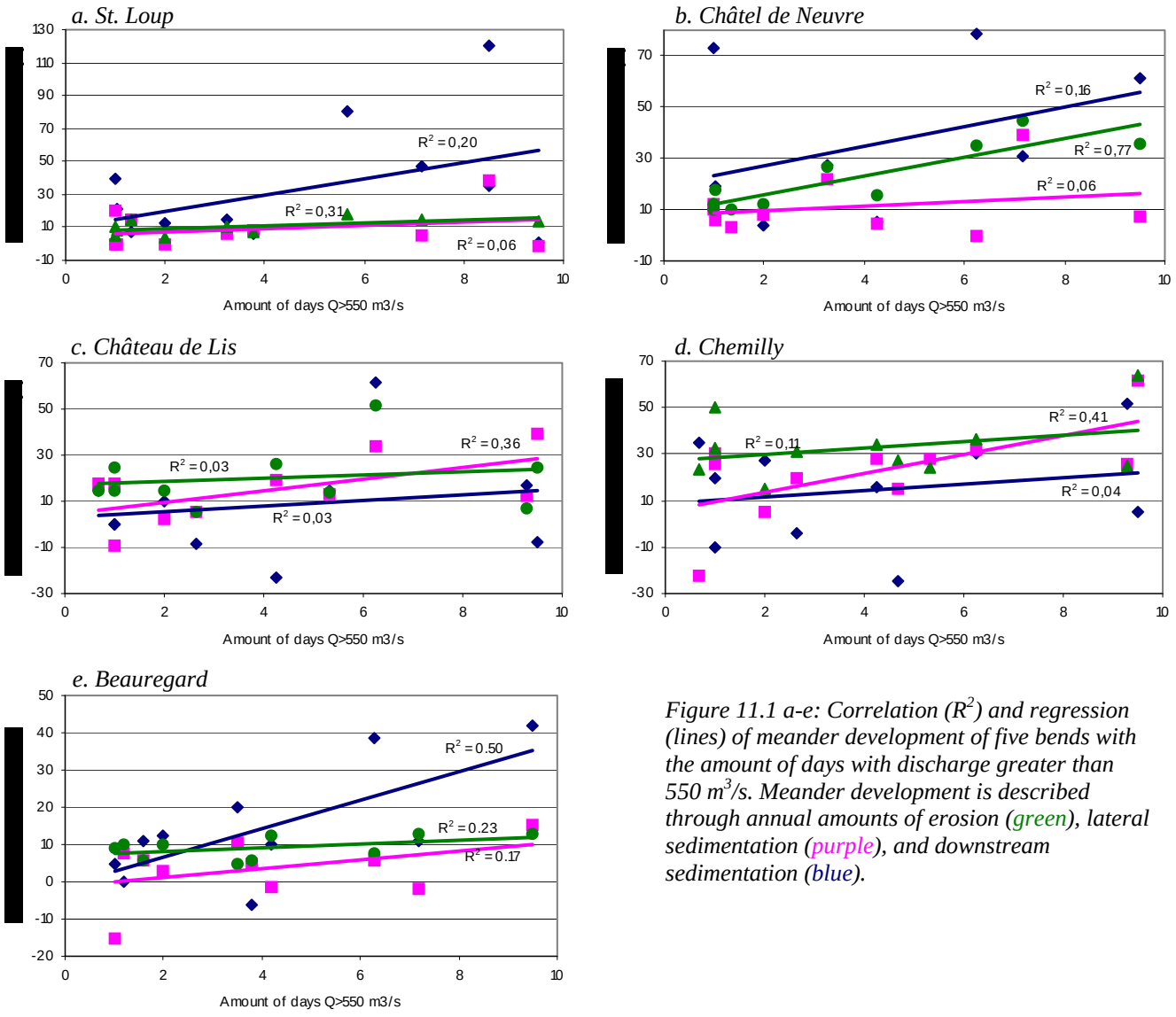

Figure 11.1 a-e: Correlation (R^2) and regression (lines) of meander development of five bends with the amount of days with discharge greater than 550 m^3/s. Meander development is described through annual amounts of erosion (green), lateral sedimentation (purple), and downstream sedimentation (blue).

The strongest relationship (statistically significant) between discharge and erosion was found at Châtel de Neuvre (b), $R^2 = 0.77$, where resistant banks were absent and the meander had the freedom to migrate. At the complex bends of Château de Lis and Chemilly (c,d) discharge correlated significantly ($R^2 = 0.36$ and 0.41) with lateral sedimentation, while this relationship was the weakest in the other bends. In the three shorter bends meander changes, related to higher (>550 m^3/s) discharges, took place predominantly at the downstream end of the bend. Erosion at St. Loup and Châtel de Neuvre (a,b), $R^2 = 0.31$ and 0.77, and downstream sedimentation at Beauregard (e), $R^2 = 0.50$, showed the strongest correlation (only erosion at St. Loup is not significant). In complex bends such as Chemilly and Chateau de Lis, high discharges cause lateral expansion, near the bend apex, moving inwards at the end of the long bend hampering outer bank erosion and downstream sedimentation.

11.2 General relationship discharge – meander development (all bends combined)

11.2.1 Direct correlation and regression

Meander migration showed trends with variable gradients and correlation (significance) when related to discharge. The variance is related to local variables such as bank resistance, pointbar vegetation and the state of meander development (chapter 13). The combination of the results of all bends caused the elimination of local variables and revealed the general influence of discharge on sedimentation and erosion (figure 11.2).

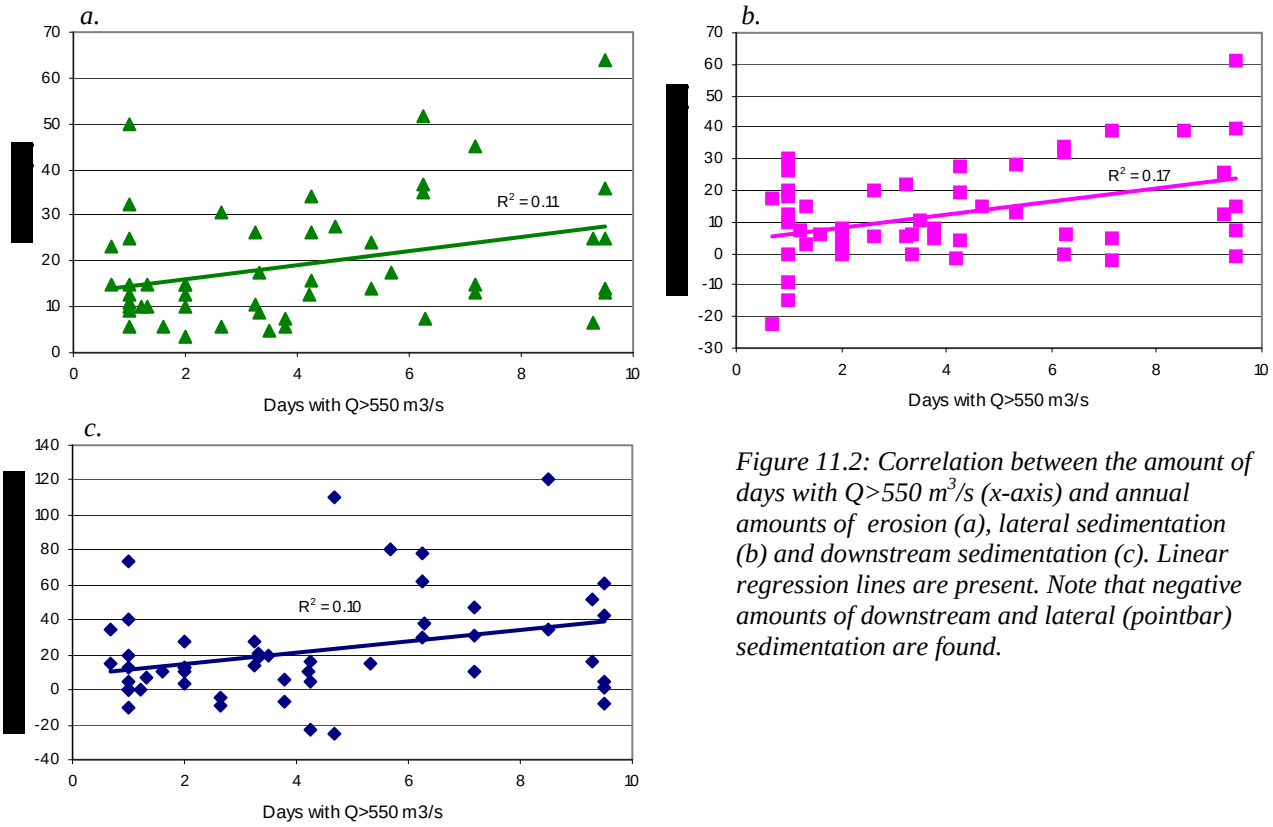

Figure 11.2: Correlation between the amount of days with Q>550 m^3/s (x-axis) and annual amounts of erosion (a), lateral sedimentation (b) and downstream sedimentation (c). Linear regression lines are present. Note that negative amounts of downstream and lateral (pointbar) sedimentation are found.

Trendlines show that increasing amounts of erosion and sedimentation are related to longer periods of high discharges. The trends however remain weak, even though they are statistically significant.

11.2.2 Correlation strength with varying discharge measures and corrections

To determine the influence of (measuring) inaccuracies, stochastic variables and the value of the results, sensitivity analyses was applied. Meander migration, erosion and lateral / downstream sedimentation, was correlated with three measures for discharge (table 11.1; with no correction). The strength of correlation was also determined between discharge measures and erosion and sedimentation that was corrected for bend radius (table 11.1; correction was carried out using the curves from figure 12.2). The third case is based on data excluding the 1950's, where deviant stage-discharge relationships existed (erosion and sedimentation were also corrected for bend radius). The last set of correlation coefficients is based on data measured over periods of two years or less (a mere 13 data sets instead of approximately 50). Discharge is highly variable and can influence meander development on a short timescale, one to two years).

	correction	erosion	lat. sed.	down. sed.
days Q>550 m3/s	none	0.11	**0.17**	0.10
	R (bend radius)	**0.22**	**0.20**	0.11
	R + 1950's	**0.33**	**0.19**	0.11
	R + timescale	-	**0.44**	**0.43**
Q average	none	-	0.12	**0.16**
	R (bend radius)	**0.35**	0.10	0.10
	R + 1950's	**0.35**	0.10	0.12
	R + timescale	-	-	0.26
Q maximum	none	0.11	**0.14**	-
	R (bend radius)	**0.15**	**0.18**	-
	R + 1950's	**0.22**	**0.18**	-
	R + timescale	-	**0.49**	-

*Table 11.1: Determination coefficients (R^2) between different discharge measures (days Q>550 m^3/s, Q average and Q maximum) and meander migration (erosion, downstream and lateral sedimentation). Correlation is done without correction, with correction for bend radius, for data from the 1950's and for data measured over periods longer than 2 years. Statistically insignificant R^2 values (uncertainty > 5%) are omitted and significance with an uncertainty of less than 1% is displayed in **bold**.*

The discharge measure that correlates best (significant) with meander migration is the amount of days with discharge greater than 550 m^3/s, although the relation is weak.

11.2.3 Lateral extent of erosion and sedimentation

The majority of the determination coefficients (R^2) indicate statistically significant relationships, but they show different results in the corrected scenarios. Erosion has a varying correlation with discharge measures in the different scenarios (table 11.1). On average it has the strongest correlation with discharges above 550 m^3/s (figure 11.3 a). Correlation with the other discharge measures is however barely lower and most often significant (table 11.1). Lateral sedimentation shows slightly weaker relationships, with the strongest and most significant correlations existing with discharges above 550 m^3/s (figure 11.3 b) and maximum discharge (table 11.1). Decreasing the time scale of measurements led to an increase in the correlation coefficients of lateral (and downstream sedimentation), while erosion showed worse and statistically insignificant correlation (table 11.1). Sedimentation has a strong relation with discharges on a shorter time scale, while erosion shows more continuous development on a larger time scale.

The most representative or strongest relationships (statistically significant) between discharge and lateral erosion and sedimentation are displayed in figure 11.3. Both trendlines have a slope of 0.25. Erosion shows a weak linear relation, with data scattered above and below the linear trend line (figure 11.3 a). A more clear linear trend is visible with lateral sedimentation,

but a lower determination coefficient (R^2) is found, that can be assigned to a few extreme values (figure 11.3 b).

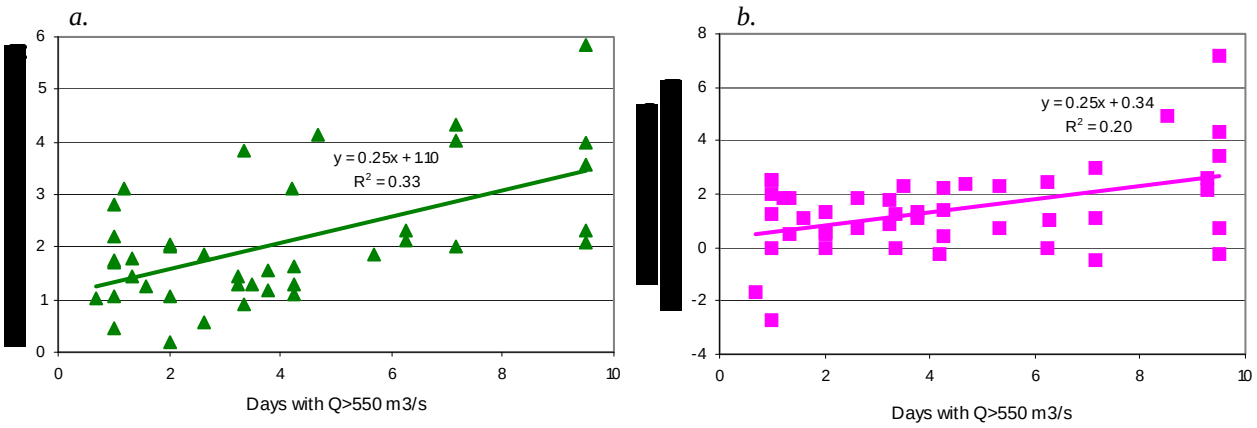

Figure 11.3: Correlation between the amount of days with Q>550 m^3/s (x-axis) and annual amounts of erosion (a) and lateral sedimentation (b) corrected for bend radius. Observed amounts of erosion were corrected for bend radius, by dividing them with expected values based on bend radius. Linear regression lines are present.

Discharge has a limited, though significant, influence on actual pointbar development, even though it determines a rivers capacity to cause erosion, transport and sedimentation. The influence of discharge on erosion can be great, up to 30%. Correlation varies little between erosion and the three discharge measures (table 11.1), but is strongest with discharges greater than 550 m^3/s. The actual influence of discharge on erosion shows great variation around regression line (figures 11.2 a and 11.3 a) and in correction scenario's (table 11.1). The relation between discharge and erosion is bound by constraints that vary from bend to bend, such as resistant banks, bend radius and upstream meanders (chapters 6 – 10, 13). The influence of discharge on lateral sedimentation (pointbar expansion) is more constant at about 20 %. Variation in correlation is low between bends (figure 11.3 b; little variation around regression lines) and in correction scenario's (table 11.1; the same applies for downstream sedimentation). Lateral sedimentation shows the strongest significant correlation with discharges above 550 m^3/s, where strong helicoidal, and therefore lateral, flow develops.

Sedimentation amounts are dependent on short term variations in discharge (table 11.1). Other factors such as bend radius, pointbar vegetation and upstream meanders remain more or less constant on a time scale of one to two years. Pointbar expansion, both lateral and downstream, occurs during specific discharges, alternating with periods of no change and phases of erosion. Outer bank erosion correlates stronger with discharge (over longer periods) because episodes of sedimentation do not occur, while local turbulence and bank processes (mass movement) ensure that erosion develops more continuously.

11.2.4 Amounts of erosion and transport

Correlating observed (lateral) sedimentation and erosion extents (in meters) with discharge indexes resulted in mostly significant but weak relationships (11.2.3). Daily sediment transport index values were calculated, based on discharge, and totalled over periods of years that correspond to observed periods of erosion (section 3.3.2). This led to the correlation of eroded distances with annually totalled transport indexes: the Meyer-Peter & Muller transport parameter and flow velocities exceeding the threshold of sediment motion (figure 11.4 a,b).

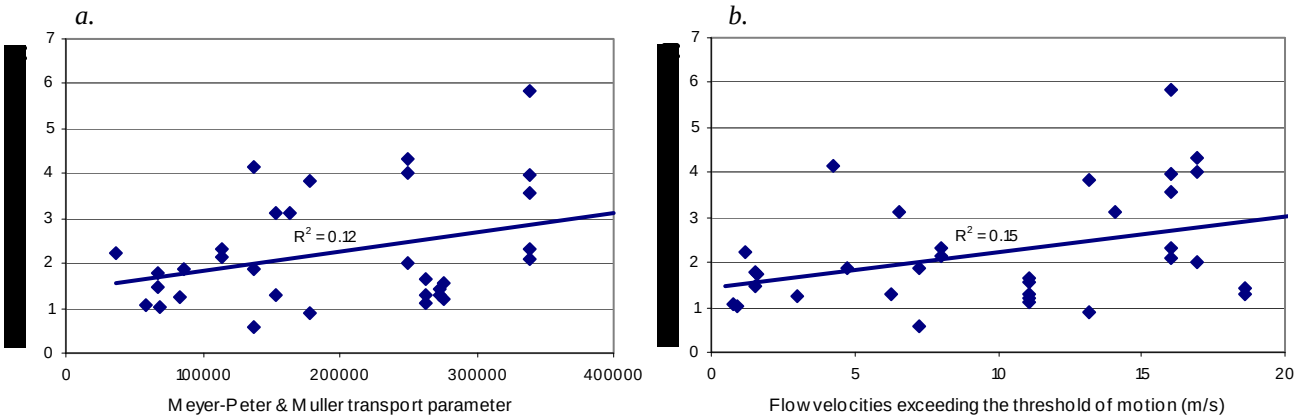

Figure 11.4 a,b: Transport parameters totalled over periods between 1960-1998 (stage and discharge data were complete) correlated to corresponding amounts of erosion. Observed amounts of erosion were corrected for bend radius, by dividing them with expected values based on bend radius.

The relationships between erosion and the transport measures show statistically significant increasing linear relationships, but are not stronger than relationships with discharge (section 11.2.3). The trend of the sediment transport index, m ~ m/s (figure 11.4 b) can be deduced from eroded volumes, m^3, that are proportional to flow velocities to the power 3, $(m/s)^3$ (section 3.3.1). A relation was expected between eroded distance (m) and the cubed root of the Meyer-Peter Muller transport parameter $(m^3)^{1/3}$, but this correlated even weaker than in figure 11.4 a. Calculating (representative) flow velocities and associated amounts of transported sediment add extra assumptions and uncertainties that prevent the improvement of the relationship between erosion and discharge.

Eroded floodplain areas were measured for a limited set of situations to add an extra dimension to maximum extents of erosion (section 4.1.2). The relation between eroded distance and area is weak because of varying meander form, that determines where and how intense erosion is (sections 3.3.3, 3.4.1). Eroded areas were correlated with the amount of days with discharge above 550 m^3/s and the flow velocity exceeding the threshold of motion (figure 11.5 a,b), that both showed the strongest relationship with eroded distance (figures 11.3 a, 11.4 b). The eroded area shows statistically significant increasing trends with the discharge and transport measures.

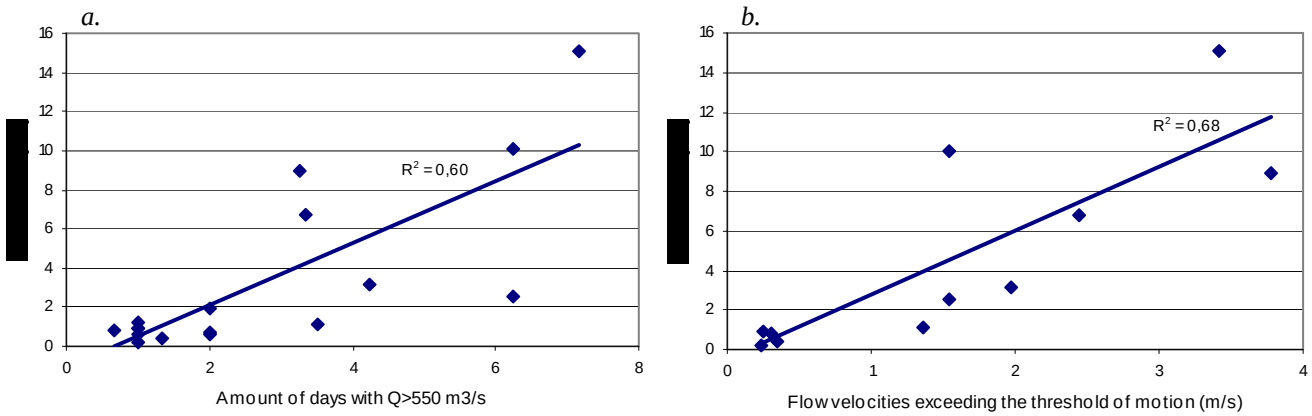

Figure 11.5 a,b: Eroded area correlated with the amount of days with Q > 550 m^3/s and the flow velocity exceeding the threshold of motion (transport index).

11.2.5 Downstream component of sedimentation and erosion along meanders

Similar to lateral erosion and sedimentation, the downstream sedimentation data of all bends was combined and corrected for various influences (table 11.1). Downstream sedimentation correlated significantly, though weakly, with discharges of nearly all heights (figure 11.6; average discharge), except the maximum values (table 11.1). The correlation remains constant despite accounting for errors and additional factors (table 11.1).

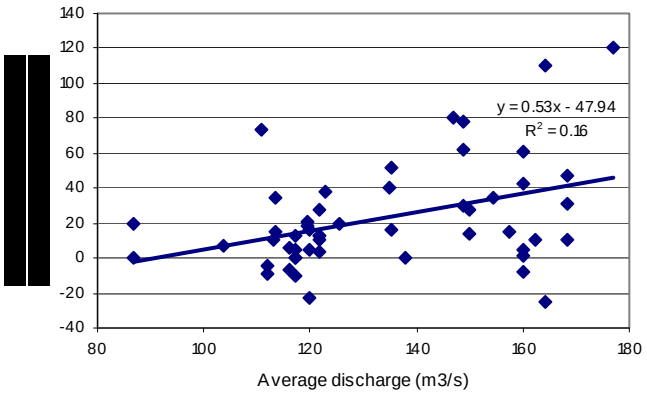

Figure 11.6: Correlation between average discharge and the downstream erosion and sedimentation.

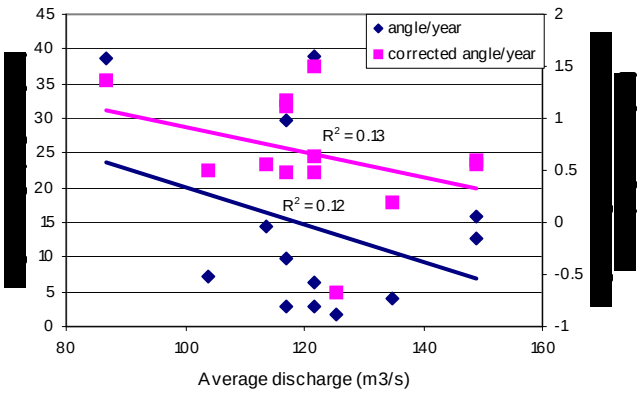

Figure 11.7: Correlation between average discharge and the downstream angle change of the center of erosion around the bend axis.

The component of erosion along the channel (downstream) was determined through comparing the center of erosion over a period of time (based on area) with the initial location of the bend apex (figure 4.4). The angle of rotation between these locations around the bend axis was determined for a set of bends (without cutoffs or resistant banks and corrected for bend radius, by dividing by expected value) and correlated to the different measures for discharge. No statistically significant relations were found, but with the exception of maximum discharge ($R^2 = 0.01$) weak negative gradients were found. The strongest relation is found between angle change and average discharge (figure 11.7). Both downstream erosion and sedimentation are related to lower discharges, represented by average discharge. The relation between downstream erosion and discharge is however not significant. Average discharge does significantly correlate with downstream sedimentation accounting for a mere 10 – 15 % of variation.

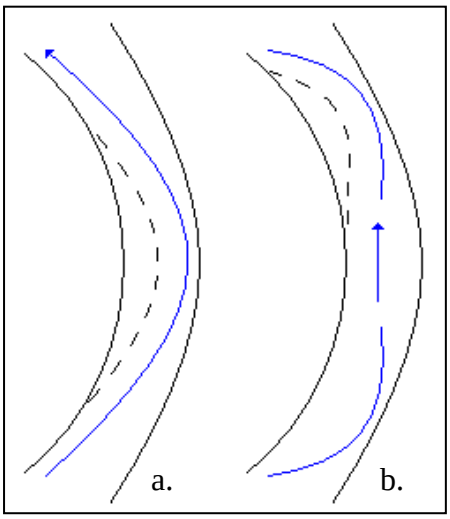

Discharge height influences where in a bend (helicoidal) flow is fully developed, causing meander migration (figure 3.7; section 3.4.1). Discharge also determines where flow moves towards the inner bend; halfway through a meander developing a compound bend, at the downstream end of a bend or overshooting it. The adjustment lengths of flow and morphology develop differently with increasing discharge; the adjustment length of sedimentation decreases, while that of flow increases (figure 3.8). Flow and morphology adjust simultaneously resulting in overall adjustment lengths of about 300 – 500 meters, which is 63% of the adjustment to equilibrium. Bend length and upstream meander development are therefore important for meander

Figure 11.7: The downstream location of erosion and sedimentation along a meander bend depending on discharge height; high (a) and low(b).

development in downstream direction. Meanders in the Allier are characteristically 800 – 1200 meters long and often have a complex nature (including rotational and compound bends). Because of the relative length and complexity of bends high discharges approach equilibrium halfway the bend (after approximately 500 meters; figure 3.8), where it causes lateral meander migration. Lower discharges have a lower sediment transport capacity, but shorter adjustment lengths that allow them to “meander” within a (compound) bend (figure 11.7 b; section 3.2.2). High discharges caused lateral expansion near the bend apex in long, complex bends such as Chemilly and Chateau de Lis (section 11.1). Flow then moves inwards at the end of the (long) bend limiting outer bank erosion and hampering downstream sedimentation (figure 11.7 a).

12. Influence of bend radius on meander development

12.1 The development of bend radius

Hickin (1977) described the progressive sharpening of a meander. Such behavior was seen over periods up to 25 years at St. Loup, since 1980 (figure 6.11), and Chemilly, until 1978 (figure 8.14). These cases did not show an accelerated increase in bend radius, which is expected with strengthening helicoidal flow.

Hickin (1974) found that the focus of erosion occasionally shifts, causing an increase in bend radius. Shifts in the location of erosion were caused by influences such as bank resistance, upstream meander development and a varying discharge. These factors caused the fluctuating development of bend radius at Châtel de Neuvre and Chemilly (figures 7.11 and 8.14) among others. Discharge influences the location of erosion and sedimentation along a bend (section 3.4.1 and 11.2.5) and therefore also influences the development of the bend radius. Discharges of different heights erode at different locations along the outer bend. In long bends varying locations of erosion can be differentiated, caused by yearly fluctuations in discharge (Chemilly and Chateau de Lis, figures 8.8 and 9.8). The bend at Beauregard (10.13) showed a more or less continuous increase in bend radius until the 1980's that was related to bend length and upstream meander development.

12.2 Relation bend radius – meander development of individual bends

On average bend radii of the individual bends correlated slightly worse with meander changes when compared to discharge (figure 12.1 a-e). The only statistically significant relationship was found at Châtel de Neuvre, between bend radius and erosion (b). With the exception of Château de Lis (d), bend radius showed the best (least poor) correlation with erosion.

Correlation with determination coefficients (R^2) higher than 0.1, even though they are not significant, show inclined trendlines that relate sedimentation and erosion to bend radius (figure 12.1) like at Châtel de Neuvre, Château de Lis (downstream sedimentation) and Chemilly (erosion). In these cases sedimentation and erosion increase with a decrease in bend radius (increase in bend curvature).

Linear trends reveal basic relationships using limited amounts of data, but are not anticipated when relating bend radius with meander development (section 3.3.3). Maximum migration values (bend radius approximately 2.5) and exponential decreases (with increasing bend radii above 2.5) are expected for standard meander development (Hickin, 1977; figure 3.6). Maximum erosion was found at Chemilly near a bend radius of 2.5 and erosion decreases with increasing bend radius, while at Châtel de Neuvre an exponential decrease in lateral erosion is recognizable (figure 12.1 b,c). Factors additional to discharge and bend radius also influenced the development of individual meanders, that deviated from standard meander development as described by Hickin (1977). At Beauregard and St. Loup, however, increased amounts of erosion correspond to increasing bend radius (figure 12.1 a,e). Although the determination coefficients are nearly negligible (R^2 = 0.08 , 0.09) the relation opposes that of a standard meander system (figure 3.6) and earlier relationships (figure 11 b,c). In both bends flow entered the bend fairly straight, due to the absence of an upstream bend. This allowed the bends to expand, taking a longer path along which (strong) helicoidal flow developed leading to (lateral) erosion (this will be further discussed in chapter 13). At Château de Lis, that was a compound bend for the largest part of the time, downstream sedimentation correlated best with bend radius (figure 12.1 d). The length of the bend caused meander development (before

and) after the apex of the compound bend (section 3.2.2), leading to downstream meander development (figure 11.7 b).

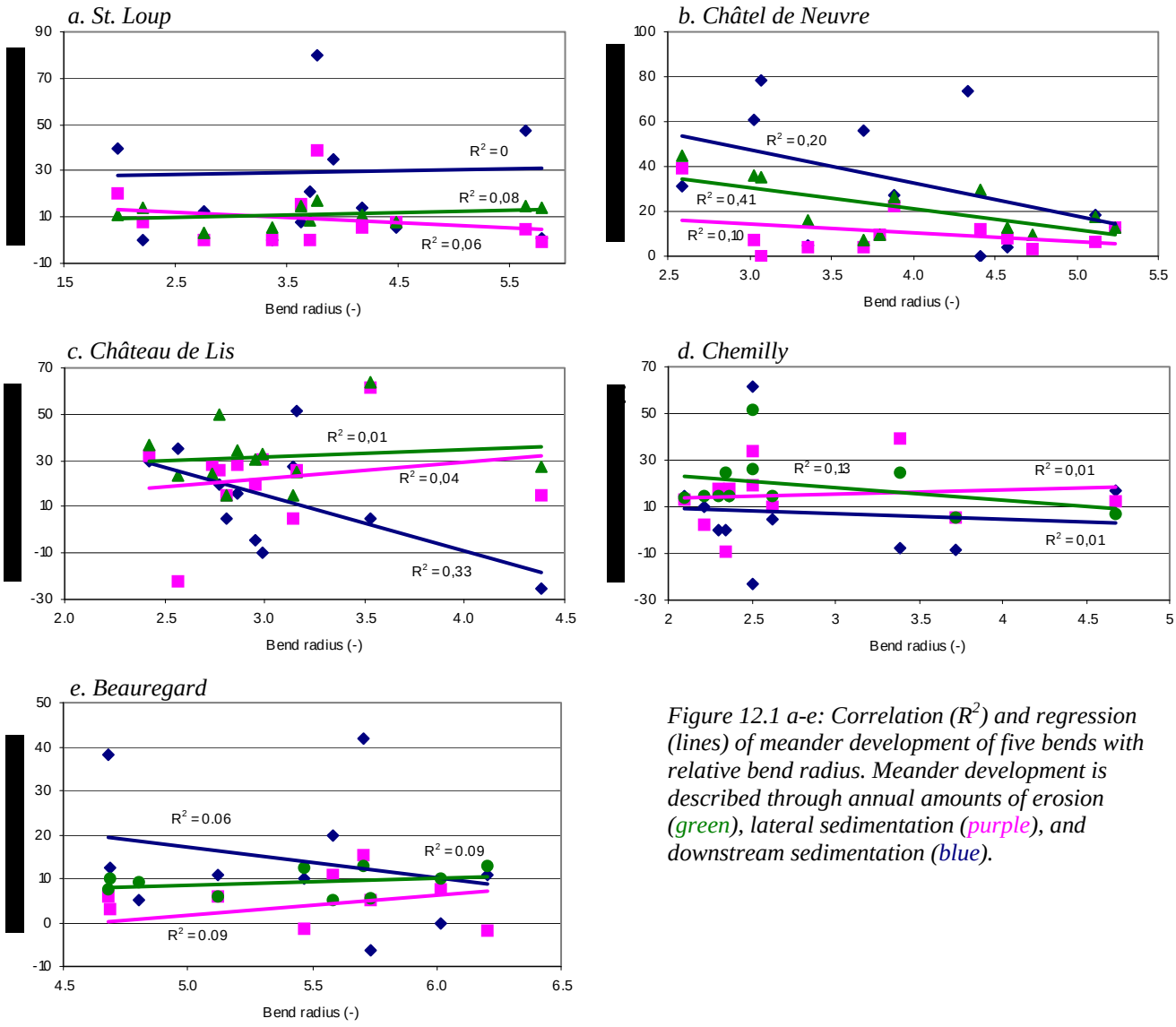

Figure 12.1 a-e: Correlation (R^2) and regression (lines) of meander development of five bends with relative bend radius. Meander development is described through annual amounts of erosion (green), lateral sedimentation (purple), and downstream sedimentation (blue).

12.3 General relationship bend radius – meander development (all bends combined)

12.3.1 Correlation and regression

Meander migration of individual bends showed weak (mostly insignificant) linear trends with bend radius, although exponential relations were also discernible (section 12.1). Combining the results of all bends neutralized the influence of remaining (local) factors on the relationship between bend radius and sedimentation / erosion, and therefore providing a more detailed view on this relationship (figure 12.2).

Trends based on bend radius were found in maximum sedimentation and erosion amounts rather than all the observed values (figure 12.2). Exponential regression lines through maximum values form envelopes around the results. Maximum meander migration (outer bank erosion and pointbar accretion) increases with a decreasing bend radius until a maximum

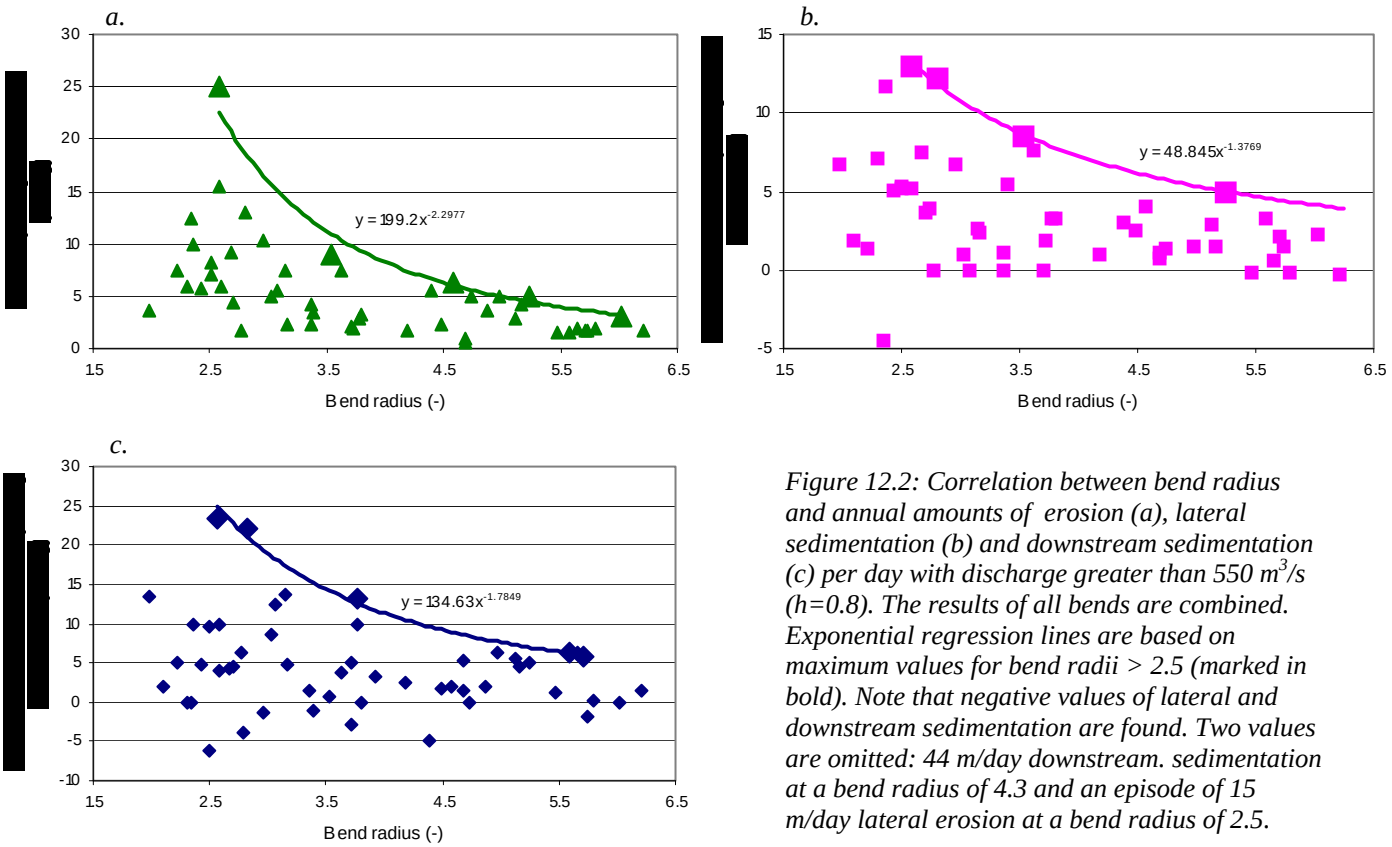

Figure 12.2: Correlation between bend radius and annual amounts of erosion (a), lateral sedimentation (b) and downstream sedimentation (c) per day with discharge greater than 550 m^3/s (h=0.8). The results of all bends are combined. Exponential regression lines are based on maximum values for bend radii > 2.5 (marked in bold). Note that negative values of lateral and downstream sedimentation are found. Two values are omitted: 44 m/day downstream. sedimentation at a bend radius of 4.3 and an episode of 15 m/day lateral erosion at a bend radius of 2.5.

is reached at a radius of 2.5 (section 3.3.3). This trend agrees with results of individual bends (section 12.1), Hickin (1977) and de Kramer et al. (2000). The sharpest, most pronounced, peak is found with maximum erosion, indicating that erosion varies considerably with bend radius (figure 12.2 a). De Kramer (2001) found a similar trend for meander migration (erosion) in the Allier (figure 3.6). He found maximum erosion values near a bend radius of 2 that were considerably lower than in this research. This is most likely the result of a smaller amount of data (about half), particularly near bend radii between 2 and 3 (where maximum erosion is expected).

Fitting regression curves through all values (not shown), a significant relationship was found between bend radius and erosion, with a determination coefficient (R^2) of 0.39. Erosion already showed the strongest correlation with bend radii of individual bends (section 11.2). Lateral and downstream sedimentation showed no correlation with bend radius ($R^2 \approx 0$).

Outer bank erosion is the only variable of meander migration that is related to bend radius. The correlation is stronger than any relation between discharge and erosion or sedimentation (section 11.2.2). Considering the trends in maximum values, bend radius acts as a limiting factor in meander development. Bend radius determines the potential amount of erosion or sedimentation. Maximum sedimentation is indirectly dependent on bend radius through erosion. Amounts of erosion restrict the amount of space and with it flow resistance that allow sedimentation (section 3.5.2).

12.3.2 Area of pointbar accretion

Accreted units along a pointbar showed a statistically insignificant relation with bend radius (figure 12.3). The size of the accreted area, however, increases with decreasing bend radius, where accreted distances did not correlate with bend radius (section 11.2.1). Correlation between accreted area and discharge revealed a poorer relationship. Analysing areas of sedimentation brings complications because sedimentation occurred at various locations along a pointbar (lateral, downstream, in a swale behind the pointbar), but also in the vertical on the pointbar (bars, splays, sediment caught by vegetation). Apart from sedimentation, erosion also occurred on pointbars (at the upstream end, downstream crossing channels, opposite from revetments).

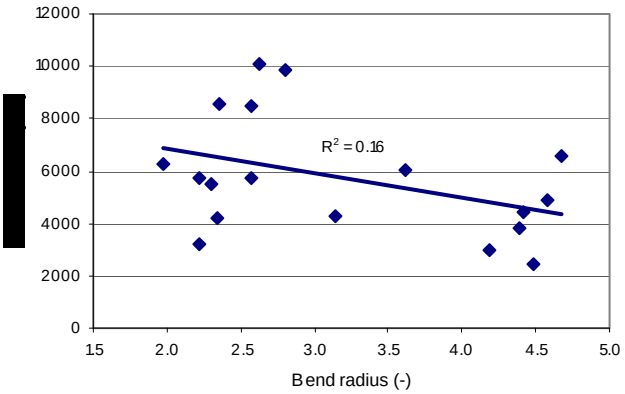

Figure 12.3: The area of pointbar accretion related to bend radius.

13. Planform pointbar development

13.1 Lateral and downstream displacement

The prominent direction of sedimentation can be deduced from the form of a pointbar and the location of its scroll bars. A pointbar that had gone through a period of downstream sedimentation was typically long and developed scroll bars that follow each other in downstream direction (figure 13.1 a), as visible in figures 6.3 and 7.9. With prominent lateral sedimentation a shorter pointbar developed and scroll bars lied laterally next to each other at the downstream end of the pointbar (figure 13.1 b). A lateral sediment stroke grew near the bend apex that tapered off (becomes narrow) near the ends of the pointbar, where there was little sedimentation (figures 6.1 and 8.3). With dominant downstream sedimentation, vegetation did not settle at the downstream end of the pointbar, while this sometimes occurred with dominant lateral sedimentation.

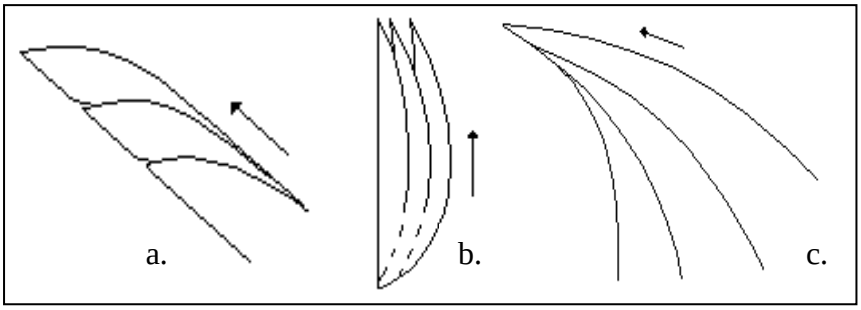

Figure 13.1: Pointbar development through the addition of scroll bars in downstream direction (a), laterally (b) and both downstream and laterally (c).

Dominant downstream bend propagation (as in figure 13.1 a) in the Allier is characterised by a straight approach of flow. This can be related to a *resistant bank* (Lagasse et al, 1995) such as in St. Loup (between 1960 and 1985) where it directed incoming and outgoing flow in downstream direction. Straight incoming flow and downstream meander propagation was also found after a *cutoff* like at Châtel de Neuvre (1990's) and initially at the two compound bends at Château de Lis (figure 9.4). Hickin (1974) and Friedkin (1945), however, argued that downstream sedimentation is characteristic for more developed meanders near equilibrium conditions. This is the case for meanders that are limited in their development by lateral confinement, but not for recently cut-off meanders. Lateral development was stimulated by the settlement of *vegetation* on a pointbar that forced flow outwards in a sharp bend, allowing the development of helicoidal flow such as found at Chemilly (1960's), St. Loup (figure 6.6) and Châtel de Neuvre (figure 7.9). Helicoidal flow, that causes lateral development, needs a certain *bend length* to develop (adjustment length; section 11.2.5). At Châtel de Neuvre (figure 7.9) lateral development followed a period of extensive downstream development that lengthened the bend to about 800 meters. The same occurred at St. Loup, with the aid of vegetation (figure 6.6), while at Beauregard the lateral component of erosion and sedimentation steadily increased as the bend grew in length (until the outer bank was fixed by revetments). Lateral and downstream meander development depend on local conditions (i.e. direction of incoming flow, presence of vegetation, resistant banks) and cannot directly be assigned to bend maturity or equilibrium conditions.

13.2 Complex and compound bends

Hooke (2004) found that meanders show gradual evolution and an increase in form complexity. In the Allier, at Chemilly and Château de Lis, lateral development evolved during the 1990's into rotational (Chemilly) and compound bend formation (Château de Lis).

The occurrence of compound bends is related to the *length of a bend* (Lancaster and Bras, 2001), as was the case at Château de Lis and Châtel de Neuvre (1975-1980). At Château de Lis a (partial) cutoff (figure 9.7) was the direct cause of bend development at the beginning and end of the cutoff, as was also temporarily the case in 1978 (figure 9.4). Lancaster and Bras (2001) and Sun et al. (1996) also stressed the importance of *bank heterogeneity* (resistant banks; 12.3.3) in the formation of compound bends. This occurred at Beauregard in the 1990's, where bends developed at the beginning and end of the resistant stretch.

13.3 Bend development along a resistant bank

When the channel of the Allier encountered a resistant bank, it was characterised by a sharp turn or kink, followed by a straight stretch (along a dike) and a point where flow moved away from the resistant bank. Meander development was forced in up- or downstream direction, which most often caused the development of a compound bend (section 13.2). Sedimentation along the pointbar attempted to copy the form of the outer bend in order to establish an equilibrium. The pointbar straightened opposite from a the resistant bank (figure 6.9 and 10.12) and at St. Loup a downstream sedimentation occurred in the form of a "bulge" at the end of the pointbar, opposite from an old channel (figure 6.9; 4). Flow kept its helicoidal character and inner bank sedimentation and allowed the pointbar to expand slightly and remain "smooth" opposite from the kinks in the outer bend (figure 6.8; 5,6). In Beauregard, the channel section along the resistant bank became longer and wider while helicoidal flow was disrupted (figure 10.11; 2,3). Because no energy was used detaching material from the outer bend and the thalweg was redirected inwards, pointbar erosion occurred.

The meander at Beauregard remained present throughout time, while it lies at the end of a straight stretch of river with a braiding character (section 10). The outer bank of the meander experienced increased resistance caused by resistant bedrock and had to bend away (to the north) introducing centripetal forces (figure 13.1). The meander will remain present as long as the resistant bank initiates a change in flow direction. Flow moved along the resistant bank and eroded further downstream, increasing the bend radius. With an increasing bend radius the length of the bend increased, giving flow a longer route to develop a (strong) helicoidal or lateral component. Figure 10.13 shows an increasing bend radius and (lateral) erosion till about 1985, while correlation between radius and lateral erosion / sedimentation show a similar (linearly) increasing trend (figure 12 e). At St. Loup the same trend is visible, where a dike straightened the channel upstream from the bend (figure 6.7) and where increasing bend radii are related to increased amounts of erosion (figure12 a).

13.4 Cutoffs

13.4.1 Meander cutoff

The meander cutoffs of Chemilly and Château de Lis (including the bend that lies in between) occurred in the same period around 1978 (section 11.2, figure 13.2). The placing of a dike south of Chemilly acted as an important factor (trigger) that led to (anthropogenic) cut-off of the bend. The cutoff caused an increase in downstream flow momentum, instead of the development of lateral flow. During high discharges the downstream momentum caused the cut-off of downstream bends. The cutoffs however, did not cascade downstream (figure 13.2). First the bends at Château de Lis and Chemilly were cut off (1978-1980) followed by the bend in between and the bend downstream of Château de Lis (1980-1985). The cutoffs were the result of meander evolution that attained a critical state (Hooke, 2004; Bak et al. 1987; Stolum 1996) and lead to the cut-off of a group of meanders.

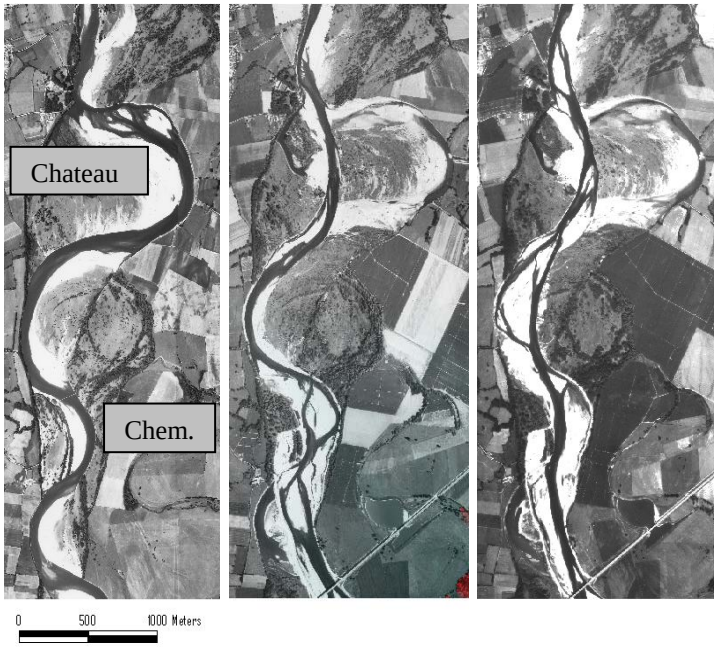

Figure 13.2: Cut-off ~~sequence (1978-1980-~~1985) near Chateau de Lis and Chemilly.

13.4.2 Chute cutoff

Chute cutoffs took place at the bends downstream of Château de Lis (figure 9.12) and Chemilly (figure 8.12). Bars, that showed weak lateral development towards the downstream pointbar, were isolated by chute channels that crossed over the pointbar. New chute channels took over the function of main flow, while old channels were abandoned and filled with sediment. Bars that belonged to the downstream pointbar were eventually (after multiple cutoffs) added to downstream end (outer bend) of the pointbars at Chemilly and Château de Lis.

The chute cutoffs were enabled by the following conditions:

- Two consecutive sharp bends (Thorne, 1992) followed each other closely.
- The channel was orientated perpendicular to valley gradient, resulting in a low local gradient that supports sedimentation.
- A fixed downstream limb of the second bend prevents lateral erosion. Only up- and downstream migration is possible.

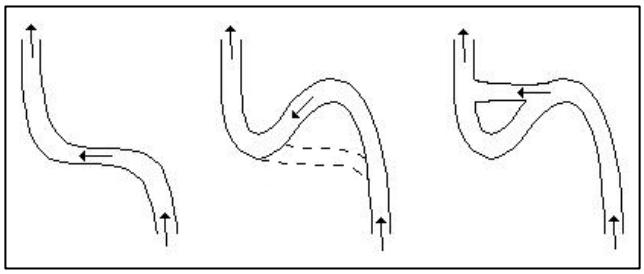

Figure 13.3: Development of counter pointbars through chute cutoff.

Outer bend erosion moved the channel and pointbar of the upstream (composed) bend to the north (figure 13.3; first two situations). The downstream bend did not develop expand laterally, in southern direction, because the necessary helicoidal flow could barely develop in the short bend. With high discharges a small part of the downstream pointbar is cut off by a chute channel (figure 13.3; last situation).

At Beauregard a chute cut-off occurred after a period of upstream channel development along a resistant bank (figure 10.9). This process is similar to processes found by Wolfert (2002), shown in figure 3.4. At Beauregard, however, the meander initially expanded upstream (figure 10.10) along the resistant bank instead of downstream as shown in figure 3.4.

14. Equilibrium between erosion and sedimentation

14.1 Relation sedimentation / erosion

Maximum erosion and lateral sedimentation showed significant linear correlation (figure 14.1). Observed sedimentation distances, however, were only about two thirds of the amount of corresponding outer bend erosion. This is the result of concentrated erosion, along a relatively short section of the outer bank where flow conditions were sufficiently strong to cause bank failure and/or sediment entrainment. Sedimentation on the opposite bank occurred along a large part of the pointbar (lateral, downstream and vertical) and in the channel.

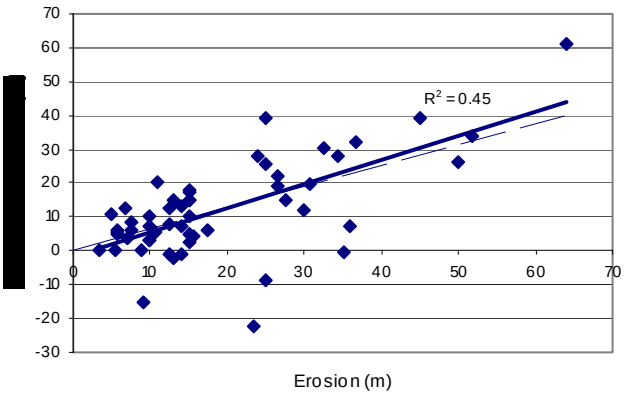

Figure 14.1: Correlation between erosion and lateral sedimentation. The dotted line represents equilibrium, where average erosion equals average lateral sedimentation.

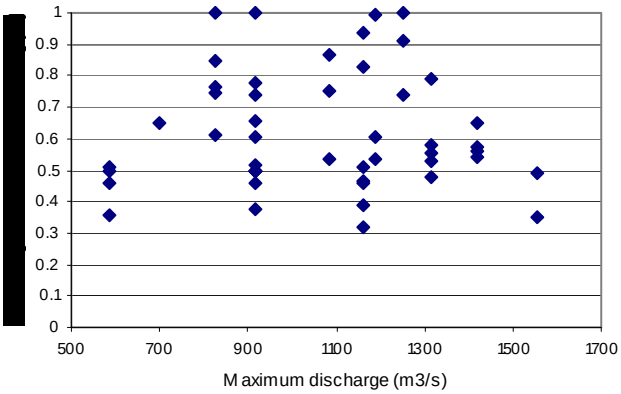

Figure 14.2: The relative amount of erosion as part of total meander migration (erosion and sedimentation) related to maximum discharge.

The regression line in figure 14.1 shows that the ratio between erosion and lateral sedimentation varies. Erosion and sedimentation intensities develop differently according to local conditions (section 13.1) and discharge (section 11.2.3). During low discharge, erosion dominates and lateral sedimentation hardly takes place. Flow conditions are sufficient for erosion to occur, that shows constant development (section 11.2.3), but not for lateral sedimentation. During higher discharges sedimentation becomes of increasing importance (relative to erosion). Lateral sedimentation correlated best with high discharges, greater than 550 m^3/s and maximum (section 11.2.3). The different conditions with which erosion and sedimentation occurred caused disturbances of the equilibrium between flow and morphology. During low discharges lags in sedimentation occur that lead to the development of swales.

The equilibrium between erosion and sedimentation depends on discharge, as both processes behave differently with respect to discharge (section 11.2). Maximum discharge exerted influence on the relative amount of erosion (as part of total meander migration, erosion and sedimentation; figure 14.2) that occurred. Erosion occurred at all discharges, while lateral sedimentation correlated best with discharges higher than 550 m^3/s (section 11.2.3; table 11.1). Therefore, with high maximum discharges, sedimentation distances approach equilibrium with erosion (ratio = 0.5; figure 12.4). With “normal” maximum discharges (between 800 – 1200 m^3/s) sedimentation often lags behind erosion (ratio > 0.5). Short periods in time (one to two years) had low maximum discharges (590 and 700 m^3/s). On this timescale lateral sedimentation showed a stronger correlation with discharge (table 11.1) causing its share in meander migration to increase to 0.5.

14.2 Equilibrium pointbar slope

Prayoyo and Struiksma (1985) determined the asymmetry of a channel cross section in equilibrium near the bend apex (equation 7, section 3.4.2). The equilibrium slope of a typical pointbar in the Allier was calculated with a waterdepth of 2.5 m (waterdepth halfway up the pointbar during bankfull discharge), sediment d90 of 1.4 cm (section 2.2) and a variable bend radius (figure 14.3). The results of slopes measured in the field and the presence of scroll bars are shown in figure 14.3. The observed slopes do not coincide with the equilibrium determined by Prayoyo and Struiksma (1985). The blue regression line of the data describes the equilibrium slope as found for a couple of bends in the Allier. The trend is statistically insignificant, but describes a slight increase in pointbar steepness with decreasing bend radius. This is similar to the equilibrium slope of Prayoyo and Struiksma (1985), although the slopes in the Allier are systematically greater. through a weak, statistically insignificant trend. The presence of scroll bars will be discussed in the following chapter.

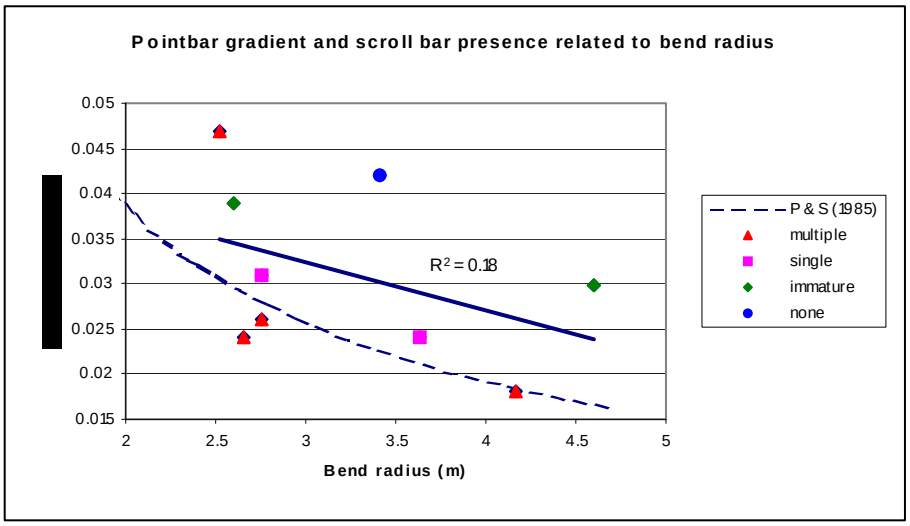

Figure 14.3:The slope of the pointbar surface (near bend apex) related to bend radius, including linear regression line. Scroll bar presence is indicated with data colour/symbols. The dotted line represents the equilibrium pointbar gradient as described by Prayoyo and Struiksma (1985).

When outer bend erosion came to a halt, the pointbar slope became steeper (figure 6.8; 5,6), due to partially lagging sedimentation (section 12.1.1). The inner bend had yet to come to an equilibrium as described by Prayoyo and Struiksma (1985). When the inner bank reached dynamic equilibrium with the (stationary) outer bank, phases of local sedimentation and erosion (figure 6.8; 5, 2002) occurred as result of fluctuating discharges (section 6.2.2). Other factors that can influence the development of the pointbar slope (equation 7), bendform and roughness (sediment size, large scale morphology and vegetation) remained constant.High discharges smoothened the pointbar and lower discharges (slowly) eroded the base of the pointbar (similar to Anthony and Harvey, 1991).

15. Scroll bar development

15.1 Ridge and swale topography

15.1.1 Scroll bar characteristics

Most scroll bars in the Allier had an arcuate, symmetric plan shape (figure 8.3; 2 and 6.10a; 1996). They formed directly along the pointbar or accumulated in scroll bar complexes (figure 7.2; 2 and 9.7; 2). Scroll bars were oriented more or less parallel to the pointbar, but often extended into the channel in up- or downstream direction. This depended on their means of development and interaction with adjacent riffles.

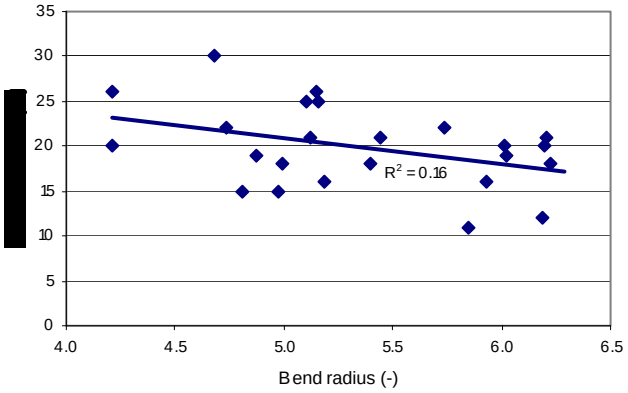

Figure 15.1: Scroll bar width related to bend radius at Beauregard.

Scroll bar widths were determined in Beauregard (figure 10.14), where the bars were readily distinguishable due to the large bend radius. Scroll bars varied in size, ranging between 15 and 30 meters in width. The relation between scroll bar width and bend radius is barely significant, showing an increasing trend with decreasing bend radius (figure 15.1). Scroll bar amounts (figure 14.3) and size (figure 15.1) increase with the rate of bend migration (Reading, 1996), which is related to bend radius. Scroll bar width showed no relation with annual discharge, because the development of scroll bars can take multiple years (while the amount of observations was limited).

Scroll bars had gently sloping surfaces near the end of the pointbar (figure 7.10; 3). They were mainly formed by the lateral component of helicoidal flow, that decreased in strength towards the end of the pointbar and caused scroll bars to becomes less high and narrower. Slipfaces or steep gradients, as found by De Kramer, 1998 (figure 3.9), developed at the end of splays and chutebars (not scroll bars; figure 7.14). These bars formed higher on the pointbar with finer sediment that was transported by (downstream) flow across the pointbar.

15.1.2 Swale development

Swales allow the distinction of scroll bars and their characteristics. The development of swales is often attributed to a lag in sedimentation in which a scroll bar can only partially respond, leaving behind a swale. The amounts of erosion that led to swale development varied considerably. Solely large distances of erosion are not sufficient for swale development (figure 9.6, 8.9, 7.4; highest erosion for these bends). Swales were present in bends where erosion was larger than sedimentation. Swales were particularly notable where this annual difference in distance was ten meters or greater (figures 6.3, 7.2, 10.6; difference erosion – sedimentation: 11, 17.5 and 13 meters). The development of swales or isolated scroll bars is related to bend radius. The smaller the bend radius, the less room there is on the inner bend and the less likely swales can develop. The three examples without swale development and high amounts of erosion had bend radii of 2.5, 2.5 and 3.5. The three notable swales developed with bend radii of 5.1, 5.1, 6.2. Swales can develop in sharp bends, but erosion must be much larger than sedimentation (figure 9.8, R = 2.4, erosion – sedimentation = 50).

The length along which erosion takes place in a tight bend is much longer than where sedimentation can take place. Strong helicoidal flow “fills” the inner bend, continuously expanding the pointbar with sediment, not allowing the formation of swales. For a bend with a large radius this difference is minimal and there is a surplus of room for sedimentation and the development of swales.

On the point bar the relief was strengthened by the processes of sedimentation and erosion. With high water, sedimentation occurred in shallow (high) areas. Flow here diverged and was influenced more by the bottom roughness (low Chezy value, with low water depth). In deeper parts water was concentrated, especially during falling stage encouraging erosion. When vegetation developed, usually in lower parts, the added roughness caused sedimentation which overcompensated the concentration of flow due to relief and relief could be inversed.

15.2 Circumstances facilitating scroll bar development

15.2.1 Pointbar slope

Scroll bars are not discernible on all pointbar slopes. Profiles from different bends showed that low pointbar gradients, under the equilibrium line of Prayoyo and Struiksma (1985), were characterised by multiple scroll bars (figure 14.3, with one exception). Active sedimentation took place, in the form of scroll bars, to achieve a steeper pointbar gradient and approach equilibrium. Just above the equilibrium line of Prayoyo and Struiksma (1985), but still below the blue regression line from the Allier, single scroll bars were present on the pointbar slope (figure 14.3). On even steeper gradients above the blue regression line, scroll bars were barely present. Immature bars were found that stagnated (underwater) because of minimal outer bend erosion through a resistant outer bank and the achievement of an equilibrium slope on the inside of the bend. the temporary development of these small bars is shown in figures 6.8; 6 and 7.10; 1. With gradients (much) higher than the equilibrium slope, scroll bars cannot develop (erosion can take place).

Scroll bars developed best where lateral migration is maximum (figure 12.2), near a bend radius of 2.5 (figure 14.3). In sharper bends lower gradients were found than expected with the equilibrium of Prayoyo and Struiksma (1985) and scroll bars were absent. With bend radii smaller than 2.5, helicoidal flow was disturbed and erosion took place along the inner bend (de Kramer 1998), hindering the development of scroll bars. Larger bend radii developed weak lateral motion, making conditions less favourable for scroll bar development.

15.2.2 Sediment composition

Sediment in the Allier is characterised by a relative abundance of coarse sand and gravel/pebbles (figure 2.3). Scroll bars were found in both size ranges but were in different states of development. Scroll bars that consisted of pebbles were in the order of 20 cm high and have gentle slopes. The form of sand bars was more lobe-like and they were higher and steeper. Consecutive bars (in development) were not the result of a relative abundance of certain grainsizes along a velocity gradient from the thalweg onto the pointbar, as proposed by Nanson and Hickin (1983).

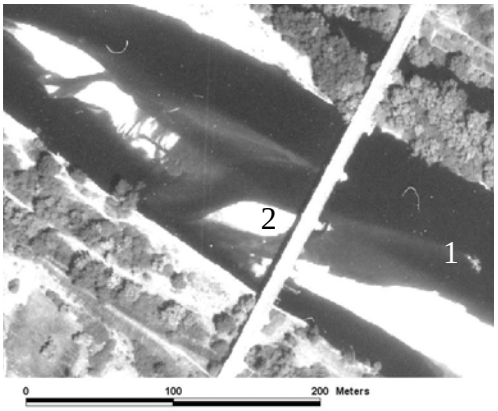

Figure 15.2: 1985 aerial photo from St. Loup showing bar development behind obstacles in the channel.

15.2.3 Flow obstruction

Channel flow was occasionaly obstructed by debris. This included material that was eroded from the outer bank, mainly trees (figure 15.2; 1), or man made features in the channel, such as bridge pillars (2). Sedimentation occurred at the lee of an obstacle where calm flow conditions were present. Continued sedimentation led to the formation of a bar that could grow downstream. The development of a bar could move inwards due to helicoidal flow, becoming a characteristic scroll bar (2).

15.3 Interaction between riffle and scroll bar development

15.3.1 Riffle development

A riffle consists of a diagonal bar that connects the end of a pointbar to the beginning of the following pointbar on the opposite bank (figure 3.10). Erosive crossing channels carry flow from one bank to the other during low discharges, dividing the riffle up into bars (figures 9.10, 9.11; 3). In straight or low sinuous river stretches riffles could easily move in up- and downstream direction, influencing pointbar formation (Beauregard, figure 10.5b). This movement was caused by upstream meander development and varying discharges (section 11.2.5). Varying discharge and adjustment length also influenced the location of crossing channels that formed thalwegs of different low discharges. These channels were present at the upstream end of the riffle (downstream end of pointbar), where low discharges with a short adjustment length cross. Higher discharges crossed further downstream, where the deep water was hindered less by the elevated bedding near the riffle and crossing channels barely formed. The location of crossing channels varies not only with discharge, but with bend form and length (section 11.2.5; figure 10.11).

15.3.2 Interaction erosion and sedimentation

Riffle morphology is characterised by low-water erosive channels that cross the riverbed. Scroll bars on the other hand are characterised by high water sedimentation processes with a lateral character. Changes in (annual) discharge cause changes in flow conditions that determine channel morphology. In the Allier scroll bar and riffle development often overlapped, causing morphological entities to be characterised by multiple processes.

Both erosion and sedimentation show distinct characteristics. Bar edges that were curved on the channel side depicted a sedimentary nature (figure 6.5; 2 and 6.6). Erosive channels tended to be more straight (riffle channels figure 9.9), lacking helicoidal flow, and developed plumes of sediment at their downstream end (crossing channel figure 7.8). These channels had irregular cross profiles, steep channel edges (crossing channel figure 7.10; 3) and on a pointbar typically widened in downstream direction where more water from the pointbar had to be drained (erosive swale figure 7.12).

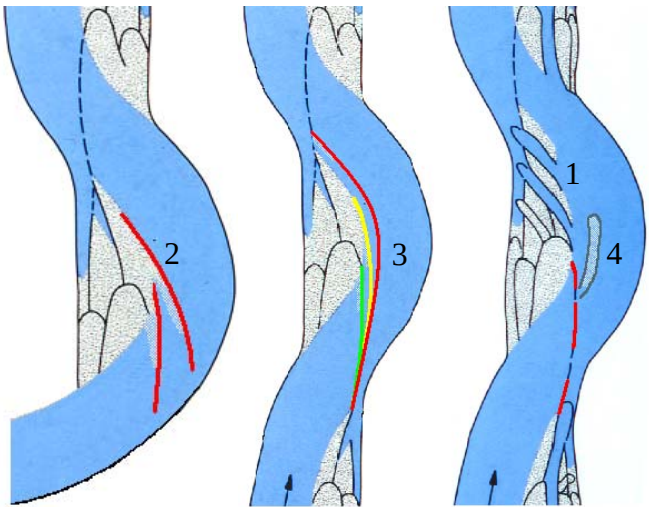

Figure 15.3: Riffle / scroll bar interaction. In situation 1 the pointbar is crossed by low-water flow channels, in 2 riffle/scroll margins (red) develop along a long (complex) bend, in 3 riffle margins (green, yellow and red) overlap, to various extents, with the pointbar and in situation 4 a bar develops at the end of an erosive crossing channel.

Swales form as a lapse in sedimentation leaving behind a through. They occasionally developed an erosive nature through the concentration of water that was drained from the pointbar (figure 7.12). Swales could also function as part of a riffle, carrying flow to the opposite bank. The island in figure 6.1 can be assigned to lateral bar formation and to riffle development, where an erosive channel separated it from the pointbar. A combination of sedimentary and erosive processes took place, depending on temporary discharge conditions. Important types of interaction between riffles and scroll bars are summarised in figure 15.3 and discussed in the following sections.

15.3.3 Overlap downstream riffle with scroll bars

Apart from sedimentation a pointbar could get eroded through the crossing of flow. When downstream sedimentation was high, the downstream end of the pointbar came into the influence zone of the riffle. Erosive channels that crossed the pointbar from the main channel to the swale developed because of a steeper water gradient (figure 6.7, 7.8). With a long pointbar, flow had to take a long path before reaching the riffle. During low or decreasing discharges there was no transverse watergradient and a path across the pointbar was shorter. There was no difference in waterlevel between the riffle and swale, because the swale held stationary water during low discharges and was connected to the riffle at its downstream end. During high discharges flow was elevated in the outer bend and the swale discharged water, causing flow to take the outer bend. This resulted in the development of islands that belonged to the pointbar but were separated by channels that crossed over to the opposite bank (figure 6.5, 1 and figure 6.7). The development of crossing channels was also related to revetments at St. Loup that redirected flow inwards.

15.3.4 Riffle presence along a pointbar

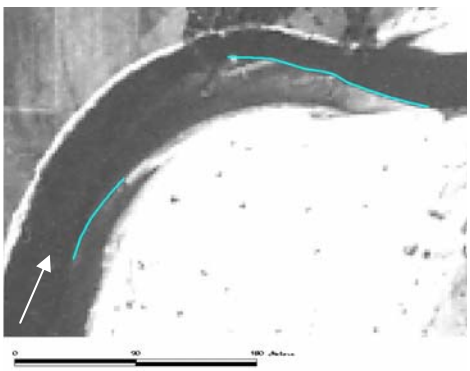

Figure 15.4: Scroll bar formation along a riffle in a complex bend north of Chateau de Lis (1960).

A riffle can act as the basis for scroll bar development in long and complex bends. Riffles developed along the pointbar as a result of the unsustainability of helicoidal flow throughout long bends (section 3.2.2). Figures 8.9, 9.2 and 15.4 show that bars were attached at their downstream end and moved towards the outer bank in upstream direction (schematically shown in figure 15.3; situation 2). These bars were part of a riffle that developed in long complex bends, although the riffle was not as pronounced as one between bends with opposing curvature. During high discharge, helicoidal flow is stronger and reached further downstream, partly remoulding the bars at the riffle. The riffle however

remained the basis and sediment source of scroll bar formation. In figure 10.12 riffle bars encompassed the second half of the compound bend at Beauregard. This riffle was well developed and marks the future lateral expansion of the (second half of the) bend.

15.3.5 Overlap upstream riffle with scroll bars

The development of scroll bars can also be related to a riffle lying upstream from it. Morphological units are hard to distinguish and lie in each others extension. Figure 9.10 shows a riffle from 1995 that bordered the upstream edge of a scroll bar complex. In figures 9.11 (1998) and 6.1 the riffle and scroll bar merged into each other without clear margins. The riffle could also encompass or surpass the area of scroll bar development such as in figures 9.11 (1997) and 7.5 b. The riffle formed the newest phase of scroll bar development as an underwater bar. These three extents to which a riffle can overlap with scroll bar development are shown in figure 15.3, situation 3.

In the case of figure 9.11 (1997), the flow directions with low and high water were somewhat different (flow predominantly from channel 1 and 2 respectively). With low discharge, flow followed a short and sharp bend just downstream of the riffle. With high discharge flow was already concentrated in the outer bend and its helicity remoulded the low water riffle in downstream direction. This led to the development of scroll bars, where the riffle acted as sediment source.

15.3.6 Scroll bars originating from the riffle

Figure 15.5: Scroll bar development from a riffle, north of Chateau de Lis (1954).

Apart from the whole downstream migration of a riffle, sections or plumes can move downstream and develop as scroll bars along the pointbar (figure 15.3, scenario 4). Crossing channels developed sediment plumes at the downstream margin of riffles. Sediment was eroded from the riffle complex, by the cross channels with a high gradient, and was deposited at the downstream end of these channels, where the gradient decreased and flow entered the main stream. This led to the development of bars that are characterised by their upstream attachment to the pointbar (figure 15.5 and 10.6). The bars moved outwards in downstream direction, because helicoidal flow had not yet developed. They also often lacked typical scroll bar asymmetry (figure 8.11; 3). Scroll bars that originated from a riffle are flanked by long throughs that have the same origin and carry flow from one bank to the other. This process is comparable to Sundborg's (1956) transformation of transverse bars to longitudinal bars. Scroll bars develop from a (transverse) riffle, across which migration is faster near a crossing channel and slower on its inside.

15.4 Bars in the outer bend

Bars in outer bends formed as up- or downstream extensions of scroll and pointbars. In Beauregard (figure 13.11; 5 and further upstream), trees eroded from the outerbank caused flow deflection and allowed sedimentation to occur in the area sheltered by trees (in agreement with Wallerstein and Thorne, 2004). Bars were also found near a sharp deviation in

channel direction at the outer bend (figure 6.8; 5, year 2003). There was obstruction to the normal line of flow and backflow could develop. The mentioned bars are of small scale and temporary nature.

Counter pointbar development in a sharp outer bend, as described by Nanson and Page, 1983 (section 3.5.3) was only found at Chateau de Lis (figure 9.10; 1995). In the Allier scroll bars were separated from a pointbar through chute cutoffs (section 13.4.2). Different phases of cutoffs moved channels northwards, while old channels (on the southside) were filled with sediment and the bars that once belonged to the downstream pointbar were attached at the downstream end (in the outer bend) of the upstream pointbar. The bars were slightly remoulded but kept their structure that showed development towards the inner bend (figures 8.11 and 9.10).

16. Conclusions

16.1 Meander development

In the period 1960 – 2003, five researched meanders in the Allier illustrated various types of large scale development in time and space. These included downstream, lateral, rotational and compound bend development, while cutoffs also played an important role in the development of (new) meanders. The type of development largely determined meander / pointbar form (radius) and characteristics (including the location and development of riffles, scroll bars and vegetation).

Meanders showed periods up to 25 years long (Chemilly until 1978 for example), with a constantly decreasing bend radius as described by Hickin (1977). This was the result of constant lateral meander development, where the focus of erosion remained unchanged (halfway down the bend). Short pointbars developed, with scroll bars located (laterally) next to each other, reaching the downstream end of the pointbar. Bend length and radius increased when bank erosion dominated at the downstream end of a bend (Beauregard until the 1980's for example). Downstream meander development develops typically long pointbars with scroll bars that follow each other in downstream direction. Natural, unrestricted, meanders evolve towards complex forms (rotational and compound; Chemilly for example) with relatively constant bend radii of about 2.5. This process however required enough space and time with a constant direction of meander development.

The direction of bend development depended on local conditions and could not directly be assigned to bend maturity or equilibrium conditions (as determined by Hickin, 1974). Bends with low curvature had to be long (>800 m) in order for helicoidal flow and lateral meander development to develop (adjustment length, de Vriend and Struiksma, 1983). Lateral development also occurred where pointbar vegetation forced flow outwards. Downstream meander propagation was related to resistant banks (also found by Lagasse et al, 1995) and recent cutoffs, that orientated flow in downstream direction. Composite bends developed in long bends where secondary flow could not be sustained and riffles appeared. Composite bends also expanded at the up- and downstream end of resistant outer banks (also found by Lancaster and Bras, 2001) and straight cutoff channels. Opposite of resistant banks, sedimentation attempted to establish an equilibrium between outer bend erosion (restricted) and inner bend sedimentation. Helicoidal flow was hampered and pointbars adapted their form to that of the outer bank, forming straight inner banks. Bend cutoffs were part of meander evolution that attained a critical state (Hooke, 2004) leading to the cut-off of a group of meanders (not propagating downstream). Series of typical chute cutoffs were found where sharp bends followed each other closely (Chemilly and Chateau de Lis). The upstream bend expanded towards the downstream bend, that remained stationary due to a resistant bank and the inability of (strong) helicoidal flow to develop over the short distance. This led to the sequential cut-off of the sharp downstream bend.

Meander migration was quantified by sedimentation and erosion extents (in lateral and downstream direction). They were correlated to discharge, that determines the river's capacity to cause morphological change, over periods of one to eight years. In all cases sedimentation and erosion showed increasing trends with discharge. Erosion correlated significantly with various measures of discharges, though best with discharges above 550 m^3/s that accounted for about 30 % of its variation. Actual amounts of erosion varied, because they were bound by local constraints such as resistant banks and the direction of incoming flow. Lateral sedimentation also showed the strongest correlation with discharges above 550 m^3/s that

constantly (for all bends and correction scenarios) accounted for about 20 % of its variation. Discharges above 550 m^3/s cover the range of discharges capable of substantial sediment transport and developed strong helicoidal flow leading to lateral erosion and sedimentation. Lateral erosion and sedimentation increased along a gradient of 0.25 with the amount of days with discharge greater than 550 m^3/s. On a time scale of one to two years, sedimentation correlated significantly with discharge, while this was not the case with erosion, that showed more continuous long term development. The different development of erosion and sedimentation in time caused lags in sedimentation and disturbances of the equilibrium between flow and morphology.

Downstream sedimentation correlated strongest with average discharges that accounted for about 10-15 % of its variation. It increased along a gradient of 0.53 with average discharge. The downstream component of erosion (adjustment length of flow) showed the least poor relation with average discharge (not statistically significant). Flow and morphology adjusted (63 %) about 300-500 meters into a bend, that was characteristically 800-1200 meters long. Secondary flow during high discharges was fully developed halfway most bends, causing lateral development. Lower discharges “meandered” within a bend causing bend expansion near the downstream end (and upstream end in case of a compound bend).

Similar to discharge sedimentation and erosion were correlated to bend radius, which generally resulted in worse correlation. Bend radius showed significant correlation with observed erosion, where a curve accounted for about 40% of variation. No correlation was found with lateral or downstream sedimentation. Bend radius was however related to maximum observed sedimentation and erosion extents, through exponential trends. Bend radius erosion and sedimentation potential, with maximum values near a bend radius of 2.5. The steepest and clearest trend was found with erosion. Sedimentation was related to bend radius through erosion that restricted the amount of space and consequently flow resistance that allowed sedimentation. Pointbar accretion correlated weakly with bend radius, because sedimentation occurred at different locations along and on a pointbar together with erosion.

Bend radius and discharge provided conditions that controlled potential erosion and sedimentation, while local factors (vegetation, bank resistance, upstream meander development etc.) limited actual amounts.

16.2 Sedimentation processes

Pointbar slopes, perpendicular to the channel, showed a trend with bend radius similar to that of a pointbar in equilibrium (Prayoyo and Struiksma, 1985). On average the slope increased from 0.025 to 0.035 with decreasing bend radius (till 2.5) and strengthening helicoidal flow. Sedimentation intensity, visible through the presence and amount of scroll bars, was greatest where slopes deviated most from the steeper equilibrium slope. After outer bend erosion came to a halt (revetments), pointbar slopes still increased due to lagging sedimentation. When the pointbar (slope) reached equilibrium, temporary phases of sedimentation and erosion occurred as a result of fluctuating discharge (other factors of influence remained constant on the short term). Scroll bars were barely present on slopes steeper than equilibrium (opposite of resistant banks) and none were distinguishable with bend radii smaller than 2.5, where helicoidal flow was disturbed and erosion often took place along the inner bend.

Scroll bars were characterised with an arcuate and more or less symmetric plan shape. They were mainly formed by the lateral component of helicoidal flow, that decreased in strength towards the end of the pointbar. This caused scroll bars to gently become lower in height (no

slipface) and narrower near the end of a bend. Scroll bars were distinguished by swales, that developed best in large bends, where there is more space for their development along the inner bend than in sharp bends. High amounts of erosion in sharp bends, that could cause a lapse in sedimentation and the development of swales, were of secondary importance. The relation between scroll bar width and bend radius was barely significant, showing a slightly increasing trend with bend radius.

Observations and calculation indicated that scroll bars developed in waterdepths of 1 – 1.5 meters, where flow velocities of 1.5 – 2 m/s were capable of sediment transport (maximum Froude number is 0.5). Pointbar morphology and scroll bar development were often influenced by the crossing of flow (riffles). Erosive channels often crossed long, narrow pointbars to a swale located on the inside of the pointbar. The short crossing provided an advantage in waterlevel gradient for flow that alternatively had to follow the long pointbar to the riffle, where the swale was connected to the main flow. Riffles developed along long complex pointbars, where helicoidal flow could not be sustained with regular discharges. During high discharge, however, helicoidal flow was stronger and reached further downstream, partly remoulding the bars at the riffle that eventually were added to the pointbar. At the upstream end of a pointbar, riffles occasionally encompassed or surpassed the area of scroll bar development. Riffles migrated downstream as a whole forming the newest phase of scroll bar development. Sections of a riffle or plumes extending from a riffle also developed in downstream direction, becoming scroll bars.

The potential of meanders in the Allier to cause erosion and sedimentation is largely determined by bend radius and discharge. Actual meander development, form and direction, is related to the local factors vegetation, bend length, bank resistance and upstream meander development.

References

Andrle, R. (1994): Flow structure and development of circular meander pools. Geomorphology 9, p. 261-270.

Anthony, D.J. and Harvey, M.D. (1991): Stage-dependent cross-section adjustments in a meandering reach of Fall River, Colorado. Geomorphology 4, p. 187-203.

Bak, P., Tang, C. and Wiesenfeld, K. (1987): Self-organised criticality: an explanation of I/f noise. Physical Review Letters 59, p. 381-384.

Bouchardy, C. (1991): Rivières et vallées de France, L'Allier. Privat.

Brice, J.C. (1974): Evolution of meander loops. Geol. Soc. of America Bulletin 85, p. 581-586.

Brice, J.C. and Blodgett, J.C. (1978): Countermeasures for Hydraulic Problems at Bridges, Vol. 1, Analysis and Assessment. FHWA/RD-78-162, Washington.

Bridge, J.S., Alexander, J., Collier, R.E.Ll., Gawthorpe, R.L. and Jarvis, J. (1995): Ground-penetrating radar and coring used to study the large-scale structure of point-bar deposits in 3-D. Sedimentology 42 (6), p. 839-852.

Chang, H.H. (1988): On the cause of river meandering. White, W.R. (ed) International Conference on River Regime, p. 83-93.

Daniels, M.D. and Rhoads, B.L. (2003): Influence of a large woody debris obstruction on three-dimensional flow structure in a meander bend. Geomorphology 52 (1), p. 159-173.

De Kramer, J. (1998): Oevererosie en meandermigratie in de Allier. MSc thesis, department Physical Geography, Utrecht University.

De Kramer, J., Wilbers, A., Van den Berg, J. and Kleinhans, M. (2000): De Allier als morfologisch voorbeeld voor de grensmaas, deel II: Oevererosie en meandermigratie. Natuurhistorisch maandblad 89, p. 189-198.

De Kramer J. (2001): Observations on the influence of morphology and morphological processes on vegetation development in the Lower Volga River, Russia. RIZA Working Document 2001.162x, 53 p.

De Vriend H.J. and Struiksma, N. (1983): Flow and bed deformation in river bends. In: River Meandering. Proc. Of the conf. Rivers '83, New Orleans, USA, p. 810-828.

Dury, G.H. (1964): Theoretical implications of underfit streams. U.S. Geol. Surv., Prof. Paper 452c, 42 p.

Engelund, F. and Hansen E. (1967): A monograph on sediment transport in alluvial streams. Danish Technical Press, Copenhagen.

Expedia Maps (2005): http://www.expedia.com

Friedkin, J.F. (1945): A laboratory study of the meandering of alluvial rivers, US Waterways Exp. Stat. Vicksburg Miss., 40 p.

Helmer, W., Overmars, W. and Litjens, G. (1991): Toekomst voor een grindrivier. Research done for the provence of Limburg. Stroming bv, 64 p.

Hickin, E.J. (1974): The development of meanders in natural river channels. American Journal of Science 274, p. 414-442.

Hickin, E.J. (1977): Hydraulic factors controlling channel migration; Research in Fluvial Systems; Dacidson-Arnott, R. and Nickling, W., Proceedings of the 5th Guelph Geomorph. Symp., Geobooks, Norwich, p. 59-72.

Hooke J.M. (2004): Cutoffs galore!: occurrence and causes of multiple cutoffs on a meandering river Geomorphology 61, p. 225-238.

Hooke, J.M. and Harvey, A.M. (1983): Meander changes in relation to bend morphology and secondary flows; Modern and ancient fluvial systems. Eds. Collinson, J.D. and Lewin, J., Basil Blackwll, Oxford, p.121-132.

Ikeda, S., Parker, G. and Sawai, K. (1981): Bend theory of river meanders, part 1:lineair development. Journal of Fluid Mech. 112, p. 363-377.

Kolkhuis Tanke, J.E. (1997): De vorming en evolutie van banken en eilanden in de Allier (Midden - Frankrijk). MSc thesis, department Physical Geography, Utrecht University.

Lagasse, P.F., Schall, J.D., Johnson, F., Richardson, E.V. and Chang F. (1995): Stream Stability at Highway Structures FHWA-IP-90-014 HEC 20, Ayres Associates, Fort Collins.

Lambeek, J.J.P. and Klaassen, G.J. (1994): Haalbaarheidsstudie referentie-onderzoek Grensmaas; Bureaustudie Waterloopkundig Laboratorium. Rijkswaterstaat Directie Limburg.

Lancaster S.T. and Bras, R.L. (2002): A simple model of river meandering and its comparison to natural channels. Hydrological Processes 16 (1), p. 1-26.

Leclerc, R.F. and Hickin, E.J. (1997): The internal structure of scrolled floodplain deposits based on ground-penetrating radar, North Thompson River, British Columbia. Geomorphology 21, p.17-38.

Leopold, L.B., Bagnold, R.A., Wolman, M.G. and Brush, Jr, L.M. (1960): Flow resistance in sinous or irregular channels. U.S. Geol. Surv. Prof. Paper 282D, p. 111-134.

Meyer-Peter, E. and Müller, R. (1948): Formulas for bed-load transport. Proc. I.A.H. R., Stockholm.

Nanson, G.C. (1980): Point bar and floodplain formation of the meandering Beatton River, northeast British Columbia, Canada. Sedimentology 27, p. 3-29.

Nanson, G.C. and Croke, J.C. (1992): A genetic classification of floodplains. Geomorphology 4, p. 459-486.

Nanson, G.C. and Hickin E.J. (1983): Channel migration and incision on the Beatton River. Journal of Hydr. Eng. ASCE 109-3, p. 327-337.

Nanson, G.C. and Page, K. (1983): Lateral accretion on meandering rivers. Spec. Publs. Int. Ass. Sediment 6, p. 122-143.

NEDECO (1959): River studies and recommendation on improvement of Niger and Benue. North Holland publishing, Amsterdam, 1000p.

Nijman, W. and Puigdefabregas, C. (1978): Coarse-grained point bar structure in a molasse-type fluvial system, Eocene Castisent Sandstone Formation, South Pyrenean Basin. In Miall, A.D., ed., Fluvial Sedimentology. Canadian Soc. Petrol. Geol. Memoir 5, p. 487–510.

Prandtl, L. (1952): Essentials of fluid dynamics. Blackie, London, 452 p.

Prayoyo, E. and Struiksma, N. (1985): Movable bed experiments in a straight flume with transverse sloping bed R657-XLVII. Delft Hydraulics.

Richards, K. (1982): Rivers. Form and process in alluvial channels. Methuen, London and New York, 358 p.

Roy Richardson, W.R. (1997): Secondary Flow and Channel Change in Braided Rivers. Submitted thesis, University of Nottingham.
http://www.geog.nottingham.ac.uk/~thorne/roy-richardson

Rozovski, I.L. (1960): Flow in bends of open channels. Jerusalem, Israel Prog. for Sci. Translations.

Reading, H.G. (1996): Sedimentary Environments: Processes, Facies and Stratigraphy. Blackwell, Oxford. 688 p.

Schumm, S.A. (1968): River adjustment to altered hydrologic regimen: Murrumbidgee River and palaeochannels, Australia. US Geological Survey Professional Paper 596.

Stolum, H.H. (1996): River meandering as a self-organisation process. Science 271 (5256), p. 1710-1713.

Struiksma, N., Olesen, K.W., Flokstra, C. and De Vriend, H.J. (1985): Bed deformation in curved alluvial channels. Journal of Hydraulic Research 23 (1), p. 57-79.

Struiksma, N. and Crosato, A. (1989): Analysis of a 2-D bed topography model for rivers; River Meandering, AGU, Water Resources Monograph 12, Eds. S. Ikeda and G. Parker, p 153-180.

Sundborg, A. (1956): The River Klaralven: A Study of Fluvial Processes. Geografiska Annaler 38 (3). p. 238-316.

Sun, T., Meakin, P., Jøssang, T. and Schwarz, K. (1996): A simulation model for meandering rivers. Water Resources Research 32 (9), p. 2937-2954.

Thompson, A. (1986): Secondary flows and the pool-riffle unit: a case study of the processes of meander development. Earth Surface Processes and Landforms 11, p. 631-41.

Thompson, D.M., Wohl, E.E. and Jarrett R.D. (1999): Velocity reversals and sediment sorting in pools and riffles controlled by channel constrictions. Geomorphology 27, p. 229–241.

Thorne, C.R (1992): Bend scour and bank erosion on the meandering Red River, Louisiana; Lowland floodplain rivers: Geomorphological perspectives, Eds Carling, P.A. and Petts, G.E. Wiley, New York, p. 95-115.

Thorne, C.R. and Hey, R.D. (1979): Direct measurements of secondary currents at a river inflexion point. Nature 280 (5719), p. 226-228.

Thorne, C.R. and Rais, S. (1983): Secondary current measurements in a meandering river: River Meandering: Proceedings of the Conference Rivers ’83. ASCE, New York, p. 675-685.

Toebes, G.H. and Sooky, A.A. (1967): Hydraulics of meandering rivers with flood plains, Proceedings of the ASCE, Journal of Waterways and Harbors Div. 92 (WW2), p. 213-236.

Van den Berg, J.H. and Balyuk, T. (2004): Interaction of vegetation and morphodynamics in pointbars of the Lower Volga (Russia) and the Allier (France). ICG 04-3, Utrecht, 34 p.

Van Looy, K. (2003): Natuurrapport 2003, Grensmaas. Instituut voor natuurbehoud, p.112-116.

Van Rijn, L.C. (1990): Principles of fluid flow and surface waves in rivers, estuaries, seas and oceans. Aqua Publications, Amsterdam, 335 p.

Wallerstein, N.P. and Thorne, C.R. (2004): Influence of large woody debris on morphological evolutionof incised, sand-bed channels. Geomorphology 57, p. 53-73.

Wilbers, A. (1997): De Allier, Een rivier met twee patronen. MSc thesis, department Physical Geography, Utrecht University. http://globis.geog.uu.nl/users/Wilbers/research.html

Wolfert, H.P. (2002): Geomorphological change and river rehabilitation: case studies on lowland fluvial ystems in the Netherlands. Phd thesis Utrecht University.